Natural genetic variation and gene expression patterns underlying lateral shoot (tiller) development in barley (*Hordeum vulgare* L)

A Dissertation
SUBMITTED TO THE FACULTY OF THE
UNIVERSITY OF MINNESOTA
BY

Allison M. Haaning

IN PARTIAL FULFILLMENT OF THE REQUIREMENTS
FOR THE DEGREE OF
DOCTOR OF PHILOSOPHY

Gary J. Muehlbauer, Advisor

January 2019

Acknowledgements

First, I would like to thank my advisor, Professor Gary Muehlbauer, for his continued support throughout my time in his lab. With his guidance and knowledge, he has been essential for shaping my research and has encouraged me to step out of my intellectual comfort zone. He has also helped me to improve skills that will be essential for a successful career in research, such as critical thinking and questioning, scientific writing, and trying to see the big picture amidst heaps of data. I would also like to thank members of my advisory committee, Professors Nathan Springer, Kevin Smith, Candice Hirsch, Michael Scanlon, and Neil Olszewski, for providing extremely helpful feedback and pushing me towards completing this dissertation.

I would like to thank Candice beyond her role on my advisory committee and Professors Chad Meyers and Lin Li for teaching me computational biology skills that have been essential for completing this work. I would also like to thank Kevin beyond his advisory role and members of his lab, especially Edward Schiefelbein and Guillermo Velasquez, for providing seeds and assistance with planting. All members of the Muehlbauer lab have contributed to my academic growth in some capacity, but I would especially like to thank Liana Nice, María Muñoz-Amatriaín, Suma Sreekanta, and Ron Okagaki for going out of their way to provide valuable suggestions and advice that have helped shape my projects.

I was fortunate to enter graduate school with an amazing cohort of students. Diana Trujillo, Derek Nedveck, Leland Werden, and Eli Krumholz became good friends with whom I was able to share both the challenges of graduate school and fun experiences, like exploring various parts of beautiful northern Minnesota. Diana deserves special thanks as a good friend and carpooling companion for going on impromptu camping trips and patiently listening to me vent about teaching and writing in my final semester. Other students in my graduate program, especially Beth Fallon, Mandy Waters, and Christina Smith, are also close friends who have helped to maintain my happiness and sanity. Friends from my home state of Indiana, especially Stacy Crouch and Brandy Snider, have also provided their love and support throughout the years and have held onto the hope that I might move back to Indiana someday.

Finally, I would like to thank my family. My parents, Claudia and Kevin Haaning, have been a constant source of love and support. Besides me, three of my siblings have also pursued careers in plant sciences, probably influenced by exposure to nature through hikes and camping trips, so I thank them for instilling in me a love of plants and learning that has led me down this trajectory. My sisters, Kelsey Rapier and Nicole Haaning, are close friends and confidantes who enrich my life with their love and humor. Nicole, along with her husband, Zeb Curtin, and children, Gus and Mabel, live nearby and have made me part of their family by including me in holidays, vacations to the Yucatán, and weekend plans. They have made Minnesota feel like home.

Synopsis

The main shoot and other above-ground tissues develop from the shoot apical meristem (SAM), including axillary meristems (AXM) from which lateral branches develop. In barley, lateral branches called tillers contribute directly to grain yield and define shoot architecture. Two studies were completed to gain a better understanding of the genetic control of tiller development. One focused on characterizing natural phenotypic and genetic variation in tiller number throughout development in a large, diverse germplasm collection; and the second focused on identifying meristem-specific genes and characterizing gene expression patterns that varied by meristem type (SAM or AXM) and morphological stage. Results from the first study revealed that correlations between tiller development (tillering) and factors previously shown to influence tiller development, like photoperiod response and spike row-type, varied depending on environment and genetic background. Furthermore, no major trade-offs existed between tiller number and other traits, and natural genetic variation associated with tillering largely overlapped variation associated with days to heading and spike row-type. Results of the second study revealed a set of genes upregulated in most meristems compared to non-meristem tissues, many of which have been characterized in other species and are likely important for general meristem maintenance or function. Results also suggested that gene expression was primarily differentiated by genotype, meristem type, and morphological stage; however, expression profiles of SAM and AXM were very similar at later developmental stages. A small number of genes were only expressed in SAM or AXM, and clustering based on expression across all meristems revealed genes

upregulated in AXM that may be important for tiller development, as some, like *UNICULME4* and *INTERMEDIUM-C* (*TEOSINTE BRANCHED 1* ortholog) have already been implicated in tiller development. Genes that were upregulated in ligules compared to leaves were also identified, and clustering of these genes revealed some that were expressed more highly in ligules and AXM that may, as in other species, have dual functions in leaf and tiller development.

Table of Contents

List of Tables

Main Tables:

Supplementary Tables (see online supplementary materials):

Chapter 2 Supplementary Tables:

List of figures

Main Figures:

Supplementary Figures:

Chapter 1. Literature Review

Historically, modifying different shoot architecture attributes of economically important grasses has improved yield. For example, introduction of semi-dwarf alleles into small grain crops like wheat, rice, and barley improved yield by decreasing stem lodging and increasing the proportion of photosynthetic assimilates allocated to grain production (Flintham et al., 1997; Mickelson and Rasmusson, 1994; Rebetzke and Richards, 2000; Saisho et al., 2004; Sasaki et al., 2002; Spielmeyer et al., 2002). Modifying other attributes of shoot architecture, like leaf angle and inflorescence morphology, have also improved yield (Heng et al., 2018; Nan Su San et al., 2018; Sakamoto et al., 2006; Tang et al., 2017; Truong et al., 2015). The number and quality of modified lateral branches called tillers are a defining characteristic of barley shoot architecture and contribute directly to grain yield. Improving aspects of tiller development (tillering) could potentially increase yield, but a more comprehensive understanding of sources of variation that impact tillering and genetic control of tillering are first necessary. In this chapter, the current body of literature surrounding meristem initiation and maintenance, lateral branching, and tiller development was reviewed to provide scope and background for the experimental objectives addressed in Chapters 2 and 3.

Meristem Initiation, Maintenance, and Function

Lateral branches and all other aboveground structures of plants are derived from stem cells initiated in a dome-shaped organ called the shoot apical meristem (SAM),

which forms during embryonic development. SAM stem cells, also called initials, are located in a region near the top and center of the SAM called the central zone (CZ), where they divide slowly and continually replenish themselves as cells are displaced from the CZ (reviewed in Barton, 2010 and Meyerowitz, 1997). Cells that are displaced into regions adjacent to the CZ called peripheral zones (PZ) divide more rapidly and differentiate to form lateral organs like leaves and axillary meristems (AXM), and cells that are displaced into a region below the CZ called the rib meristem also divide more rapidly and differentiate to form the central cells of stems (reviewed in Barton, 2010 and Meyerowitz, 1997).

SAMs of most angiosperms consist of clonally distinct cell layers, called the tunica and corpus, from which all above-ground organs are derived (reviewed in Barton, 2010 and Meyerowitz, 1997). In many grasses, including barley, the tunica consists of a single layer (L1) that is one cell-thick and maintained by anticlinal cell divisions (Döring et al., 1999). Leaves in barley are derived from both tunica (L1) and corpus (L2), the epidermis and part of the mesophyll are derived from L1, and all other cells are derived from L2. Tillers develop from AXM, which are located at the growing tips of axillary buds (AXB) and are also derived from both layers (Döring et al., 1999).

During early embryogenesis before any organs are visible, a class 1 *KNOTTED-LIKE HOMEOBOX* (*KNOX*) gene, called *KNOTTED 1* (*KN1*) in maize (Kerstetter et al., 1997), *SHOOT MERISTEMLESS* (*STM*) in Arabidopsis (Long et al., 1996), and *ORYZA SATIVA HOMEOBOX 1* (*OSH1*) in rice (Sato et al., 1996), is expressed at the site of SAM formation. Loss-of-function mutant phenotypes are species-dependent and range in

severity from complete loss of SAM in Arabidopsis (Long et al., 1996) to defective boundary formation between the SAM and leaf primordia in rice (Tsuda et al., 2014). In maize, *KN1* loss of function resulted in failure to develop new organs after the coleoptile was formed, but penetrance of the phenotype depended on inbred background and ranged from very low (<5% after four backcrosses in B73) to very high (77-100% after four backcrosses in W23) (Vollbrecht et al., 2000). In addition to being expressed in the SAM, these genes are expressed in all shoot meristems, including axillary meristems and floral meristems, and are commonly used as markers for meristem identity (e.g. Jackson et al., 1994).

Other class 1 *KNOX* genes are expressed in SAM and other meristems as well and appear to have both overlapping and distinctive functions. For example, Arabidopsis *BREVIPEDICELLUS* (*BP*, also called *KNAT1*) is also expressed in SAM, but instead of being expressed in the central zone like *STM*, it is expressed in peripheral zones and loss of function causes defects in inflorescence architecture (Venglat et al., 2002). In addition to their role in initiating meristematic tissues and maintaining stem cells, *KNOX* genes are important for proper meristem function by specifying cell fate, and ectopic expression or overexpression typically results in abnormal organ patterning or ectopic meristem formation (reviewed in Barley and Waites, 2002 and Hake et al., 2004). For example, the *Hooded* mutant in barley develops extra floral organs instead of awns on the palea of the caryopsis, caused by overexpression of *HvKNOX3*, the barley ortholog of *KN1* (Müller et al., 1995). Loss of function mutations in rice *OSH15*, another class 1 *KNOX* gene, caused

defects in organ patterning, including shortened internodes and abnormalities in cell shape and vascular bundle formation (Sato et al., 1999).

In Arabidopsis, SAM size and maintenance of stem cells is regulated by a negative feedback loop consisting of WUSCHEL (WUS) and CLAVATA (CLV) proteins, where levels of WUS, which promotes stem cell fate, are restricted by CLV signaling (Schoof et al., 2000). CLV3 in Arabidopsis is a member of the CLV3/ ENDOSPERM SURROUNDING REGIONS (CLE) peptide family and is secreted from stem cells in meristems (reviewed in Somssich et al., 2016). Several receptor-like proteins (RLPs), including CLV1 and CLV2, are localized to plasma membranes of cells in a region of the meristem called the organizing center (OC) where they perceive secreted CLV3. Though the role of CLV signaling in meristem size and maintenance appears to be conserved, WUS orthologs/paralogs are not expressed in the central zone in rice or maize as they are in many dicots, and they do not appear to have the same function (reviewed in Pautler et al., 2013). For example, *TILLERS ABSENT1* (*TAB1*), the rice ortholog of *WUS*, is only expressed in AXM and appears to influence AXM initiation (Tanaka et al., 2015); and the two *WUS* paralogs in maize, *ZmWUS1* and *ZmWUS2*, are expressed in SAM but appear to be respectively restricted to cells of the prospective node/internode and leaf primordia (Nardmann and Werr, 2006). On the other hand, the *WUSCHEL-related homeobox4* (*WOX4*) gene in rice appears to be functionally similar to *AtWUS* and is negatively regulated by FON2-LIKE CLE PROTEIN1 (FCP1), which is homologous to AtCLV3, suggesting that WOX/CLV feedback may be conserved in grasses (Ohmori et al., 2013).

Establishment of boundaries through regulation of gene expression and protein signaling is important for meristem initiation, maintenance, and function; and many genes involved in boundary formation restrict expression of class 1 *KNOX* genes. In Arabidopsis, *CUP-SHAPED COTYLEDON* (*CUC*) genes, *CUC1*, *CUC2*, and *CUC3* are expressed early in the region between cotyledons, where the SAM develops, and later in the SAM itself, where they establish boundaries between meristem tissue and newly forming leaf primordia (Raman et al., 2008; Vroemen et al., 2003). *CUC* genes encode NO APICAL MERISTEM/*Arabidopsis thaliana* activating factor 1 and 2/CUP SHAPED COTYLEDON 2 (NAC) domain transcription factors that are important for boundary formation in various tissues. Boundary formation is important for meristem initiation, and like *stm* mutants, *cuc1 cuc2* double mutants do not form a SAM and do not survive past embryogenesis (Aida et al., 1997). Moreover, the *KNOX* gene *STM* is not expressed in *cuc1 cuc2* double mutants, indicating that CUC1 and CUC2 induce *STM* expression, and STM, in turn, is required for proper spatial expression of *CUC1* and *CUC2* (Aida et al., 1999; Takada et al., 2001). All three *CUC* genes in Arabidopsis are somewhat functionally redundant, but *CUC2* and *CUC3* play additional roles in initiation of axillary meristems and leaf patterning (Blein et al., 2008; Nikovics et al., 2006; Raman et al., 2008). Besides CUC proteins, other transcription factors, like ASYMMETRIC LEAVES 1 (AS1) and BLADE-ON-PETIOLE 1 (BOP1) and BOP2 are important for regulating *KNOX* gene expression and establishing and maintaining boundaries in meristems and other tissues (Khan et al., 2012; Ori et al., 2000).

Hormone signaling is also important for formation of boundaries and meristem maintenance and function. For example, functional meristems maintain low levels of gibberellin (GA) and relatively high levels of cytokinins (CK). Class 1 *KNOX* genes have been shown to inhibit expression of GA20 oxidases, enzymes necessary for GA biosynthesis, and induce expression of GA2 oxidases, enzymes that deactivate GA, in several species (Bolduc and Hake, 2009; Hay et al., 2002; Jasinski et al., 2005; Sakamoto et al., 2001). Cytokinin biosynthesis, on the other hand, is induced by KNOX proteins, and like KNOX proteins, cytokinins repress GA levels by enhancing expression of GA2 oxidases (Jasinski et al., 2005). The most important function of meristems is to initiate new organ primordia, like leaves and axillary meristems, and auxin is required for this function. Auxin maxima form in the SAM at sites where new organ primordia initiate, and mutations in genes that affect auxin transport result in various abnormalities, like the inability to establish axillary meristems in inflorescences, as seen in *pin-formed* and *pinoid* mutants in Arabidopsis and *barren* mutants in maize (Friml et al., 2004; Gälweiler, 1998; McSteen and Hake, 2001; McSteen et al., 2007; Ritter et al., 2002).

Lateral Organ initiation and Patterning

As previously mentioned, the most important function of meristems is to initiate new organs that make up the shoot, and establishment and maintenance of boundaries in the SAM are important for establishment of new organ primordia. In Arabidopsis, proper expression of the boundary genes *CUC2* and *CUC3* are important for proper lateral organ initiation and patterning. Development of lateral branches is impaired in *cuc2 cuc3* double mutants, and overexpression of miR164 in these mutants nearly abolishes AXM

initiation. Expression of *LATERAL SUPPRESSOR* (*LAS*), a gene required for AXM initiation, is reduced in *cuc2 cuc3* mutants and nearly absent in *cuc2 cuc3* mutants overexpressing miR164, which is the likely reason that mutants have impaired lateral branching (Raman et al., 2008). On the other hand, *mir164* mutants form accessory axillary buds in leaf axils and have increased *LAS* expression, indicating that *CUC2*, *CUC3*, miR164, and *LAS* all cooperate in AXM initiation in Arabidopsis. *LAS*, tomato *LATERAL SUPPRESSOR* (*LS*), and rice *MONOCULM1* (*MOC1*) are orthologous genes that encode nuclear GRAS family proteins necessary for AXM initiation (Greb et al., 2003; Li et al., 2003; Schumacher et al., 1999).

Some genes influence both vegetative and reproductive axillary meristem development. For example, orthologous genes rice *LAX PANICLE1* (*LAX1*) and maize *BARREN STALK1* (*BA1*) are required for vegetative and reproductive AXM initiation (Komatsu et al., 2003; Oikawa and Kyozuka, 2009). *BA1* and *LAX1* encode basic helix-loop-helix (bHLH) transcription factors expressed in boundaries between organs, in leaf axils, and in newly forming AXM (Gallavotti et al., 2004; Oikawa and Kyozuka, 2009). Maize *ba1* and rice *lax1* mutants are defective in both vegetative and inflorescence branching, and *lax1 moc1* double mutants have an additive phenotype with more severely reduced branching (Oikawa and Kyozuka, 2009). *BA1* acts downstream of and is a direct target of the protein kinase BIF2, a PINOID ortholog important for polar auxin transport (Skirpan et al., 2008, 2009). Like *ba1* mutants, *bif2* are defective in both vegetative and inflorescence branching (Ritter et al., 2002). Barley low tillering mutants, like *uniculm2*

(*cul2*) and *absent lower laterals* (*als*), also have abnormal inflorescence branching (Babb and Muehlbauer, 2003; Dabbert et al., 2009).

Some genes important for forming and maintaining boundaries are important for leaf patterning in addition to their role in axillary meristem initiation. For example CUC2 in Arabidopsis and NAC domain transcription factors in other species, like GOBLET (GOB) in tomato, regulate leaf margin patterning and are negatively regulated by miR164 (Berger et al., 2009; Nikovics et al., 2006). Some genes involved in lateral branching in barley are also involved in leaf patterning. For example, ligules, strips of epidermal tissue that form at the blade-sheath boundary of many grass leaves, are absent or reduced in *uniculme 4* (*cul4*) low tillering mutants (Tavakol et al., 2015). Strong *eligulum-a* mutant alleles also cause a low tillering phenotype and loss of both ligules and auricles, flaps of tissue that form at leaf margins of the blade-sheath boundary (Okagaki et al., 2018).

Development of Lateral Branches in Plants

Shoot development occurs continuously throughout the life of a plant in repeating, stacked units called phytomers, which in barley consist of an upper and lower half-node separated by a portion of stem called an internode, with leaf primordia developing on the upper half-node and axillary buds (AXB) and root initials developing on the lower half-node (Forster et al., 2007). The SAM is located at the growing tip of the main shoot, and eventually it develops into an inflorescence meristem during transition from vegetative to reproductive development, forming specialized phytomers that make up the inflorescence

(Sussex, 1989). Axillary meristems (AXM) are located at the tips of AXB. Like the SAM, AXM consist of pluripotent cells that can divide and differentiate to form phytomers that make up lateral shoots, and they can also develop into inflorescence meristems to form inflorescences during reproductive growth (Sussex, 1989).

Environmental and endogenous factors influence lateral branch development primarily through hormonal signaling. Although auxin is required for AXM initiation, high concentrations of auxin inhibit internode elongation in the AXB. Internode elongation has been correlated with auxin transport out of AXB through PINFORMED (PIN) proteins, auxin efflux carriers that localize to the cell membrane (Balla et al., 2011; Prusinkiewicz et al., 2009). Under the canalization model of auxin transport, polarized auxin transport from the source (shoot apex) to the sink (roots) through the stem is regulated by sink strength (Balla et al., 2011; Müller and Leyser, 2011; Prusinkiewicz et al., 2009; Sauer et al., 2006). In plants that exhibit apical dominance, the sink strength is weak, which prevents transport of auxin out of AXB into the stem. Removal of the shoot apex in pea increased sink strength, triggering polarization of PINs in AXB, auxin efflux from AXB, and subsequent AXB outgrowth (Balla et al., 2011).

Strigolactones are also hormones that inhibit AXB internode elongation. In Arabidopsis, they are synthesized in the roots by enzymes encoded by *MORE AXILLARY GROWTH* (*MAX*) genes and then transported acropetally to AXB (Gomez-Roldan et al., 2008). Arabidopsis *max1* mutants have increased axillary branching associated with increased expression of *PIN1* and increased auxin transport (Bennett et al., 2006; Shinohara et al., 2013). This increased branching phenotype is dependent on the

overexpression of *PIN1*, as *max1*/*pin1* double mutants exhibit fewer lateral branches (Bennett et al., 2006). Based on these results, it is possible that strigolactones inhibit internode elongation by inhibiting transcription of *PIN* genes, preventing auxin efflux out of AXB. Strigolactones may also induce expression of orthologous transcription factors maize *TEOSINTE BRANCHED 1* (*TB1*), rice *FINE CULM1* (*FC1*), and Arabidopsis *BRANCHED1*, which act downstream of strigolactones to inhibit internode elongation (Aguilar-Martínez et al., 2007; Doebley et al., 1995; Finlayson, 2007; Minakuchi et al., 2010).

Unlike auxin and strigolactones, cytokinins are hormones that promote AXB outgrowth. However, the exact way in which they promote it is unknown. In pea, applying cytokinins externally to dormant axillary buds promotes outgrowth, while increasing the amount of auxin in adjacent stems. The specific cytokinin that released the most buds from dormancy also resulted in the most auxin accumulation in adjacent stem, indicating that internode elongation is dependent on auxin accumulation (Li and Bangerth, 2003). Inducing overexpression of cytokinins in young transgenic Arabidopsis plants rapidly resulted in increased auxin biosynthesis in the shoot apex and roots (Jones et al., 2010). Under the canalization model, increasing cytokinin-regulated auxin biosynthesis in axillary buds could increase their sink strength, allowing them to export auxin into the stem to escape dormancy (reviewed in Müller and Leyser, 2011).

Development of Tillers in Barley

The phytomer structure of barley and other grasses differ somewhat from other plants in that the axillary buds of some early-forming phytomers can develop into modified lateral shoots called tillers. Tillers are different from other types of lateral shoots in that they are located near the base of the plant because internodes of tiller forming phytomers do not elongate. They can also develop root systems independent of the main shoot because root initials of tiller forming phytomers can develop into nodal or adventitious roots. Phytomers in barley and some grass species also differ from many other plant species in that AXB development is typically suppressed in the phytomers with elongated internodes that make up the culm or stem.

Tillering in barley begins during seedling development. New AXB develop adjacent to the internode, covered by the leaf sheath of the previously formed phytomer. Typically, two AXB are already formed in mature embryos, one that formed in the axil of the coleoptile (T_0 AXB) and another that formed in the axil of the first leaf (T_1 AXB) (Kirby and Applegate, 1981). The first tiller is usually visible when seedlings have three leaves, and most spring barley lines continue to produce tillers for approximately two weeks after the first tiller emerges (Anderson et al., 2013). Plants can develop primary, secondary, and, in some cases, tertiary (and beyond) tillers, which develop from SAM-derived, primary tiller AXM-derived, and secondary tiller AXM-derived tissue, respectively (Kirby and Applegate, 1981). The number of tillers that develop depends upon the genotype and environmental conditions, and cessation of tillering usually coincides with the onset of stem elongation (Anderson et al., 2013; Miralles and Richards, 2000). Some tillers will develop grain-bearing inflorescences called spikes,

while other tillers die or fail to form spikes; and, like tiller number, the proportion of tillers that survive and develop spikes depends on the genotype and environmental conditions (Anderson et al., 2013).

Tillering is influenced by many different environmental variables. Many studies have demonstrated that more tillers develop when there is sufficient availability of water, light, and nutrients; and their development is inhibited when any of these factors is limited (Aspinall, 1961, 1963; Aspinall et al., 1964; Davis and Simmons, 1994; Fletcher and Dale, 1974; Skinner and Simmons, 1993). Planting density can affect tiller number as well because it influences the amount of resources available to individual plants (Kirby and Faris, 1972; Simmons et al., 1982). Tiller number is also influenced by temperature; for example, García del Moral and García del Moral (1995) observed that tillering is inhibited by high temperature. Photoperiod also influences tiller number by influencing the duration of the vegetative growth phase. Though photoperiod sensitivity in barley varies, in general, barley is considered a long-day plant and flowers in response to long photoperiods (> 12 hours of daylight). Miralles and Richards (2000) demonstrated that tiller number is inversely related to photoperiod. Tiller number increased as photoperiod decreased, due to delayed flowering and a longer vegetative growth period, and tillering rate increased as photoperiod decreased.

Functional genetics of tillering has been characterized in several low and high tillering mutants. To date five tillering genes have been isolated: *JUBEL2*, *UNICULME4* (*CUL4*), *ELIGULUM-A* (*ELI-A*), *MANY NODED DWARF* (*MND*), and *INTERMEDIUM-C* (*INT-C*) (Table 1-1). *JUBEL2* encodes a BEL-like homeodomain transcription factor

orthologous Arabidopsis *BELLRINGER* (*BLR*) and is mutated in the low tillering mutant *low number of tillers 1* (*lnt1*) (Dabbert et al., 2010). *CUL4* encodes a BROAD COMPLEX, TRAMTRACK, BRIC-À-BRAC (BTB)-ankyrin domain containing protein homologous to *Arabidopsis thaliana BLADE-ON-PETIOLE 1* (*BOP1*) and *BOP2*, and *cul4* mutants produce very few primary tillers and no secondary tillers (Tavakol et al., 2015). The *eli-a* mutant, was identified as a suppressor of the *uniculm2* (*cul2*) mutant phenotype (Okagaki et al., 2018). Typically, *cul2* mutants do not produce any tillers, but when crossed with mutants containing strong *eli-a* alleles, they developed at least one tiller. *ELI-A* encodes a conserved protein that may be a transposon, and, despite their ability to inhibit the *cul2* mutant phenotype, single mutants with strong *eli-a* alleles are low tillering and typically produce about half as many tillers as non-mutants (Okagaki et al., 2018). Unlike the other three genes, mutation of *INT-C* and *MND* result in high tillering phenotypes. INT-C is an ortholog of the branching inhibitor maize TB1 and a member of the TB1, CYCLOIDEA (CYC), PROLIFERATING CELL NUCLEAR ANTIGEN FACTOR1/2 (TCP) family of transcription factors, and loss-of-function mutants have a moderate high tillering phenotype (Ramsay et al., 2011). *MND* encodes a cytochrome P450 in the CYP78A family homologous to rice *PLASTOCHRON1* (*PLA1*), and *pla1* mutants have a similar phenotype as *mnd* mutants (Mascher et al., 2014).

Many uniculm and low tillering mutant phenotypes are epistatic to high tillering phenotypes. These epistatic interactions are apparent when different low tillering and uniculm mutants, like *absent lower laterals* (*als*) and *cul2*, are crossed with different high tillering mutants like *granum-a* (*gra-a*) and *mnd1*. In all cases hybrid plants have a low

tillering or uniculm phenotype, probably due to the inability of some uniculm or low tillering plants to initiate or maintain AXMs and/or AXBs (Babb and Muehlbauer, 2003; Dabbert et al., 2009; Okagaki et al., 2013). Crossing the low tillering mutants *lnt1* and *als* with another low tillering mutant *intermedium-b* resulted in a more severe uniculm phenotype, suggesting the possibility that two independent pathways may control tiller development (Dabbert et al., 2009, 2010).

By comparing gene expression of tillering mutants and non-mutant progenitor lines, differentially expressed genes were identified that may be involved in axillary growth. Many of the genes upregulated in low-tillering mutants are involved in stress and defense related responses, like production of reactive oxygen species, glutathione synthesis, and calcium signaling (Dabbert et al., 2009; Okagaki et al., 2013). Many of these stress and defense related responses have also been shown to be involved in embryogenesis and organ development (reviewed in Beveridge et al., 2007).

In addition to the previously discussed exogenous and endogenous factors that influence tillering in barley, pleiotropic effects of photoperiod response and spike morphology also influence tillering. Pleiotropic effects of photoperiod sensitivity and spike morphology on tillering were observed before any of the genes influencing these traits were elucidated. For example, Guitard (1960) observed that initiation of tillering occurred earlier in an early flowering line as photoperiod increased, while it was delayed in a late flowering line; and Kirby and Riggs (1978) demonstrated that barley with two-row spike morphology (2-rows) developed more tillers than barley with six-row spike morphology (6-rows). Today, many genes and genetic pathways underlying photoperiod

sensitivity and spike morphology in barley have been identified and described (Table 1-1); and differences in tillering have been described between lines carrying different alleles of the most influential genes. For example, studies have shown that lines carrying a dominant allele of *PHOTOPERIOD-H1* (*PPD-H1*), a major regulator of photoperiod response in barley, flowered earlier and had fewer tillers than lines with the recessive allele (Alqudah et al., 2016; Karsai et al., 1999); and 2-rows carrying the functional allele of *SIX-ROWED SPIKE 1* (*VRS1*), had more tillers than 6-rows with the non-functional allele (Alqudah and Schnurbusch, 2014; Liller et al., 2015). *PPD-H1* and *VRS1* are also common candidate genes for quantitative trait loci (QTL) associated with tillering (Alqudah et al., 2016; Karsai et al., 1997; Laurie et al., 1994; Nice et al., 2017).

To date, most of the genes implicated in circadian clock and photoperiod response in barley have been previously identified and characterized in other species, especially in the model long day plant *Arabidopsis thaliana*. Perception of circadian rhythms by clock genes is important for many different processes in plants, including flowering. Campoli et al. (2012a) identified barley genes that were likely orthologs of Arabidopsis clock genes based on diurnal and circadian expression, and showed that variation in *PPD-H1*, an ortholog of the Arabidopsis clock gene *PSEUDO RESPONSE REGULATOR 7*, did not influence expression of clock genes but did influence expression of genes that induce flowering. Genetic pathways that induce flowering have also been well characterized in Arabidopsis, and, like clock genes, the major players appear to be conserved in barley. Barley lines carrying the photoperiod sensitive *PPD-H1* allele had elevated expression levels of *VERNALIZATION-H3* (*VRN-H3*), an ortholog of Arabidopsis *FLOWERING*

LOCUS T (*FT*) (Campoli et al., 2012a; Turner et al., 2005). In Arabidopsis, CONSTANS (CO) activates *FT* transcription under long days. CO is a zinc finger transcription factor containing a CO, CO-LIKE, and TIMING OF CAB EXPRESSION 1 (CCT) domain, and its transcription is activated under long days by the clock proteins GIGANTEA (GI) and FLAVIN KELCH F BOX 1 (FKF1), a ubiquitin ligase with a light-sensing chromophore (reviewed in Andrés and Coupland, 2012). *FT* is expressed in leaves where light signals are perceived, and its protein product is transported through phloem to the SAM where it forms a hetero-hexameric flowering activation complex (FAC) with FLOWERING LOCUS D (FD), a basic leucine zipper (bZIP) transcription factor, and 14-3-3 proteins. The FAC activates transcription of floral meristem identity genes like *FRUITFUL* (*FUL*), *LEAFY* (*LFY*), and *APETALA 1* (*AP1*) (reviewed in Andrés and Coupland, 2012). In addition to having elevated *VRN-H3* expression, barley lines with a photoperiod responsive *PPD-H1* allele had elevated expression of other genes that induce flowering, like *HvCO-like 1* (*HvCO1*) and *HvCO2* and the *AP1* ortholog *VRN-H1*. Circadian clock and flowering genes previously characterized in barley are summarized in Table 1-1.

Lateral spikelet fertility in barley influences tiller number, most likely by affecting resources available for tiller development (Liller et al., 2015). Barley spikelets contain three florets, one central and two lateral. In barley with 2-row spike morphology, the ancestral state, the central floret is fertile and develops into a grain, while the two lateral florets are infertile and do not develop into grains; whereas in 6-rows, all three florets are fertile and develop into grains. In general, 6-rows produce more seeds on average than 2-rows, and they also produce fewer tillers and have wider leaves (Alqudah

et al., 2016; Liller et al., 2015; Pasam et al., 2012). Spike row-type is primarily determined by variation in *VRS1*, which encodes a homeodomain leucine zipper protein (Komatsuda et al., 2007; Sakuma et al., 2017), or *VRS4*, which encodes an ortholog of the maize transcription factor RAMOSA2 (Koppolu et al., 2013); and loss-of-function mutation of either gene is sufficient to cause a 6-row spike type. Both of these genes probably encode inhibitors of lateral floret differentiation based on mutant phenotypes and localization and timing of mRNA expression. Both are expressed in lateral florets at the glume primordia stage (Waddington Stage 2.5) (Komatsuda et al., 2007; Koppolu et al., 2013; Sakuma et al., 2017), which occurs when plants have 3.5-6 leaves and are actively developing tillers (Anderson et al., 2013; Digel et al., 2015; Waddington et al., 1983). Variation in several other genes besides *VRS1* and *VRS4,* like *INT-C* (Ramsay et al., 2011) and *VRS3* (Bull et al., 2017; van Esse et al., 2017), also influence spike row-type and/or inflorescence morphology and are summarized in Table 1-1.

The overall goal of the following two chapters was to add to the current body of knowledge about tiller development in barley. In the second chapter, we grew and measured various traits in a large number of lines that allowed us to characterize relationships between tillering and other traits. We also identified natural genetic variation that could potentially be useful for optimizing tiller number or morphology. In the third chapter, we analyzed gene expression in SAM and AXM to identify sets of genes that are likely important for meristem development in barley. We also identified sets of genes with higher expression in AXM that may be specifically important for AXM or tiller development. Both studies have generated new information regarding genetic

control of tiller development in barley and may be useful for improving shoot architecture.

Table 1-1. Genomic locations of genes and mutants related to tiller development, photoperiod sensitivity, circadian clock, and spike row morphology in barley (Chr: Chromosome, Pos: Position).

Gene ID	Gene/Mutant Name	Protein Annotation	Chr	Gene/ Interval Start (bp)	POPSEQ Pos (cM)	References
Tillering Genes						
HORVU2Hr1G011730	*ELIGULUM-A* (*ELI-A*)	Putative transposon with RNase H domain	2	24295416	15.52	(Okagaki et al., 2018)
Not applicable (NA)	*many noded dwarf1 (mnd1)*	NA	2	100641977	52.61-56.77	(Druka et al., 2011)
NA	*absent lower laterals (als)*	NA	3	601474414	86.44-109.61	(Druka et al., 2011)
HORVU3Hr1G085720	*JUBEL2*	BEL1-like homeodomain transcription factor	3	613897933	92.71	(Dabbert et al., 2010)
HORVU3Hr1G106880	*UNICULME4* (*CUL4*)	BLADE-ON-PETIOLE (BOP) 1/2-like BTB-ankyrin repeat containing protein	3	671495852	137.71	(Tavakol et al., 2015)
HORVU4Hr1G007040	*INTERMEDIUM-C* (*INT-C*)	TCP transcription factor (TEOSINTED-BRANCHED1 ortholog)	4	17599033	32.04	(Ramsay et al., 2011)
HORVU5Hr1G081060	*MANY NODED DWARF* (*MND*)	Cytochrome P450	5	562934361	97.09	(Mascher et al., 2014)
NA	*uniculm2* (*cul2*)	NA	6	423193924	60.19-60.72	(Druka et al., 2011; Okagaki et al., 2013)
NA	*granum-a* (*gra-a*)	NA	7	636617013	126.2	(Druka et al., 2011)
Circadian Clock and Flowering Genes						
HORVU1Hr1G076430	*PHOTOPERIOD-H2* (*PPD-H2*)	FLOWERING LOCUS T-like	1	514098182	94.01	(Faure et al., 2007; Laurie et al., 1995)
HORVU1Hr1G094980	*praematurum.a-8* (*mat.a-8*)/ *early maturity 8* (*eam8*)	EARLY FLOWERING3-like, Nuclear protein involved in phytochrome B signaling	1	556900385	132.54	(Boden et al., 2014)

HORVU2Hr1G013400	*PHOTOPERIOD-H1*	Two-component pseudo response regulator	2	29123785	19.15	(Turner et al., 2005)
HORVU2Hr1G023180	*FLOWERING LOCUS T 4*-like (*FT4*)	FLOWERING LOCUS T-like	2	68833704	47.46	(Faure et al., 2007)
HORVU2Hr1G063800	*MADS8*	APETALA1-like MADS box transcription factor	2	432051592	58.76	(Kobayashi et al., 2012; Schmitz et al., 2000)
HORVU2Hr1G072750	*CENTRORADIALIS* (*CEN*)	Phosphatidylethanolamine-binding protein	2	523377523	58.7	(Comadran et al., 2012)
HORVU2Hr1G085910	*CONSTANS 4*-like (*CO4*)	Transcription factor with a CCT domain	2	620631167	65.61	(Griffiths et al., 2003)
HORVU3Hr1G021140	*GIGANTEA* (*GI*)	Nuclear protein involved in phytochrome B signaling	3	67421434	45.8	(Russell et al., 2016)
HORVU3Hr1G027590	*FLOWERING LOCUS T 2*-like (*FT2*)	*FLOWERING LOCUS T-like*	3	119252011	45.5	(Russell et al., 2016)
HORVU3Hr1G079640	*FLOWERING LOCUS D 4*-like (*FDL4*)	bZIP transcription factor	3	584357437	76.45	(Li et al., 2015)
HORVU3Hr1G086000	*LUX ARRHYTHMO*-like (*LUX*)/ *early maturity 10* (*eam10*)	Myb family transcription factor	3	615106969	92.71	(Campoli et al., 2013)
HORVU4Hr1G021010	PSUEDO RESPONSE REGULATOR 59-like (PRR59)	Two-component pseudo response regulator	4	105940577	51.3	(Campoli et al., 2012a)
HORVU4Hr1G039300	*FLAVIN-BINDING, KELCH REPEAT, F-BOX 1*-like (*FKF1*)	Flavin-Binding, Kelch Repeat, F-Box protein	4	300696992	52.5	(Calixto et al., 2015)
AK361423††	*FLOWERING LOCUS D 5*-like (*FDL5*)	bZIP transcription factor	4	427458289	51.51	(Li et al., 2015)
HORVU4Hr1G090390	*FLOWERING LOCUS T 5*-like (*FT5*)	*FLOWERING LOCUS T-like*	4	645064417	116.98	(Faure et al., 2007)
HORVU5Hr1G060000	*EARLY FLOWERING 4-like* (*ELF4*)	Nuclear protein involved in phytochrome B signaling	5	469024048	48.4	(Russell et al., 2016)
HORVU5Hr1G081620	PSUEDO RESPONSE REGULATOR 95-like (PRR95)	Two-component pseudo response regulator	5	565156282	97.1	(Calixto et al., 2015)

HORVU5Hr1G095630	*VERNALIZATION-H1* (*VRN-H1*)	MADS box transcription factor	5	599122941	126.01	(Fu et al., 2005)
HORVU6Hr1G022330	*ZEITLUPEb* (*ZTLb*)	F-box protein, part of SCF complex that degrades TOC1	6	70576253	49.32	(Calixto et al., 2015)
HORVU6Hr1G057630	*TIMING OF CHLOROPHYLL A/B BINDING PROTEIN 1* (*TOC1*)	Two-component pseudo response regulator	6	374866560	55.4	(Calixto et al., 2015)
MLOC_75496[†]	*CONSTANS 2*-like (*CO2*)	Transcription factor with a CCT domain	6	504463498	68.23	(Calixto et al., 2015)
HORVU7Hr1G024610	*VERNALIZATION-H3* (*VRN-H3*)	FLOWERING LOCUS T-like	7	39679905	33.67	(Yan et al., 2006)
HORVU7Hr1G043030	*CONSTANS 1*-like (*CO1*)	Transcription factor with a CCT domain	7	127667781	67.91	(Calixto et al., 2015)
HORVU7Hr1G070870	*LATE ELONGED HYPOCOTYL*-like (*LHY*)	Myb family transcription factor	7	385861846	70.8	(Campoli et al., 2012a; Ford et al., 2016; Russell et al., 2016)
HORVU7Hr1G099010	*ZEITLUPEa* (*ZTLa*)	F-box protein, part of SCF complex that degrades TOC1	7	599452510	97.3	(Calixto et al., 2015)
Spike Morphology Genes						
HORVU1Hr1G051010	*SIX-ROWED SPIKE 3* (*VRS3*)	Histone demethylase	1	378411487	49.02	(van Esse et al., 2017)
HORVU2Hr1G092290	*SIX-ROWED SPIKE 1* (*VRS1*)	Homeodomain leucine zipper protein	2	652031057	80.22	(Komatsuda et al., 2007)
HORVU2Hr1G113880	*ZEOCRITON* (*ZEO*)	APETALA2-like ethylene-responsive element binding protein	2	730026693	127.08	(Houston et al., 2013)
HORVU3Hr1G016690	*SIX-ROWED SPIKE 4* (*VRS4*)	RAMOSA2-like lateral organ boundary (LOB) domain protein	3	40939171	41.71	(Koppolu et al., 2013)
MLOC_61451.6[††]	*laxatum-a* (*lax-a*)	BOP1/2-like BTB-ankyrin repeat containing protein	5	332395826	44.09	(Jost et al., 2016)

HORVU5Hr1G061840	*DENSE AND ERECT PANICLE 1* (*DEP1*)/ *Breviaristatum-e* (*ari-e*)	DEP1/ari-e	5	482214542	53.36	(Huang et al., 2009)
NA	*intermedium-b* (*int-b*)	NA	5	556603279	91-139.11	(Druka et al., 2011)
NA	*intermedium-m* (*int-m*)	NA	5	640705320	150.7-158.23	(Druka et al., 2011)
Hormone Signaling Genes						
HORVU1Hr1G060810	*GA INSENSITIVE DWARF 1* (*GID*1)/ *GA SENSITIVITY 1* (*GSE1*)	α subunit of a GTP-binding protein	1	441473715	57.4	(Chandler et al., 2008)
HORVU3Hr1G068000	*semi-brachytic* (*uzu*)/ *BRASSINOSTEROID-INSENSITIVE 1* (*BRI1*)	Leucine-rich repeat receptor-like kinase	3	516134759	58.34	(Chono et al., 2003)
HORVU3Hr1G089980	*GIBBERELLIN 20-OXIDASE 3*-like (*GA20-OX*3)	Gibberellin 20-oxidase (GA biosynthesis)	3	630544688	104.41	(Xu et al., 2017)
HORVU3Hr1G090980	*semidwarf 1* (*sdw1*)/*denso*/ *GIBBERELLIN 20-OXIDASE 2*-like (*GA20-OX*2)	Gibberellin 20-oxidase (key gene in GA biosynthesis)	3	634077597	108.74	(Jia et al., 2015; Xu et al., 2017)
HORVU4Hr1G006930	*SLENDER1* (*SLN1*)	GRAS family transcription factor (repressor of GA signaling)	4	16668801	32.04	(Chandler et al., 2002)
AK363454[†]	*DWARF14* (*D14*)	Strigolactone esterase (conversion of strigolactone to bioactive form)	4	573727760	66.71	(Marzec et al., 2016)
HORVU7Hr1G003090	*GA-RESPONSIVE DWARF 5* (*GRD5*)	CYP88A cytochrome P450, ent-kaurenoic acid oxidase (GA biosynthesis)	7	5917105	8.76	(Helliwell et al., 2001)
HORVU7Hr1G008720	*BRACHYTIC 1* (*BRH1*)	α subunit of heterotrimeric G protein (GA signaling)	7	11332545	8.76	(Ito et al., 2017)

[†]Aligned to 2016 high confidence gene but gene was annotated improperly

[††]Did not align well to a 2016 high or low confidence gene, but did align well to expected 2016 pseudomolecule.

Chapter 2. Tiller development in barley is primarily associated with plant fitness, heading date, and spike row-type

This chapter is a draft of a manuscript that will be submitted to a peer-reviewed journal with the following authors:

Allison M. Haaning[1], Kevin P. Smith[2], Gina L. Brown-Guedira[3], Shiaoman Chao[4], Priyanka Tyagi[3], and Gary J. Muehlbauer[1,2*]

Author Affiliations

[1] Department of Plant and Microbial Biology, University of Minnesota, Saint Paul, Minnesota, United States of America

[2] Department of Agronomy and Plant Genetics, University of Minnesota, Saint Paul, Minnesota, United States of America

[3] Eastern Regional Small Grains Genotyping Lab, United States Department of Agriculture-Agricultural Research Service, Raleigh, North Carolina, United States of America

[4] Department of Cereal Crops Research, Red River Valley Agricultural Research Center, United States Department of Agriculture-Agricultural Research Service, Raleigh, North Carolina, United States of America

Synopsis

In barley (*Hordeum vulgare* L.), lateral branches called tillers contribute to grain yield and define shoot architecture. To examine relationships between tiller development (tillering) and other traits, we grew 761 lines from the USDA National Small Grains Core Collection, genotyped using genotyping-by-sequencing (GBS) and a 50K SNP array, and collected data over three years for weekly tiller number, productive tiller number (tillers with grain bearing spikes), days to heading (heading), and traits relating to vegetative and inflorescence development. Across the three years, productive tiller number varied with plant fitness, indicating fitness is a major driver of tiller survival. Analyses using subsets

of lines based on spike row-type (2-row and 6-row) and *PHOTOPERIOD-H1* genotype (*Ppd-H1* and *ppd-H1*) confirmed that spike row-type and photoperiod response are correlated with tillering, but the extent and timing depended on environment and genetic background. Evidence also suggested minor trade-offs between tiller number and other vegetative traits. Thirty-three quantitative trait loci (QTL) were associated with tillering in 2014 and 2015. Of these, ~40% overlapped QTL associated with heading and ~22% overlapped QTL associated with spike row-type. Only four tillering QTL were identified in both years, and the QTL that explained the most variance in each year, one overlapping *PPD-H1* in 2014 and one on 3H at 135.4 cM in 2015, were not identified in both years. Results suggest that tillering is mainly influenced by environment, primarily through its effect on plant fitness, and by pleiotropic influences of heading and spike row-type.

Introduction

Grasses form modified lateral branches called tillers that develop from axillary meristems (AXM) located in leaf axils near the base of the plant. Barley shoot architecture is largely defined by the number and vigor of tillers, which are often indistinguishable from the main shoot, and, like the main shoot, usually form grain-bearing inflorescences called spikes that contribute to grain yield. Historically, modifying shoot architecture has been beneficial for improving crop yield. For example, introduction of semi-dwarfing genes in economically important grasses like wheat (Flintham et al., 1997; Rebetzke and Richards, 2000), rice (Sasaki et al., 2002; Spielmeyer et al., 2002), and barley (Mickelson and Rasmusson, 1994; Saisho et al., 2004) has increased grain yield by decreasing stem lodging and, in some cases, increasing the proportion of photosynthetic assimilates allocated to grain production. Breeding for more erect leaves to allow for denser planting (Nan Su San et al., 2018; Sakamoto et al., 2006; Truong et al., 2015) and improving inflorescence morphology through increasing the number and/or size of seeds (Heng et al., 2018; Tang et al., 2017), two other important aspects of shoot architecture, have also been shown to enhance grain yield in grasses. In barley, tillers contribute directly to grain yield and are a defining component of shoot architecture; however, merely increasing tiller number may not increase grain yield because, as some studies suggest, it may negatively impact other traits, like seed number and weight, stem diameter, and lodging severity (Benbelkacem et al., 1984; Simmons et al., 1982; Stoskopf and Reinbergs, 1966). Therefore, a comprehensive understanding of the genetic basis of shoot architecture and potential

trade-offs with other agronomic traits is important for altering barley shoot architecture for increased grain yield.

Tiller number is a complex trait influenced by many environmental variables, including water availability, soil waterlogging, nutrient availability, planting density, temperature, photoperiod (Aspinall, 1961, 1963; Aspinall et al., 1964; Davis and Simmons, 1994; Fletcher and Dale, 1974; Kirby and Eisenberg, 1966; Kirby and Faris, 1972; Miralles, 2000; de San Celedonio et al., 2014; Simmons et al., 1982; Skinner and Simmons, 1993), and by variation in genes that are likely involved in development, hormone signaling, and stress response. Tillering has been previously characterized in various high and low tillering barley mutants. For example, *many noded dwarf* (*mnd*) (Mascher et al., 2014) and *intermedium-c* (*int-c*) (Ramsay et al., 2011) mutants produce high tiller numbers; while *uniculm2* (*cul2*) (Babb and Muehlbauer, 2003; Okagaki et al., 2013), *uniculme4* (*cul4*) (Tavakol et al., 2015), *low number of tillers1* (*lnt1*) (Dabbert et al., 2010), and *absent lower laterals* (*als*) (Dabbert et al., 2009) are all mutants that produce very few or no tillers. To date, several genes implicated in barley tillering have been isolated including: *JUBEL2* (Dabbert et al., 2010), *INT-C* (Ramsay et al., 2011), *CUL4* (Tavakol et al., 2015), *MND4/6* (Mascher et al., 2014), and *ELIGULUM-A* (Okagaki et al., 2018). With the exception of *INT-C* (Ramsay et al., 2011), which encodes the barley ortholog of maize *TEOSINTE BRANCHED 1*, none of these loci are orthologs of genes shown to influence lateral branching in other species.

In addition to being influenced by environment and different genetic loci, tillering is also pleiotropically influenced by photoperiod sensitivity and spike row-type (Alqudah

and Schnurbusch, 2014; Alqudah et al., 2016; Liller et al., 2015; Turner et al., 2005), and, consequently, several candidate genes identified for quantitative trait loci (QTL) associated with tillering have been shown to influence photoperiod sensitivity or spike row-type (Alqudah et al., 2016; Karsai et al., 1997; Laurie et al., 1995; Naz et al., 2014; Nice et al., 2017; Wang and Chee, 2010). Barley plants containing a dominant *PHOTOPERIOD-H1* allele (*Ppd-H1*) are typically photoperiod sensitive and flower in response to long days, and plants with a recessive *ppd-H1* allele are typically photoperiod insensitive (Digel et al., 2015; Turner et al., 2005). Photoperiod sensitivity in barley is also influenced by variation in other genes, including *VERNALIZATION-H3* (*VRN-H3*) (Faure et al., 2007; Loscos et al., 2014; Yan et al., 2006), *CENTRORADIALIS* (*HvCEN*) (Comadran et al., 2012), *VRN-H1* (Loscos et al., 2014; Zitzewitz et al., 2005), and several *CONSTANS*-like genes (Campoli et al., 2012b; Mulki and von Korff, 2016). Photoperiod sensitivity impacts tiller number through influencing the timing and duration of shoot elongation, as tillering typically stops shortly after shoot elongation begins (García del Moral and García del Moral, 1995; Miralles, 2000). Spike row-type also pleiotropically influences tiller number. Barley spikelets contain three florets, one central and two lateral, all of which are fertile and produce seeds in six-row barley (6-rows); whereas in two-row barley (2-rows) only the central floret is fertile. As a consequence of lateral spikelet fertility, 6-rows produce more, often smaller seeds than 2-rows, and they also tend to produce fewer tillers and have wider leaves (Alqudah and Schnurbusch, 2014, 2015; Liller et al., 2015). Spike row-type is primarily determined by variation in *SIX-ROWED SPIKE 1* (*VRS1*), which encodes a homeodomain leucine zipper protein

(Komatsuda et al., 2007), or *VRS4*, which encodes an ortholog of the maize transcription factor RAMOSA2 (Koppolu et al., 2013), both of which are inhibitors of lateral spikelet development. Plants with dominant *VRS1* or *VRS4* alleles are typically 2-rows, whereas plants with recessive alleles are typically 6-rows. Variation in other genes also influence spike row-type and/or inflorescence morphology, including *VRS3* (Bull et al., 2017; van Esse et al., 2017) and *INTERMEDIUM* genes (Lundqvist and Lundqvist, 1988; Ramsay et al., 2011).

To date, most barley tillering studies have used forward genetics or bi-parental mapping approaches, which limit detection of natural genetic variation, and typically only examine tiller number at harvest. However, a recent genome-wide association study identified numerous QTL associated with tiller number at five different developmental stages in 218 spring barley accessions grown in the greenhouse (Alqudah et al., 2016). In addition, genetic interactions between tiller number and spike row-type, photoperiod sensitivity, and plant height were also characterized (Alqudah et al., 2016). In this study, we further examined genetic interactions between these traits and tillering using 761 lines composed of spring 2-rows and 6-rows. We also examined yield related traits, such as average seeds per spike and kernel weight, and vegetative growth related traits, such as stem diameter and leaf width, to identify potential trade-offs between tillering and other important traits. The specific goals of this study were to (1) examine relationships between tillering and other traits, (2) identify natural genetic variation associated with tillering, and (3) determine the extent to which natural genetic variation associated with tillering overlaps genetic variation associated with other traits. A better understanding of

how these sources of variation are associated with tiller development will help develop a framework for a whole-plant understanding of tillering and the role that the environment plays, which can inform breeding choices to optimize tiller number and vigor for yield enhancement.

Materials and Methods

Line Selection, Field Design, and Growing Conditions

A diversity panel containing 768 accessions (Table S2-1 in online supplementary materials) from the National Small Grains Core Collection was developed for phenotypic analyses and genome-wide association studies (GWAS). The panel, split equally between 2-rows and 6-rows, was selected first by including the parents of a barley nested association mapping (NAM) population (Smith, unpublished results) and then based on their contribution to polymorphism information content (PIC), as determined by Muñoz-Amatriaín et al., 2014 (Muñoz-Amatriaín et al., 2014). All accessions grown in 2014 and 2015 were the same except for seven lines that did not flower in 2014 were replaced with different lines in 2015.

Accessions were grown in the field in St. Paul, MN in 2014 and 2015 in a Type 2 Modified Augmented Design (Lin and Poushinsky, 1985; Lin et al., 1983; May et al., 1989) containing 56 blocks, with one half containing two-row accessions (2-rows) and the other half containing six-row accessions (6-rows) (Fig. S2-1). Individual blocks contained 15 rectangular one meter by 0.25 meter plots (five plots by three plots), with the central plot always containing a primary repeated check, cv. Conlon for 2-rows and

cv. Rasmussen for 6-rows (Fig. S2-1). Eight, randomly chosen blocks also contained two repeated secondary checks, assigned randomly to plots within the block. PI584962 and PI614939 were used as secondary checks for 2-rows, and PI327860 and CIho7153 were used as secondary checks for 6-rows. All other plots contained one of the 768 accessions from the mapping panel. In 2016, 54 lines, split equally between 2-rows and 6-rows, were randomly chosen from NAM parent accessions grown in both years using the sample function in R to confirm trait correlations and assess environmental association with tiller number and other traits (Table S2-1). The 54 accessions and the primary checks Conlon and Rasmussen were grown in a complete, randomized block design with three replicates. To control weeds, prevent shading, and allow space for lodging, adjacent plots of non-vernalized winter wheat separated plots. Plots containing barley were machine planted with 30 seeds per plot and thinned to ten plants per one meter-long plot with regular spacing between plants one week after emergence.

Phenotyping, trait value adjustment, and phenotypic analyses

Vegetative traits measured included tiller number, plant height, leaf width (2015 only), and stem diameter (2014 and 2015 only). In 2014 and 2015, tillers were counted on the same plants (ten in 2014 and five in 2015) per row weekly, beginning at two weeks past-emergence (2WPE) and ending at 7WPE. Productive tillers, tillers with grain-bearing spikes at plant maturity, were counted after grain filling when plants first showed signs of senescence (yellowing of awns and flag leaves). Tillering rate was calculated by dividing the maximum tiller number by the time in weeks that maximum tiller number occurred. Other metrics of tillering rate were determined by calculating the differences

between mean tiller number between two consecutive weeks and by calculating slope of a line fit to mean tiller number between at least three consecutive weeks. Leaf width (2015 only) and plant height were measured at the same time that productive tillers were counted. Plant height was calculated as the mean height (cm) of the tallest shoots of all plants from soil level to the top of the spike, not including the awns. Leaf width was calculated as the mean width (mm) at the widest point of the second leaf below the flag leaf on the tallest shoot of all plants. This leaf was chosen because it was consistently green at maturity. The tallest stem of all individual plants in a row were harvested after senescence and dried in an oven at 37 °C for 72 hours. Dried stems were scanned, and the diameters (mm) were measured at the widest point of the last internode (below the peduncle) and averaged for each accession using Image J software (version 1.50).

Phenotyping of inflorescence-related traits included spike row-type, spike length, seeds per spike, spike density, and 50-kernel weight. Spikes from the tallest shoots of all plants were harvested after senescence and dried in an oven at 37 °C for 72 hours. Spikes were scanned, and ImageJ software was used to measure length (cm) of spikes from the bottom of the first seed (above peduncle) to the top of the last seed. After scanning spikes, all seeds were removed by hand and counted; and mean seeds-per-spike for the five spikes was calculated. Spike density was calculated as mean seeds-per-spike divided by mean spike length. All seeds from the five spikes were pooled together, and 50-kernel weight was calculated as the total mass (g) divided by the total number of seeds multiplied by 50.

Days to heading was recorded when spikes on at least half of the shoots in a row were at least 50% emerged from the boot. Growing Degree Days (GDD) were calculated as the average daily temperature (maximum daily temperature + minimum daily temperature / 2) minus the baseline temperature at which spring barley germinates (4.4 °C) (Anderson et al., 2013). Weather data from the UMN Saint Paul weather station (Weather station ID: GHCND:USC00218450) was used to calculate GDD and compare environmental conditions in different years. This data was downloaded for the 2014, 2015, and 2016 growing seasons from the National Oceanic and Atmospheric Administration (NOAA) database (ncdc.noaa.gov/cdo-web/search) (Table S2-2). Lodging was scored after senescence but before spikes were harvested, based on a scale of one to five, with one being completely upright and five being completely prostrate. A score of three was assigned when plants formed an approximate 45 degree angle with the ground. Scores of two were given to plants between one and three, and scores of four were given to plants between three and five.

Trait values were adjusted using two different methods developed by Lin et al. (1983) specifically for Type 2 Modified Augmented Designs and then assessed before and after correction to determine whether adjustment reduced heterogeneity of checks. One method, based on row and column averages of primary checks (method 1 – M1), is better for correcting values when the field varies in one or two directions, based on a simulation study (Lin et al., 1983). The second method, based on linear regression of primary and secondary checks (method 3 – M3), is better for correcting values when the

field varies in many directions, based on a simulation study (Lin et al., 1983). M1 adjusted trait values (*M1AdjValue*) were calculated using the following equation:

$$M1AdjValue = RawValue - Check1_{RowAve} - Check1_{ColAve} + 2Check1_{Ave}$$

$Check1_{RowAve}$ and $Check1_{ColAve}$ were the averages of all primary check trait values in the same block row and block column, respectively, as the raw trait value being adjusted. $Check1_{Ave}$ was the average of all primary check values. Method 3 adjusted trait values (*M3AdjValue*) were calculated using the following equation:

$$M3AdjValue = RawValue - Slope_{AllChecks}(Check1_{Block} - Check1_{Ave})$$

$Slope_{AllChecks}$ was the slope resulting from linear regression of primary check trait values versus the average secondary check trait values within the same block, and $Check1_{Block}$ is the value of the primary check in the same block as the raw trait value. Appropriateness of correction and selection of a correction method was based on two criteria (Lin and Poushinsky 1983, 1985; Lin et al., 1983; May et al., 1989). First, ANOVA in R (version 3.4.4) using primary check trait values was used to test for block row and column effects (Table S2-3). Second, relative efficiency of correction was calculated by dividing the average variance of raw secondary check trait values by the average variance of adjusted secondary check trait values, and values greater than one indicated that correction reduced variance due to heterogeneity in the field (Table S2-3). Raw trait values were used for phenotypic analyses to avoid individual trait adjustments from affecting trait correlations (Table S2-4), and raw and adjusted (if applicable) trait values were used for genome-wide association mapping (Table S2-5).

All statistical analyses were performed in R. Broad-sense heritability (H^2) was estimated using 2014 and 2015 raw trait values by two-way ANOVA with the following model: Trait ~ Year + Line. Genetic variance was calculated as the difference between the line sum of squares and the residual sum of squares divided by two (for two years – 2014 and 2015), and heritability was calculated by dividing genetic variance by the sum of genetic variance and the residual sum of squares divided by two (Table S2-6). Trait heritability was also estimated with 2016 raw trait values using rep instead of year in the two-way ANOVA model (Table S2-6). One-way ANOVA was performed followed by a Tukey-Kramer test for pairwise comparison of trait means between different year, spike row-type, and photoperiod sensitivity groups; and the multcompView package (version 0.1-7) was used to assign letters designating whether groups were significantly different based on FDR-adjusted p-values from the Tukey-Kramer test. Pearson and Spearman rank correlations between traits were calculated using the rcorr function from the package Hmisc (version 4.1-1) (Table 2-2 and Table S2-7). Principal components analysis (PCA) based on average weekly (two to seven weeks past-emergence) and productive tiller number was performed using the PCA function from FactoMineR (version 1.41). The first and second principal components based on tiller number were used as traits in association mapping (Table S2-5).

For multiple linear regression (MLR) analyses, the following model was fit using the lm function in R with tiller number as the response variable and other traits as predictor variables:

$$\text{Tiller Number} = \beta_{Intercept} + \beta_{Days\ to\ Heading} + \beta_{Seeds\ Per\ Spike} + \beta_{Fifty\ Kernel\ Weight} +$$

$\beta_{Leaf\ Width}$ (2015 only) + $\beta_{Plant\ Height}$ + $\beta_{Stem\ Diameter}$

Before model fitting, lines with missing values for any of the traits included in the model were removed. The boot.stepAIC function from the bootStepAIC package (version 1.2-0) was used to replicate model fitting using simulated data sets from the whole data set, and the model was fit in both directions 1000 times to choose predictor variables in the final model. The final model was refit and cook's distance was used to identify and remove outliers. Lines with the highest Cook's distance were removed iteratively, and the model was refit until the R^2 value of the model did not improve. Predictor variables were checked for collinearity using the vif function from the R package car (version 3.0-0) to ensure none of the variables had a Variance Inflation Factor (VIF) that indicated excessive correlation of predictor variables (VIF > 5). After all outlier lines were removed and the model with all predictor variables was refit, ANOVA of the final model fit was used to choose final predictor variables ($p < 0.05$) and calculate percent variance explained by final predictor variables.

Genotyping, Linkage Disequilibrium, and Population Structure Analysis

Lines were genotyped using genotyping-by-sequencing (GBS) and a 50K iSelect (Illumina, San Diego, CA) SNP array (Bayer et al., 2017). DNA was extracted from seedling leaf tissue using a Mag-Bind® Plant DNA Plus kit (Omega Bio-tek, Norcross, GA), following the manufacturer's instructions, and genomic DNA was quantified using a Quant-iT™ PicoGreen® dsDNA Assay Kit (Thermo Fisher Scientific, Waltham, MA). For GBS, reduced representation libraries were created according Poland et al. (2012) using Pst1-Msp1 restriction enzymes. Libraries were sequenced using a HiSeq 2500

system (Illumina) to obtain single-end 125 bp reads. SNP calling was performed using the TASSEL 5 GBS Version 2 Pipeline using 64 base kmers and a minimum kmer count of five (http://www.maizegenetics.net/tassel). Reads were aligned to the Morex reference genome assembly using the "aln" algorithm in the Burrows-Wheeler Aligner (BWA, version 0.7.10) (Beier et al., 2017; Mascher et al., 2017). Genotyping using barley 50K iSelect BeadChip kits (Illumina) was performed according to the manufacturer's instructions, and SNPs were scored in GenomeStudio (version 2.0.2, Illumina) using manually curated clusters developed by Bayer et al. (2017). GBS and 50K SNP datasets were filtered individually based on percent missing data and percent heterozygosity. All filtering and imputing steps were performed using TASSEL 5 (Bradbury et al., 2007). For the first round of filtering, GBS SNPs were removed if more than 50% of calls were missing and/or heterozygous and the minor allele frequency (MAF) was less than 0.03, and 50K array SNPs were eliminated if they contained more than 20% missing and/or heterozygous calls and a MAF less than 0.03. The GBS and 50K SNP datasets were then merged and missing data was imputed using the LD-kNNi imputation method in TASSEL 5 (sites = 20, Taxa = 5, maxLDDistance = -1). The merged, imputed SNP dataset was filtered again for missing data, eliminating SNPs and lines with more than 5% missing/heterozygous data. Lines were also filtered for missing data, and twenty-six lines with more than 5% missing/heterozygous SNP calls were excluded from association mapping and other genetic analyses. Three lines were removed from all genetic analyses because the spike row-type did not match what was recorded in GrainGenes (https://wheat.pw.usda.gov), GRIN (https://npgsweb.ars-grin.gov), and Muñoz-Amatriaín

et al. (2014) (see notes in Table S2-1). SNPs were then tagged using the Tagger feature in Haploview (version 4.1) (Barrett et al., 2005) with an R^2 cutoff of 0.95, resulting in 69,607 tagged SNPs for 747 lines (Table S2-8).

To analyze chromosomal linkage disequilibrium (LD) decay, pairwise R^2 values between all SNPs within a chromosome were calculated in TASSEL, and the background LD level was calculated as the 95th percentile of significant (pDiseq < 0.01) R^2 values for all SNP pairs >= 50 cM apart, the distance at which the recombination rate is 0.5 for loci on the same chromosome. A non-linear model described by Hill and Weir (1988) was fit to all significant pairwise R^2 values and their corresponding distances using the nls function in R (R Core Team, 2017), and the decay distance was calculated as the distance at which the non-linear model intersected with background LD level (Table S2-9) (Marroni et al., 2011). LD decay distances were calculated for individual chromosomes using physical and POPSEQ positions (Mascher et al., 2013) of tagged SNPs . To assess intrachromosomal patterns of LD for candidate gene analysis, pairwise comparisons were made between SNPs in 100 SNP windows. R^2 values were ordered by mean position, and the R^2 values and mean positions of 4950 pairwise comparisons (unique number of pairwise comparisons for 100 SNPs) were averaged and plotted as a line graph and a curve was fit using local regression (LOESS) (Fig. S2-7). The LD plot and haplotypes for SNPs in and around *Ppd-H1* were generated using Haploview (Fig. S2-2).

Population structure was analyzed using the program STRUCTURE (version 2.3.4) (Pritchard et al., 2000). A set of 701 SNPs for STRUCTURE analysis (Table S2-10) were chosen by selecting SNPs from individual chromosomes from the final tagged

SNP dataset that were at least as far apart as the calculated genetic decay distance (Table S2-9). Results from ten individual STRUCTURE runs for K 1-10 were analyzed using STRUCTURE Harvester (Earl and vonHoldt, 2012). The optimum number of subpopulations was chosen based on delta K (ΔK) (Fig. S2-5), which was calculated by STRUCTURE Harvester based on equations from Evanno et al. (2005).

Genome-wide Association Mapping

Genome-wide association mapping (AM) analysis was performed using compressed mixed linear models from the GAPIT R package (Genome Association and Prediction Integrated Tool, version 2.0) (Lipka et al., 2012) with the final imputed and filtered set of 69,607 SNP tags (Table S2-8) and raw and corrected (if applicable based on Table S2-3) phenotypic data (Table S2-5). The MAF cutoff was 0.03 for all lines and 0.05 for subsets based on spike row-type or *Ppd-H1* alleles. The model selection feature of GAPIT was used to choose the optimum number of principal components for each individual trait to account for population structure, and the optimal compression level determined by GAPIT was used. The percentage of genetic variance explained by individual SNPs was calculated as the difference between R^2 of models with the SNP and without the SNP. Criteria for inclusion of significant SNPs in a single QTL was determined based on genetic distance. If genetic distance of a SNP (+/- 2 cM) overlapped genetic distance of another SNP (+/- 2 cM) associated with the same trait, they were considered part of the same QTL. Information about all significant SNPs, including allelic effect size, percent variance explained, and nearest gene information is included in

Table S2-11, and all significant SNPs are shown in Fig. S2-6. Plots included in all figures were generated using the R package ggplot2 (version 3.0.0).

Results

Phenotypic Results

In 2014 and 2015, 761 lines were grown in the field, and data for weekly and productive tiller number, days to heading, plant height, stem diameter, leaf width (2015 only), seeds per spike, fifty kernel weight, and lodging (2015 only) was collected (Table S2-4). Fifty-four of the lines that were grown in 2014 and 2015 were also grown in 2016 in three complete, randomized blocks, and data for weekly and productive tiller number, days to heading, plant height, seeds per spike, and fifty kernel weight was collected (Table S2-4). Phenotypic data was analyzed in all lines and in subsets of lines based on spike row-type and *PPD-H1* alleles. Tiller number data in 2014 and 2015 is summarized in Table 2-1, and all trait data from all years is summarized in Tables S2-4 (all raw trait values) and S2-5 (raw and adjusted trait values used for association mapping).

Genetic variance for tiller number was significant (p-value < 0.0001) in 2014 and 2015 for most time points (Table 2-1). In both years for all line subsets, variance was highest for maximum tiller number and tiller number measured at later time points (5-7WPE), and it decreased for productive tiller number (Table 2-1). Tiller number at 6WPE, the time point at which average maximum tiller number occurred for all lines in 2014 and 2015, had the highest heritability estimate (0.53) of all tiller counts. Decreased heritability from 6WPE to productive tiller number was likely due to variability in tiller

survival, which appears to be strongly influenced by environment as genetic variance for percent productive tillers was not significant (Table S2-6). Heritability estimates for tillering traits based on 2014 and 2015 phenotypic data were lower than other traits measured (Table S2-6).

Heritability estimates based on 2016 data with reps instead of years in the ANOVA model showed a similar trend in which tillering traits had lower heritability estimates than non-tillering traits and the highest tillering heritability estimates were for later time points and then decreased for productive tiller number (Table S2-6). All heritability estimates were higher based on 2016 data than 2014 and 2015 data, and percent productive tillers, which did not have significant genetic variance based on 2014 and 2015 data, had a high heritability estimate (0.86) based on 2016 data (Table S2-6). These results indicate that tillering traits are fairly consistent in the same environment but are influenced by genotype-by-environment interactions.

Environmental association with tillering

Environmental association with tiller number was assessed using data for the 54 lines (27 2-rows and 27 6-rows) grown in all three years. Weekly and productive tiller number in 2014 was much lower than 2015 and 2016 (Fig. 2-1A,B). The onset of tiller development was also delayed in 2014. By 2WPE in 2014, 25.4% of all lines grown had not yet developed at least one tiller per plant on average, whereas all lines grown in 2015 had developed at least one tiller per plant by 2WPE. Maximum tiller number was not significantly different between 2015 and 2016, but productive tiller number was lower in 2016 than 2015 due to lower tiller survival (Fig. 2-1B). All three years followed a similar

trend where tiller number increased linearly until 5WPE, after which it either slowed or began decreasing (Fig. 2-1A).

Average plant height, stem diameter (measured in 2014 and 2015 only), seeds-per-spike, and fifty kernel weight followed a similar trend as productive tiller number across the three years, where trait values were highest in 2015 and lowest in 2014 (Fig. 2-1C). In years when plants developed more productive tillers on average, they were also taller with thicker stems, more seeds per spike, and heavier seeds on average (Fig. 2-1C), indicating that productive tiller number is correlated with overall plant fitness.

Rainfall and accumulated growing degree days (GDD) across the growing season were compared to examine which differed most between the three years and if it was likely that they influenced tillering and other traits. Low tiller number and the delay in tillering that occurred in 2014 were likely due to heavy rainfall (4.4 cm) that occurred one day after emergence and flooded the field (see * in Fig. S2-1). Lower productive tiller number in 2016 compared to 2015 was likely caused by drought later in the growing season. After heavy rainfall (4.1 cm) that occurred one day after the 4WPE time point in 2016 (see † in Fig. S2-1), only 0.3 cm of additional rain fell for the remainder of the growing season. Compared to 2014 and 2016, rainfall was steady across the growing season in 2015 with no particularly heavy rainfalls. Heat accumulation, assessed by GDD, did not appear to have any major effects on tillering. For the first 15 days after planting, accumulated GDD was very similar in all three years, but then GDD accumulated more rapidly in 2014 and 2016 than in 2015 (Fig. S2-1), indicating that the 2015 growing season was slightly cooler overall than 2014 and 2016 growing seasons.

Though the warmer growing season did not appear to negatively affect maximum tiller number in 2016, it is likely that it, coupled with drought in 2016, had an impact on tiller survival, as a lower percentage of tillers were productive in 2016 compared to 2015.

Pleiotropic effects of photoperiod response and spike morphology on tillering

Consistent with previous studies (Alqudah et al., 2016; Liller et al., 2015; Turner et al., 2005), our results support that spike row-type and photoperiod response have pleiotropic influences on tiller number. However, previous studies have not characterized the timing and extent that these traits influence tillering throughout development or in different environments, nor have they assessed the synergistic effects of both traits on tiller number. To gain a better understanding of these relationships, we examined tillering and other traits in 761 lines grown in both 2014 and 2015 that were split into groups based on spike row-type or *PPD -H1* genotype.

In earlier studies, variation in *PPD-H1* was shown to influence days to heading, tiller number, and tillering duration (Alqudah et al., 2016; Turner et al., 2005). One SNP included in this study, BK_14, is 308 bp upstream of and has been previously shown to be in complete or near-complete LD with SNP22, the likely causal variant underlying photoperiod sensitivity differences (Digel et al., 2016; Turner et al., 2005). Furthermore, LD analysis indicated that all SNPs in the Ppd-H1 gene and several that flanked it were in high LD (Fig. S2-2). Therefore, BK_14 was used to distinguish lines as having the photoperiod sensitive *Ppd-H1* (G) allele or the photoperiod insensitive *ppd-H1* (A) allele. Of the 761 lines grown in 2014 and 2015, 325 and 436 carried the *Ppd-H1* and *ppd-H1* alleles, respectively. As expected, average days to heading was significantly later in *ppd-*

H1 lines than *Ppd-H1* lines in both years (Fig. S2-4), and tiller number and tillering rate were also significantly higher in *ppd-H1* lines than *Ppd-H1* lines (Fig. 2-2A; Table 2-1).

Like photoperiod response, spike row-type has been shown to pleiotropically influence tiller number as well as other traits like seed number and weight and leaf area (Alqudah and Schnurbusch, 2014, 2015; Liller et al., 2015). Of the 761 lines grown in 2014 and 2015, 382 were 2-rows and 379 were 6-rows. As expected, average tiller number was higher in 2-rows than 6-rows in 2014 and 2015 (Fig. 2-2A; Table 2-1). Duration of tiller development was also slightly longer for 2-rows than 6-rows in both years, and a lower percentage of all tillers were productive in 6-rows compared to two rows in both years (Fig. S2-4). As expected, 2-rows also had longer spikes with fewer, heavier seeds and narrower leaves than 6-rows (Fig. S2-4). Two-rows also had thinner stems than 6-rows on average (Fig. S2-4), which has not been previously reported.

Because tillering is influenced by both photoperiod sensitivity and spike row-type, it is likely that they have additive effects on tiller number, so the 761 lines grown in 2014 and 2015 were grouped as follows based on both spike row-type and *PPD-H1* genotype to assess these effects: 2-row/*Ppd-H1* (96 lines), 2-row/*ppd-H1* (286 lines), 6-row/*Ppd-H1* (229 lines), and 6-Row/*ppd-H1* (150 lines). As expected, 2-row/ppd-H1 lines had the highest average tiller number in both years, but, unexpectedly, lines with the lowest average tiller number were not 6-row/*Ppd-H1* (Fig. 2-2B). In 2014 and 2015, average tiller number in 6-rows with different *Ppd-H1* alleles was not significantly different, indicating that *Ppd-H1* has very little effect in a 6-row background (Fig. 2-2B).

After seeing that *Ppd-H1* genotype appeared to have little association with tiller number in 6-rows, we were interested in determining whether photoperiod sensitivity in general was associated with tiller number in 6-rows. To assess this, we developed multiple linear regression (MLR) models with tiller number as the response variable and other traits as predictor variables to see whether days to heading, which is influenced by photoperiod sensitivity, explained a significant proportion of variance in tiller number. Interestingly, days to heading explained a larger proportion of variance in maximum tiller number for 6-rows than 2-rows in 2014 and 2015 (Fig. 2-2C), suggesting that photoperiod response regulators besides *PPD-H1* influence tiller number in 6-rows.

Trait correlations and MLR models of tiller number supported that tiller development is influenced by photoperiod sensitivity, but it was also apparent that this effect varied by environment (year). Days to heading and *PPD-H1* genotype were both positively correlated with maximum tiller number and tillering rate in all years (Table 2-2), and MLR models showed that days to heading explained a similar proportion of variance (~20%) in maximum tiller number in 2014 and 2015 (Fig. 2-2D). On the other hand, productive tiller number showed a very different trend between 2014 and the other two years. In 2014, productive tiller number was positively correlated with heading, more strongly than with any other trait (Table 2-2). However, in 2015 and 2016, heading and productive tiller number were not significantly correlated in any line subset (Table 2-2). Furthermore, while days to heading explained the most variance (23.2%) in the MLR model for productive tiller number in all lines in 2014, it explained a very small

proportion of variance (1.4%) in the MLR model for productive tiller number in all lines in 2015 (Fig. 2-2D).

The relationship between days to heading and duration of tillering was also examined in the 54 lines grown in all three years. In all three years, the majority of lines did not develop additional tillers after days to heading was recorded; however a larger proportion of lines in 2015 (26.1%) than 2014 (12.2%) or 2016 (14.9%) developed additional tillers after heading was recorded. This suggests that, although duration of tillering is impacted by days to heading, some lines can continue to produce tillers after heading, especially when environmental conditions are more ideal, as they were in 2015.

Trait correlations and MLR models also showed that spike row-type was associated with tillering, but like photoperiod sensitivity, its association varied by environment. Correlations between spike row-type and tiller number were consistently negative (2-rows have more tillers than 6-rows) and were stronger for productive tiller number than for maximum tiller number in all years. However, correlations between spike row type and tiller number were very weak in 2014 compared to 2015 and 2016 (Table 2-2). Tiller number MLR models showed similar results as trait correlations. Seeds per spike, which is inherently different between 2-rows and 6-rows, explained a significant proportion of variance in MLR models of maximum and productive tiller number in all lines in 2015 but not 2014 (Fig. 2-2D). Seeds per spike did not explain a significant proportion of variance in any tiller number models for 2-rows or 6-rows, indicating that spike row-type, but not seeds per spike in general, is related to tiller number.

Trade-offs between tillering and other traits

Tiller number and other traits were compared in this study to identify potential trade-offs associated with higher tiller number. Because spike row-type pleiotropically influences tiller number and other traits, trade-offs were assessed separately in 2-row and 6-row subsets. They were also assessed using 2015 data only because additional traits were measured in 2015 (leaf width and lodging) and tiller development did not appear to be limited by overall plant fitness as in 2014. We found some evidence of minor trade-offs between tiller number and other vegetative traits. Leaf width and stem diameter were both weakly negatively correlated with productive tiller number in 2-rows and 6-rows (Table S2-7), and they also explained a significant proportion of variance and were negatively correlated in tiller number models (Fig. 2-3A).

We considered the possibility that larger trade-offs or trade-offs that were not detected by correlations or MLR modeling could be detected by comparing traits in lines with very different tillering capacities. Therefore, 2-rows and 6-rows were split into 10th and 90th percentile groups based on maximum and productive tiller number (Fig. 2-3B). Despite at least 2.5-fold or higher change in average tiller number between percentile groups (Fig. 2-3B), very few traits were significantly different between percentile groups. Stem diameter was lower in high tillering 6-rows (90th percentile, maximum and productive) than low tillering 6-rows (10th percentile, maximum and productive) but was not significantly different between high and low tillering 2-rows (Fig. 2-3C). Fifty kernel weight was also lower and lodging severity was more severe in high tillering 6-rows (90th percentile, maximum) than low tillering 6-rows (10th percentile, maximum), but they

were not significantly different between high and low tillering 2-rows (Fig. 2-3C). Interestingly, the trend in percent productive tillers between percentiles based on maximum tiller number was reversed in percentiles based on productive tiller number (Fig. 2-3D). This suggests that tiller survival had a major impact on final productive tiller number in 2015 and that variation in tiller survival prevents trade-offs between tiller number and other traits. Overall, our results suggest that trade-offs between tiller number and other traits were very minor and were slightly more pronounced in 6-rows than 2-rows, but, in general, there were no major trade-offs between tiller number and other traits independent of spike row-type.

Natural genetic variation associated with tillering

Population structure and linkage disequilibrium (LD) decay were characterized in all lines in the diversity panel prior to association mapping. As with the entire NSGC collection, population structure analysis of all lines in the diversity panel using STRUCTURE resulted in five subpopulations distinguished primarily by spike row-type, collection location, and improvement status (Fig. S2-5 and Table S2-1), and corresponding to those described in Muñoz et al. (2014). Analysis of LD decay for individual chromosomes indicated that it decayed over a fairly small genetic distance in the diversity panel, less than 1 cM for all chromosomes (Table S2-9). For genome-wide association mapping, a genetic distance of +/- 2 cM was chosen as a cutoff for including significant SNPs in the same quantitative trait loci (QTL) to account for regions with higher LD, such as around *Ppd-H1* (Fig. S2-2).

Genome-wide association mapping was performed using 2014 and 2015 raw or adjusted (if applicable based on Table S2-3) phenotypic data for all tillering traits, days to heading, spike row-type, seeds per spike, spike length, spike density, fifty kernel weight, leaf width (2015 only), stem diameter, plant height, and lodging (2015 only). Tillering QTL included SNPs significantly associated with tiller number, rate of tillering, and tillering principal components (PCs). Tiller number included 2-7WPE, productive, maximum, and non-productive tiller number (number of tillers that did not form spikes). Tillering rate included differences in tiller number between two consecutive weeks, slope in tiller number across at least three weeks, and a trait called tillering rate, which was calculated by dividing maximum tiller number by the week at which maximum tiller number occurred. Principal components analysis (PCA) was based on 2-7WPE and productive tiller number.

Very few tillering QTL were identified in both years. Out of 37 QTL associated with tillering traits in 2014 and 2015, (Table 2-3), only four were identified in both years, one on 2H at 56.82-58.76 cM (2H-58), one on 5H at 47.89-48.10 cM (5H-48), and two on 7H at 31-33.67 cM (7H-33) and 70.16-70.54 cM (7H-70) (Table 2-3, Fig. 2-4). In addition to there being little overlap between the two years, the QTL that were most significant and associated with the most traits in each year were not detected in both years, one on 2H at 13.72 – 23.24 cM (2H-19) in 2014 and one on 3H at 35.39 cM (3H-135) in 2015. The 2H-19 QTL overlapped the *PPD-H1* locus and was associated with tiller number, tillering rate, and tillering PC1 in all lines and with tiller number and tillering rate in 2-row lines (Table 2-3, Fig. S2-6). For many tillering traits in 2014, 2H-

19 was the only QTL identified (Fig. S2-6, Table S2-11), and the allelic effect size for tiller number ranged from 1.1-1.5 tillers. The 3H-135 QTL was associated with tiller number, tillering rate, and tillering PC1 in all lines and *Ppd-H1* lines and with tiller number and tillering rate in 6-rows (Table 2-3, Fig. S2-6). For many tillering traits in 2015, 3H-135 was the only QTL identified, and the allelic effect size for tiller number ranged from 1.5-4 tillers (Fig. S2-6, Table S2-11).

Measuring tiller number throughout development provided opportunities to identify QTL associated with other tillering traits besides tiller number, such as tillering rate, and to compare the number of QTL associated with tillering at different time points. Fourteen out of 23 tillering QTL in 2014 and six out of 14 tillering QTL in 2015 were only associated with tillering rate (Table 2-3). No QTL were associated with tiller number at the earliest time point, 2WPE, in either year; and no QTL were associated with the three earliest points, 2-4 WPE, in 2014 (Fig. S2-6), possibly due to low phenotypic variance (Table 2-1). Tiller number at later time points (5-7WPE, maximum, and productive) was associated with more QTL than at earlier time points (Fig. S2-6).

Including groups based on *PPD-H1* genotype and spike row-type allowed us to detect QTL that were not detected in all lines, especially in 2014, and observe that there was virtually no overlap in QTL detected in 2-rows and 6-rows or *Ppd-H1* and *ppd-H1* lines. In 2014, only four out of the 23 QTL associated with tillering were uniquely identified in all lines, whereas ten unique tillering QTL were identified in *ppd-H1* lines (Table 2-3). Two QTL were uniquely identified in 2-rows and one was uniquely identified in 6-rows in 2014 (Table 2-3). No unique QTL were identified in *Ppd-H1* lines

in 2014 (Table 2-3). In 2015, more QTL were identified in all lines than in any other group; however, including the *Ppd-H1* group enabled identification of three unique QTL (Table 2-3). No QTL were associated with tillering in 2-rows in 2015, and no uniquely identified QTL were associated with tillering in 6-rows in 2015. In addition to identifying unique QTL in each year, including groups based on spike row-type and *Ppd-H1* genotype, also enabled detection of three of the four QTL that were associated with tillering in both years. Only one of the four tillering QTL identified in both years, 2H-58, was identified in all lines in both years (Table 2-3, Fig. 2-4).

Overlap of natural genetic variation associated with tillering and other traits

Because tiller number was correlated with days to heading and spike row-type (row-type), we expected to see some overlap between tillering QTL and QTL associated with heading and row-type. In 2014, nine of 23 tillering QTL were also associated with row-type and/or heading in the same year, and in 2015, seven out of 14 tillering QTL were also associated with row-type and/or heading in the same year (Fig. 2-4). A single tillering QTL, 2H-58, which was the only one associated with tillering in all lines in both years, was the only one associated with heading and row-type in both years as well (Fig. 2-4A). In 2014 and 2015, five tillering QTL overlapped heading within each year (Fig. 2-4B). However, if all QTL associated with heading regardless of year were considered, overlap between tillering QTL and heading QTL, especially in 2014, was more extensive. Incidentally, there was very little overlap between row-type QTL and heading QTL in either year (Fig. 2-4B).

Overlap between tillering QTL and QTL associated with other traits besides row-type and heading were examined as well. A few tillering QTL overlapped QTL associated with spike density and/or seeds per spike that were not associated with spike row-type. For example, two tillering QTL on 3H at 104.41 and 108.74 cM that were detected in ppd-H1 lines in 2014 overlapped QTL associated with spike density or seeds per spike but not spike row-type. In one instance, a tillering QTL on 4H at 115.23 – 116.20 cM identified in all lines and *ppd-H1* lines in 2014 overlapped a QTL associated with leaf width in *ppd-H1* lines in 2015, but it also overlapped a QTL for row-type, which is correlated with leaf width as well as tiller number. No QTL were identified for stem diameter or plant height in 2014 or 2015 in any line subsets.

Discussion

Results of this study agreed with results from earlier studies suggesting that environment and pleiotropic effects of photoperiod sensitivity and spike row-type influence tiller number. In addition, we showed that environment appeared to influence productive tiller number, but not necessarily tiller number earlier in development. Though results supported that tiller number is influenced by pleiotropic effects of photoperiod sensitivity and spike row-type, we also observed that this effect varied by year and genetic background. Trade-offs between tiller number and other traits were assessed, and we found evidence of minor trade-offs, mainly between tiller number and other aspects of vegetative growth, that were slightly more pronounced in 6-rows than 2-rows. Finally, we identified natural genetic variation associated with tillering in 2014 and 2015, and though tillering QTL overlapped QTL associated with days to heading and

spike row-type rather extensively, there was little overlap between tillering QTL in the two years.

Environment had a large effect on tillering and associated genetic variation

The effect of year on tillering capacity was proportionately higher than pleiotropic effects of spike row-type or *PPD-H1* genotype within the same year. Lower heritability estimates for productive tiller number and weak correlations between heading and productive tiller number in 2015 indicated that productive tiller number was more strongly influenced by environment than maximum tiller number. Nice and coauthors (2017) showed that the heritability estimate for productive tiller number was very low ($H^2 = 0.11$) in an advanced backcross–nested association mapping population grown in five field environments, compared to estimates for other traits. On the other hand, heritability estimates in this study based on 2016 replicates for all tillering traits were high, especially for field-grown plants, and were similar to estimates for greenhouse-grown plants in Alqudah et al. (2016). This implies that tillering traits are genetically controlled but also strongly impacted by genotype by environment (GxE) interactions.

In addition to influencing tillering phenotypes, environment also affected identification of natural genetic variation associated with tillering. Out of 33 tillering QTL detected in 2014 and 2015, only four were detected in both years, and all four accounted for a small proportion of variance in tillering traits. In contrast, QTL that were associated with more heritable traits such as days to heading and spike density and that explained the highest proportions of variance were detected in both years. For example, QTL overlapping genes previously shown to influence heading, such as *PPD-H1* and

HvCEN, and QTL overlapping genes previously shown to influence spike density, such as *Vrs1* and *Int-C*, were detected in both years. These results suggest that growing the same accessions in different environments will be essential to further our understanding of the genetic architecture underlying tillering.

Tillering capacity is influenced by many different environmental factors, so consideration of specific environmental variables throughout a growing season will help to further our understanding of how different genotypes respond to specific stresses. In a study by Aspinall et al. (1964), barley plants that received repeated drought treatments produced fewer tillers than controls, while plants that received a single long drought treatment produced more tillers than controls. Moreover, the effect of drought treatments on tillering capacity depended on the timing and length of the drought periods. Experiments like this emphasize the need for measuring tiller number in multiple environments, as the same type of stress can have opposing effects on tiller number depending on when and how often it occurs during development. Understanding the unique environmental conditions of each growing environment could also facilitate selection of accessions that are better adapted to specific environments or that respond better to specific stresses. For example, one accession, PI357314, was very similar in 2014 and 2015 in terms of productive tiller number, seeds per spike, and 50-kernel weight. Unlike most accessions grown in 2014, fitness of this accession did not appear to be impacted by waterlogging, so it is possible that it is more resistant to this stress than most accessions.

Correlations between tiller number and spike row-type and photoperiod sensitivity varied by environment and genetic background

Consistent with other studies, we found that 2-rows produced more tillers than 6-rows and lines containing *ppd-H1* alleles produced more tillers than lines containing *Ppd-H1* alleles, but we also observed that these correlations depended on environment and genetic background (Alqudah and Schnurbusch, 2014; Alqudah et al., 2016; Liller et al., 2015; Turner et al., 2005). For example, we found *PPD-H1* genotype did not appear to have much influence on tiller number in 6-rows, and a QTL overlapping the *PPD-H1* locus was not associated with tiller number in 6-rows as in 2-rows and all lines. It also appeared that *PPD-H1* allelic state influenced tiller number more in 2014 than 2015, while, conversely, spike row-type influenced tiller number more in 2015 than 2014. No QTL associated with tiller number in either year overlapped the *Vrs1* locus, despite significant differences between 2-rows and 6-rows in both years. This result was not surprising in 2014 when the difference in tiller number between spike row-types was small, but it was surprising in 2015, considering that 2-rows had 34% more productive tillers on average than 6-rows.

Tiller survival affects the number of grain bearing spikes and likely attenuates trade-offs between tiller number and other traits

We showed that productive tiller number followed the same trend across years as other traits relating to plant fitness, like seeds per spike, kernel weight, and vegetative biomass (plant height and stem diameter). Tiller number in 2015 and 2016 was very similar until the 5WPE time point, but productive tiller number was lower in 2016 due to

decreased tiller survival, as were other traits relating to plant fitness, indicating that tiller survival was influenced by overall plant fitness. Trade-offs between tiller number and other vegetative traits were very minor in 2015 when plants made many tillers. Even when comparing groups of lines with very different tillering capacities, there was little evidence of trade-offs, but they did appear to be slightly more pronounced in 6-rows.

Because there was little evidence of trade-offs and productive tiller number followed the same trend as other traits, it is likely that tiller survival prevented major trade-offs from occurring. Few studies have described trade-offs between tiller number and other traits in barley or other small grain crops, and results have been inconsistent. For example, Kebrom et al. (2012) reported that removing tillers in wheat could induce development of larger spikes with more seeds. However, results from another study that examined yield and yield-related traits in barley under different seeding densities over two years indicated that there was no trade-off between tillers per plant and seeds per spike (Stoskopf and Reinbergs, 1966). They found that the seeding density at which seeds per spike was highest was the same density at which productive tiller number per plant was highest. Furthermore, when they compared 20 high-yielding lines and 20 low-yielding lines, they found that average seeds per spike was higher in high-yielding lines but that average tiller number was not different.

It is likely that lower tiller number in 6-rows than 2-rows is due to a trade-off with seeds per spike, which is inherently higher in 6-rows. However, there was no evidence that more seeds per spike within 2-rows or 6-rows was associated with lower tiller number. Within 2-rows or 6-rows, the number of seeds per spike is influenced by

pollination and seed filling, which typically occurs near the end of tillering or after tillering has completed (Alqudah and Schnurbusch, 2014; Digel et al., 2015; Waddington et al., 1983). The difference in seeds per spike between 2-rows and 6-rows, on the other hand, is due to lateral floret fertility, which is determined earlier in development when plants are actively tillering. *VRS1*, which encodes an inhibitor of lateral floret fertility, is strongly expressed in lateral florets at glume primordia stage, which occurs at the five-leaf stage approximately three to four weeks after emergence (Bonnett; Sakuma et al., 2017; Waddington et al., 1983). Overall, results from this study indicated that trade-offs between tiller number and seeds per spike probably only exist if the difference in seeds per spike is due to floret fertility and not pollination or seed filling.

Natural genetic variation associated with tillering was shaped by many factors

All four of the tillering QTL identified in 2014 and 2015 overlapped genes that have been previously shown to influence heading in barley (*HvCEN*, *ELF4*, *VRN-H3*, and *LHY*), and all of them were also associated with heading (Fig. 2-4). Interestingly, three of the four QTL that were identified in both years in this study were also identified in a study by Alqudah et al. (2016) (2H 56.82-58.71 cM, 5H 47.89-48.10 cM, and 70.16-70.54 cM), which also measured tiller number throughout development. In total, ten of the 33 tillering QTL identified in this study were also identified in the Alqudah et al. study, suggesting that some natural genetic variation consistently influences tillering under different environments. Measuring tiller number throughout development allowed us to identify more QTL than if we had only measured productive tiller number, and having numerous tiller number measurements throughout development enabled us to

include tillering rate in our association study, which facilitated identification of more tillering QTL than tiller number alone. Moreover, none of the four tillering QTL that were identified in both 2014 and 2015 would have been identified if tillering rate metrics were not included in this study (Table 2-3).

The 3H-135 QTL that explained the most variance in tillering and was associated with the most tillering traits in 2015 was not detected in 2014. Alqudah et al. (2016) identified a QTL at 137.71 cM, but it is unlikely that it is the same QTL, as LD in this region is very low (Fig. S2-8). A QTL spanning both 3H-135 and the QTL at 137.71 (122.78-154.68 cM based on POPSEQ map) was associated with productive tiller number in a study by Honsdorf et al. (2014). Due to extremely low LD surrounding 3H-135, it is unlikely that the tillering gene *CUL4*, which is also at 137.71 cM, is a candidate gene for this region, because LD decays below background levels between 3H-135 and *CUL4* (Fig. S2-8). The 3H-135 QTL was identified 34 times for different tillering traits or subsets of lines, but it was not identified in 2-rows due to very low minor allele frequency (0.013). A single GBS SNP, S3H_666048593, was associated in 31 instances, and for three tillering traits in all lines, a second GBS SNP, S3H_667646315 (also at 135.39 cM), was also associated. Although S3H_667646315 was in higher LD with S3H_666048593 than any other SNP, LD between the two was fairly low ($R^2 = 0.29$). Therefore, it is likely that candidate genes for 3H-135 are near S3H_666048593. The nearest gene to S3H_666048593 is HORVU3Hr1G103960, which encodes an epoxide hydrolase that is more highly expressed in developing tillers than any other tissues (based on expression data from Barlex, barlex.barleysequence.org). Another potential candidate gene is

homologous to *PLASTOCHRON3*/*GOLIATH*, which encodes a glutamate carboxypeptidase that regulates plastochron length (rate of leaf initiation) in rice (Kawakatsu et al., 2009).

Tillering is a complex trait influenced by environment, pleiotropic effects of other traits, and many loci that explain a small proportion of the genetic variance. Based on results of this study, it appeared that plants utilized resources and made more grain bearing spikes when conditions were favorable, without sacrificing other components of yield, like seed number or weight. Results from this study and others also indicate that genetic variation associated with days to heading and spike row-type consistently influences tiller number across different environments. However, identifying genetic variation associated with tiller number in different environments will be essential for gaining a full understanding of the genetic control of tiller development and may be useful for identifying variation suited for adaptation to specific environments.

Acknowledgements

The authors would like to thank Professors Rex Bernardo and Candice Hirsch for assistance with analyses and technicians Shane Heinen, Edward Schiefelbein, and Guillermo Velasquez for assistance with planting. We would also like to thank former members of Professor Gary Muehlbauer's lab: Maria Muñoz-Amatriaín, for providing information about the USDA NSGCC, and Liana Nice, for helping with field design and analysis. We would like to acknowledge the Minnesota Supercomputing Institute (MSI) at the University of Minnesota (UMN) for computing resources

(https://www.msi.umn.edu). Finally, special thanks to former UMN undergraduate students working in the Muehlbauer lab who assisted with plant phenotyping: Allison Shaw, Adam Schrankler, Calandra Sagarsky, Praloy Carlson, Raone Soares Biancardi, Lothi Yamat, Jesus Gonzalez Langa, William Corcoran, Jennifer Nguyen, Amos Kidandaire, Sonya Yermishkin, and Colin Finnegan. This work was financially supported by the USDA-NIFA Triticeae Coordinated Agriculture Project (TCAP).

Table 2-1. Summary statistics for tillering traits measured in 2014 and 2015.

Trait	Lines	Number of Lines	Mean		Standard Deviation		p-value[1]	H^2
			2014	2015	2014	2015		
Tiller Number 2WPE	All	756	1.58	3.13	0.81	0.74	2.0E-09	0.35
	2-Row	375	1.84	3.38	0.83	0.76	0.032	0.17
	6-Row	381	1.31	2.88	0.70	0.62	3.7E-03	0.24
	Ppd-H1	324	1.40	3.03	0.74	0.67	7.1E-05	0.35
	ppd-H1	432	1.72	3.21	0.83	0.77	5.3E-05	0.31
Tiller Number 3WPE	All	756	3.39	8.00	1.63	2.26	6.4E-07	0.30
	2-Row	375	3.77	9.27	1.66	2.13	0.168	0.09
	6-Row	381	3.00	6.75	1.52	1.58	0.047	0.16
	Ppd-H1	324	3.06	7.44	1.56	1.93	6.3E-04	0.30
	ppd-H1	432	3.63	8.42	1.65	2.39	3.9E-03	0.23
Tiller Number 4WPE	All	756	5.66	12.98	2.33	3.58	6.2E-11	0.38
	2-Row	375	6.08	14.13	2.26	3.47	9.4E-04	0.28
	6-Row	381	5.24	11.85	2.34	3.33	2.7E-06	0.37
	Ppd-H1	324	5.17	12.40	2.26	3.46	1.1E-07	0.44
	ppd-H1	432	6.03	13.42	2.32	3.61	3.0E-04	0.28
Tiller Number 5WPE	All	756	7.11	19.27	2.98	6.28	3.0E-16	0.45
	2-Row	375	7.53	21.51	2.98	5.76	6.0E-06	0.37
	6-Row	381	6.68	17.06	2.92	5.98	1.8E-11	0.50
	Ppd-H1	324	6.39	17.75	2.88	6.10	2.3E-11	0.52
	ppd-H1	432	7.64	20.40	2.94	6.17	1.1E-05	0.34
Tiller Number 6WPE	All	756	7.21	19.97	3.28	6.73	4.4E-25	0.53
	2-Row	375	7.99	22.47	3.29	6.14	3.4E-08	0.43
	6-Row	381	6.45	17.51	3.10	6.38	1.3E-15	0.56
	Ppd-H1	324	6.16	18.22	3.03	6.40	4.1E-15	0.58
	ppd-H1	432	8.00	21.28	3.25	6.68	3.1E-09	0.43
Tiller Number 7WPE	All	756	6.72	18.98	3.31	6.54	2.1E-22	0.51
	2-Row	375	7.53	21.90	3.31	6.07	1.8E-06	0.38
	6-Row	381	5.92	16.11	3.11	5.67	3.7E-15	0.55
	Ppd-H1	324	5.60	17.13	3.03	5.87	5.4E-12	0.54
	ppd-H1	432	7.56	20.37	3.26	6.68	9.0E-09	0.42
Tiller Number Maximum	All	756	8.01	20.90	3.45	6.88	6.3E-22	0.50
	2-Row	375	8.69	23.44	3.42	6.22	1.2E-06	0.39
	6-Row	381	7.34	18.40	3.34	6.59	3.1E-15	0.56
	Ppd-H1	324	6.95	19.29	3.24	6.71	4.2E-14	0.57
	ppd-H1	432	8.81	22.11	3.38	6.76	1.5E-07	0.39
Tiller Number Productive	All	744	6.14	13.17	3.14	4.29	4.7E-13	0.41
	2-Row	372	6.96	15.43	3.14	4.13	4.3E-03	0.24
	6-Row	372	5.32	10.90	2.92	3.09	9.9E-05	0.32
	Ppd-H1	314	4.92	11.98	2.47	3.38	6.8E-05	0.35
	ppd-H1	430	7.04	14.04	3.27	4.66	3.4E-05	0.32

[1]p-values indicate significance of genetic variance based on 2-way ANOVA.

Table 2-2. Pearson's correlation coefficients for tillering traits versus other traits for lines grown in each year. Non-significant ($p>0.01$) are denoted by n.s.

Line Subset	Seeds per Spike			Spike Row Type			Fifty Kernel Weight			Days to Heading			Ppd-H1 Genotype			Plant Height			Stem Diameter	
	2014	2015	2016	2014	2015	2016	2014	2015	2016	2014	2015	2016	2014	2015	2016	2014	2015	2016	2014	2015
Maximum Tiller Number																				
All	n.s.	-0.32	-0.35	-0.18	-0.36	-0.37	n.s.	n.s.	n.s.	0.39	0.46	0.74	0.27	0.20	0.34	0.42	n.s.	n.s.	0.15	-0.30
2-Row	0.13	n.s.	n.s.	---	---	---	n.s.	-0.14	-0.64	0.27	0.42	0.80	0.33	0.26	0.69	0.42	n.s.	n.s.	0.22	n.s.
6-Row	n.s.	n.s.	n.s.	---	---	---	n.s.	-0.22	n.s.	0.48	0.52	0.68	n.s.	n.s.	n.s.	0.44	n.s.	n.s.	0.21	-0.21
Ppd-H1	0.15	n.s.	n.s.	n.s.	n.s.	n.s.	n.s.	n.s.	-0.52	0.43	0.49	0.55	---	---	---	0.39	n.s.	n.s.	n.s.	-0.26
ppd-H1	-0.15	-0.43	-0.68	-0.19	-0.46	-0.62	n.s.	0.14	n.s.	0.26	0.37	0.73	---	---	---	0.37	n.s.	n.s.	n.s.	-0.34
Productive Tiller Number																				
All	-0.14	-0.50	-0.45	-0.22	-0.52	-0.57	0.12	0.28	0.53	0.45	n.s.	n.s.	0.29	0.23	n.s.	0.37	n.s.	n.s.	n.s.	-0.38
2-Row	0.14	n.s.	n.s.	---	---	---	n.s.	n.s.	n.s.	0.28	n.s.	n.s.	0.32	0.16	n.s.	0.42	n.s.	n.s.	0.15	-0.15
6-Row	n.s.	n.s.	n.s.	---	---	---	n.s.	n.s.	n.s.	0.59	n.s.	n.s.	0.15	n.s.	n.s.	0.37	n.s.	n.s.	n.s.	-0.24
Ppd-H1	n.s.	-0.39	n.s.	n.s.	-0.42	n.s.	n.s.	0.15	0.57	0.51	n.s.	n.s.	---	---	---	0.32	n.s.	n.s.	n.s.	-0.34
ppd-H1	-0.19	-0.48	-0.55	-0.20	-0.52	-0.65	0.18	0.32	0.54	0.32	n.s.	n.s.	---	---	---	0.34	n.s.	n.s.	n.s.	-0.43
Percent Productive Tillers																				
All	-0.19	-0.17	n.s.	-0.21	-0.15	n.s.	0.19	0.23	0.50	0.27	-0.42	-0.77	0.15	n.s.	n.s.	0.10	n.s.	n.s.	n.s.	-0.12
2-Row	n.s.	-0.15	n.s.	---	---	---	0.19	0.21	0.77	n.s.	-0.44	-0.84	0.14	-0.18	-0.73	0.14	n.s.	n.s.	n.s.	n.s.
6-Row	n.s.	n.s.	n.s.	---	---	---	n.s.	0.16	n.s.	0.38	-0.44	-0.78	n.s.	n.s.	n.s.	n.s.	n.s.	n.s.	n.s.	n.s.
Ppd-H1	n.s.	-0.26	n.s.	n.s.	-0.25	-0.53	n.s.	0.21	0.69	0.24	-0.58	-0.80	---	---	---	n.s.	n.s.	n.s.	-0.19	n.s.
ppd-H1	-0.20	-0.13	n.s.	-0.21	n.s.	n.s.	0.27	0.26	n.s.	0.24	-0.33	-0.76	---	---	---	0.12	n.s.	n.s.	n.s.	-0.16
Tillering Rate: Maximum Tiller number / Tillering Duration (Weeks)																				
All	n.s.	-0.22	-0.34	n.s.	-0.28	-0.44	n.s.	n.s.	n.s.	0.20	0.50	0.67	0.19	0.16	0.37	0.44	n.s.	n.s.	0.24	-0.25
2-Row	0.14	n.s.	n.s.	---	---	---	n.s.	-0.16	-0.63	0.14	0.49	0.79	0.26	0.26	0.70	0.43	n.s.	n.s.	0.28	n.s.
6-Row	0.14	n.s.	n.s.	---	---	---	n.s.	-0.20	n.s.	0.25	0.53	0.52	n.s.	n.s.	n.s.	0.46	n.s.	n.s.	0.30	-0.21
Ppd-H1	0.17	n.s.	n.s.	n.s.	n.s.	n.s.	n.s.	n.s.	n.s.	0.23	0.56	0.58	---	---	---	0.42	n.s.	n.s.	0.25	-0.20
ppd-H1	n.s.	-0.35	-0.68	n.s.	-0.40	-0.71	n.s.	n.s.	n.s.	n.s.	0.41	0.60	---	---	---	0.41	n.s.	n.s.	0.19	-0.31

Table 2-3. Quantitative trait loci (QTL) associated with tillering in 2014 and 2015. Letters designate whether QTL were detected for tiller number (N), tillering rate (R), or tillering PCA (P). Descriptions of QTL that were detected in 2014 and 2015 are shaded.

Chrom	Position cM	Position Mb	Candidate Gene	2014 All	2014 2-Row	2014 6-Row	2014 Ppd-H1	2014 ppd-H1	2015 All	2015 2-Row	2015 6-Row	2015 Ppd-H1	2015 ppd-H1
1H	44.01	39306516	NA	---	---	---	---	N--	---	---	---	---	---
1H	80.27	492231577	NA	---	---	---	---	---	-R-	---	---	---	-R-
2H	8.1	14055173	NA	---	---	---	---	-R-	---	---	---	---	---
2H	13.72-23.24	18658962-31111153	*Ppd-H1*	NRP	NR-	---	---	---	---	---	---	---	---
2H	43.09	54263832	NA	N--	---	---	---	---	---	---	---	---	---
2H	47.46-51.59	70305728-94010493	*FT4*	---	---	---	---	---	NR-	---	---	---	-R-
2H	56.82-58.76	170753050-500471658	*CEN* or *AP1*	-R-	---	---	-R-	---	NR-	---	---	---	NR-
2H	67.75	631099978	*CO4*	---	---	---	---	---	-R-	---	---	---	---
2H	86.67	671627122-671718762	NA	---	---	---	---	---	---	---	---	NR-	---
2H	90.15	678954955	NA	---	---	-R-	---	---	---	---	---	---	---
2H	94.15	682607357	NA	---	-R-	---	---	---	---	---	---	---	---
2H	139.93	749156584	NA	---	---	---	---	-R-	---	---	---	---	---
3H	36.95	32875005	NA	---	---	---	---	-R-	---	---	---	---	---
3H	46.40-46.73	87626129-93522710	*FT2* or *GI*	---	---	---	---	---	-R-	---	---	---	---
3H	53.78	491541454	NA	-R-	---	---	-R-	---	---	---	---	---	---
3H	75.22	582897121	*FDL4*	---	---	---	---	---	NR-	---	---	---	---
3H	104.41	627260793-631633600	*GA20ox3*	---	---	---	---	-R-	---	---	---	---	---
3H	108.74	633415954	*sdw1*	---	---	---	---	-R-	---	---	---	---	---
3H	135.39	666048593-667646315	NA	---	---	---	---	---	NPR	---	NR-	NPR	---
4H	26.04	10017450	NA	N--	---	N--	---	---	---	---	---	---	---
4H	51.53	421390780-422326469	*PRR59, FDL5,* or *FKF1*	N--	---	---	---	---	---	---	---	---	---
4H	115.23-116.20	640426479-641157608	*FT5*	-R-	---	---	---	NR-	---	---	---	---	---
5H	0.32	1131874	NA	---	---	---	---	---	N--	---	---	---	---
5H	32.04	23902955	NA	N--	---	---	---	---	---	---	---	---	---
5H	38.45	29447751	NA	---	---	---	---	---	---	---	---	-R-	---
5H	47.89-48.10	405622321-437381309	*ELF4*	---	---	---	---	-R-	-R-	---	---	---	---
5H	139.63	624883939	NA	N--	---	---	---	---	---	---	---	---	---
5H	148.01	635782594	NA	---	---	---	---	---	---	---	---	N--	---
6H	63.46	469166692	NA	---	---	---	---	-R-	---	---	---	---	---
7H	8.76	11333756-11334135	*Brh1* or *Grd5*	---	---	---	---	NR-	---	---	---	---	---
7H	31.00-33.67	37988653-42121652	*Vrn-H3*	---	-R-	---	---	-R-	-R-	---	---	---	---
7H	38.50-38.96	43145614-45702908	NA	---	---	---	---	-R-	---	---	---	---	---
7H	70.16-70.54	196348803-285713945	*LHY*	---	-R-	---	---	---	-R-	---	---	---	---

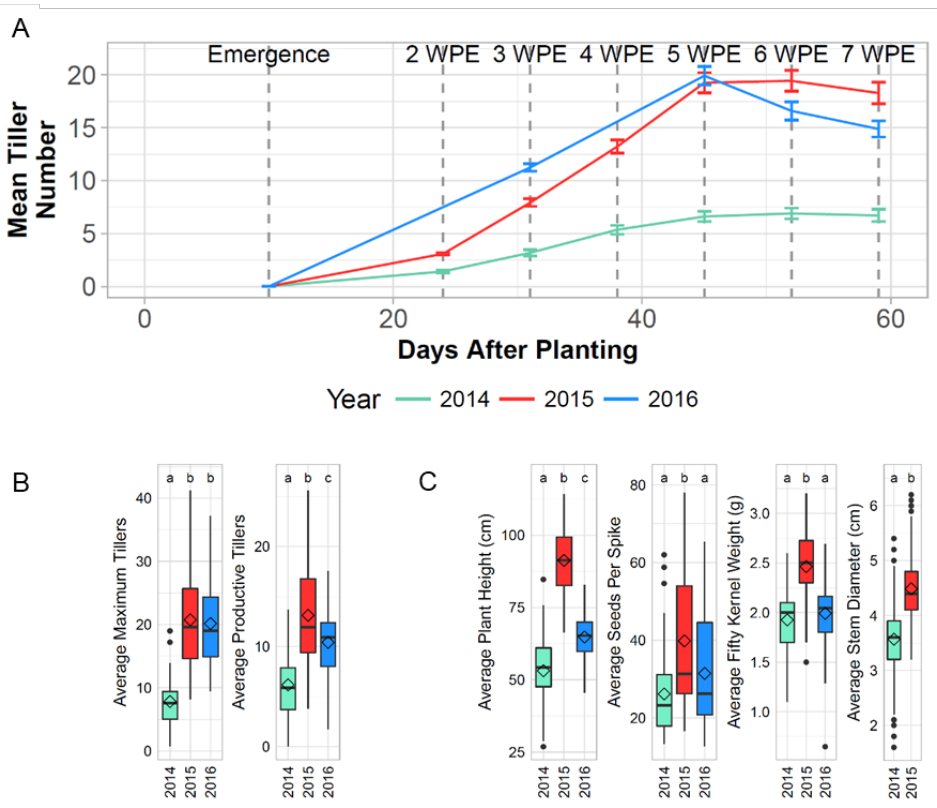

Figure 2-1. Tiller development (tillering) and other traits varied similarly by environment. A) Progression of average tiller number throughout the growing season for 54 lines grown in 2014, 2015, and 2016. B) Box plots summarizing maximum and productive tiller number for 54 lines grown in all three years. Diamonds represent mean trait values, and letters indicate whether groups are significantly different (Tukey Test, FDR-adjusted p-value < 0.01). C) Box plots summarizing non-tillering traits show that they follow the same trend as productive tiller number across the three years.

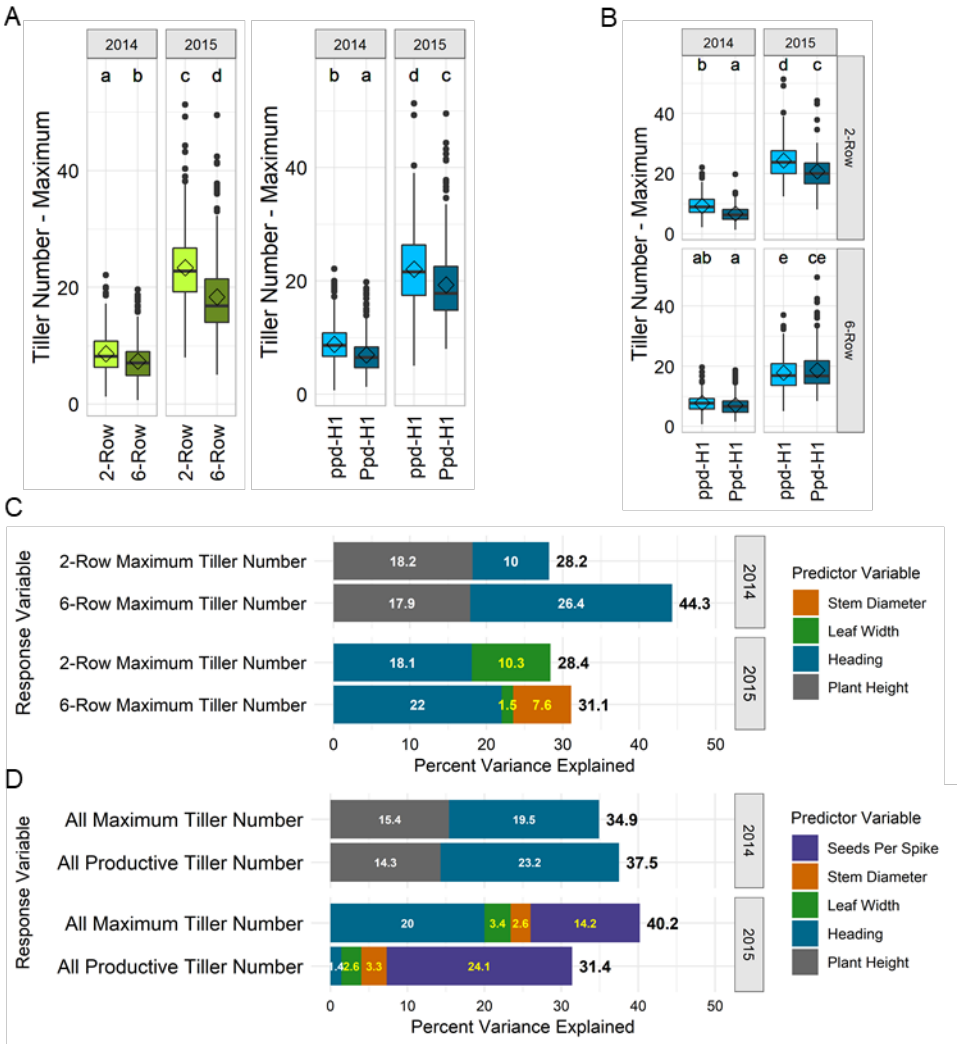

Figure 2-2. Correlation of tiller number and spike row-type and photoperiod sensitivity varied by environment and genetic background. A) Box plots comparing maximum tiller number between 2-rows (n = 382) and 6-rows (n = 379) and between lines containing *Ppd-H1* (n = 325) and *ppd-H1* (n= 436) alleles in 2014 and 2015. Diamonds represent mean trait values, and letters indicate whether groups were significantly different (Tukey Test, FDR-adjusted p-value < 0.01). B) Box plots comparing maximum tiller number between 2-rows containing either *Ppd-H1* (n=96) or *ppd-H1* (n=286) alleles and between 6-rows containing either *Ppd-H1* (n=229) or *ppd-H1* (n=150) alleles. C) Percent variance explained by predictor variables in multiple linear regression models of maximum tiller number in 2-rows and 6-rows in 2014 and 2015. Days to heading explained a larger proportion of variance in 6-rows than 2-rows in both years. D) Percent variance explained by predictor variables in models of maximum and productive tiller number in all lines in 2014 and 2015. Seeds per spike explained a significant proportion of variance in tiller number in 2015 but not 2014, and days to heading explained a large proportion of variance in productive tiller number in 2014 but not 2015.

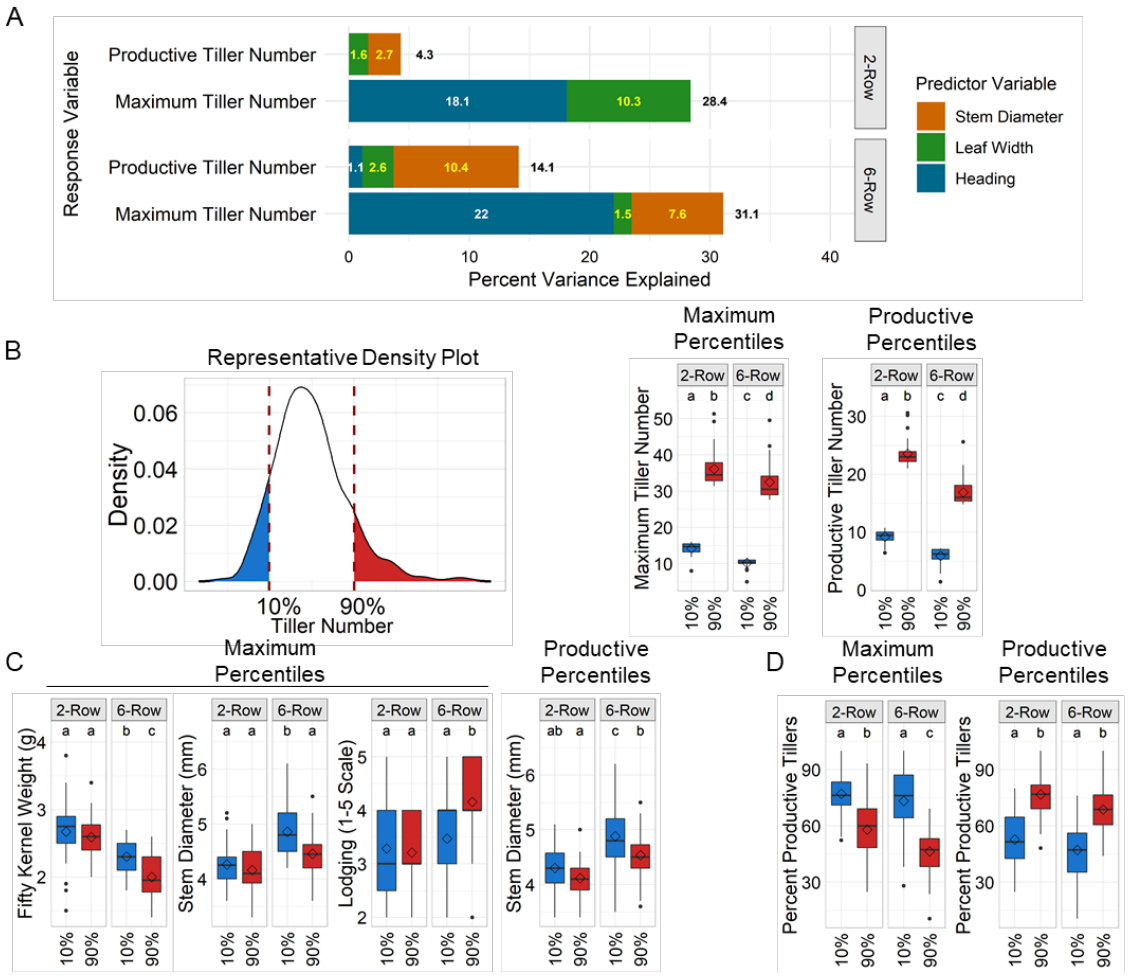

Figure 2-3. Minor trade-offs between tiller number and other traits in 2015. A) Percent variance explained by predictor variables in multiple linear regression models of maximum tiller number in 2-rows and 6-rows in 2015. Vegetative traits, stem diameter and leaf width, explained a significant proportion of variance in all models (ANOVA, p-value < 0.01). B) Representative density plot on left illustrates assignment of 2-row and 6-row lines into percentile groups based on maximum and productive tiller number. Box plots comparing tiller number in percentile groups based on maximum and productive tiller number. Diamonds represent mean trait values, and letters indicate whether groups were significantly different (Tukey Test, FDR-adjusted p-value < 0.01). C) Box plots showing traits that were significantly different between percentile groups based on maximum and productive tiller number. D) Box plots of percent productive tillers (percentage of tillers that survive and form grain-bearing spikes) shows that the trend in tiller survival is opposite in percentiles based on maximum and productive tiller number.

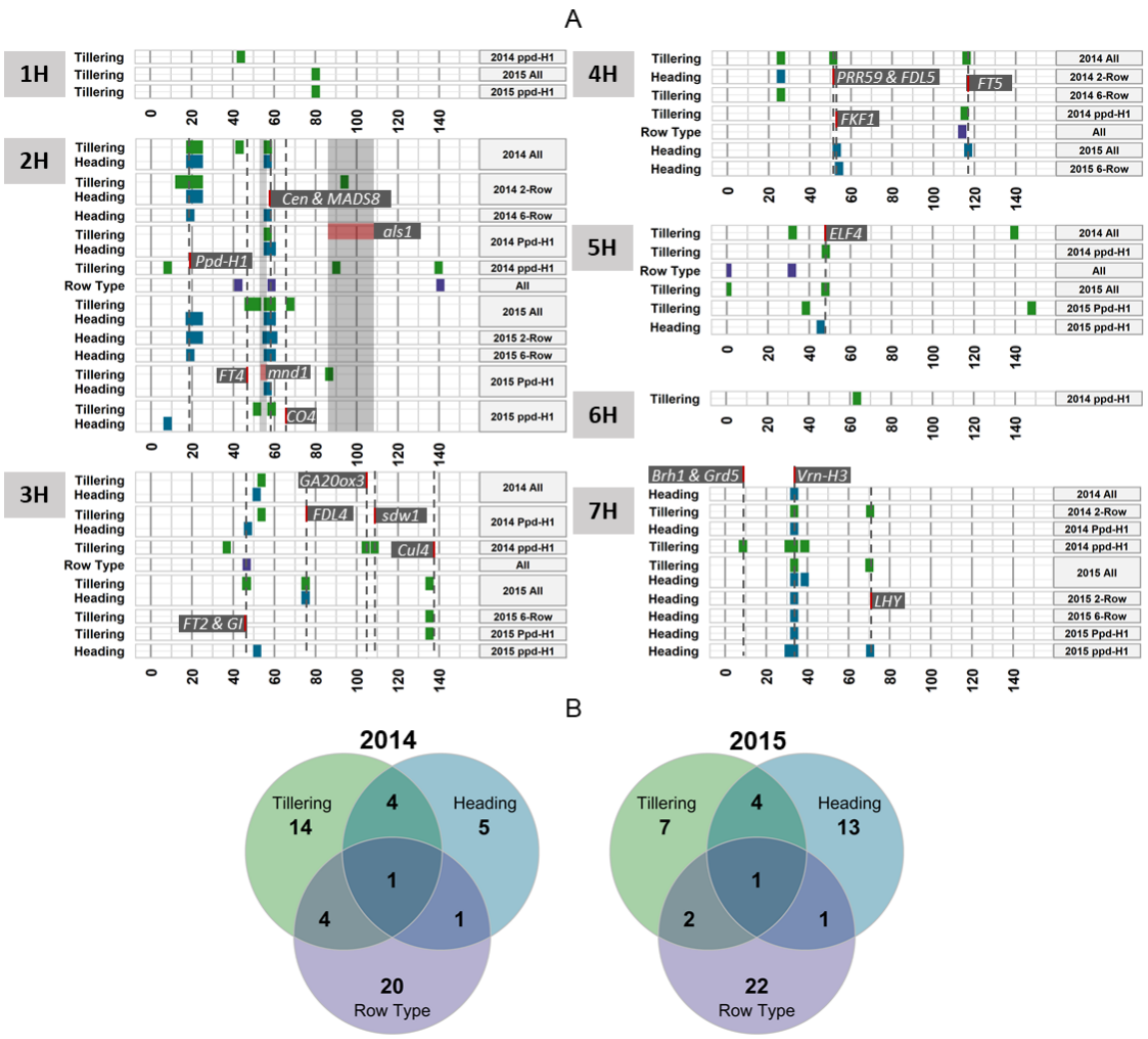

Figure 2-4. Overlap of quantitative trait loci (QTL) associated with tiller development (tillering) and other traits in two years. (A) Bars show genetic positions of significant SNPs (+/- 2 cM) associated with tillering, days to heading, and spike row-type. Gray dotted lines and gray shaded regions show positions of genes and mutant introgressions previously implicated in control of heading time, inflorescence morphology, or tiller number (Summarized in Table 1-1). Only heading and row-type QTL that overlap tillering QTL are shown. (B) Venn diagrams showing the number of QTL that overlapped for tillering, heading, and spike row-type in 2014 and 2015.

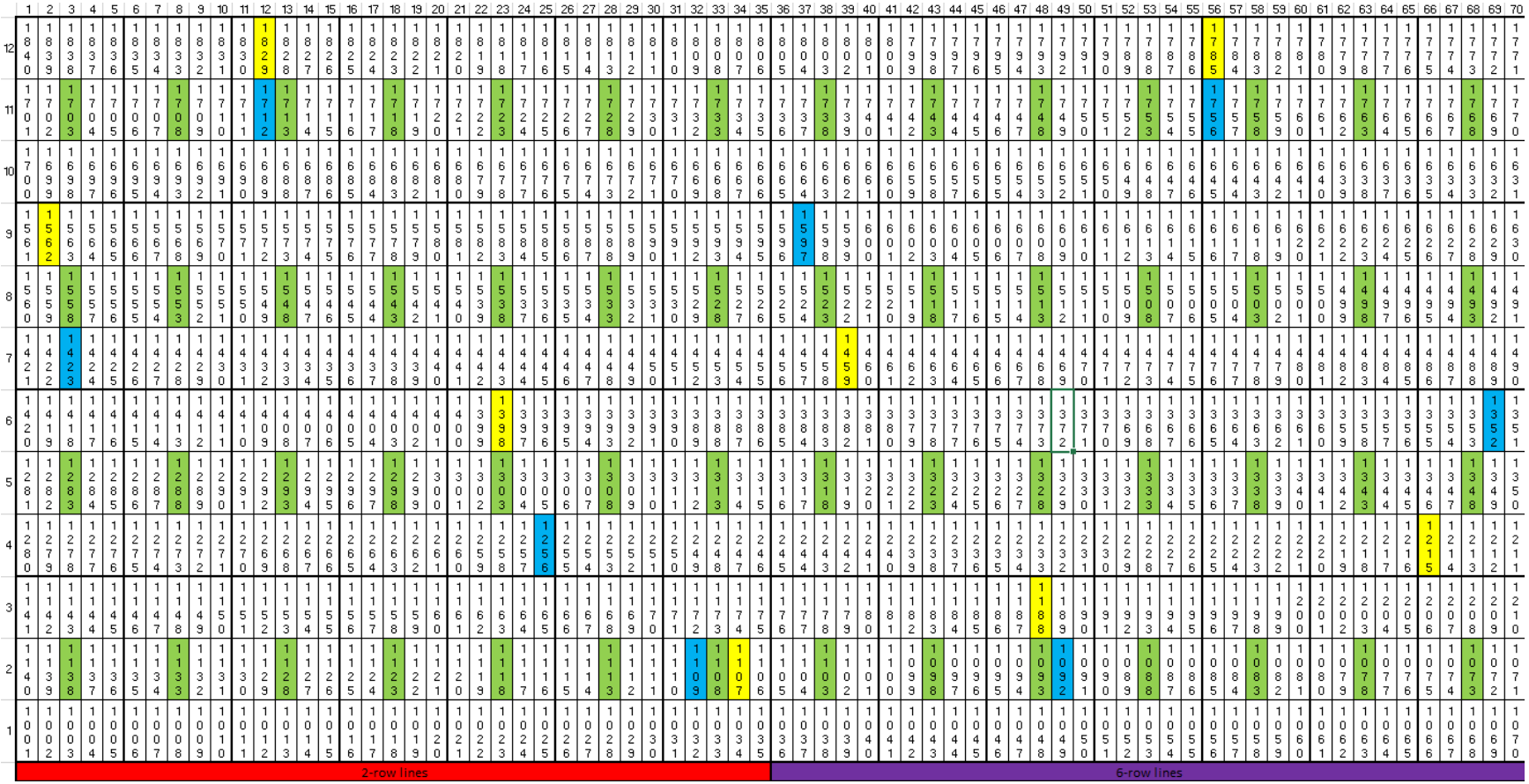

Supplementary Figure 2-1. Type 2 Modified Augmented Design – 2014 and 2015. Fields contained 56 blocks (outlined with thick, black lines), each containing a single primary check (green plots - Conlon for 2-row lines and Rasmussen for 6-row lines) and some containing two secondary checks as well (blue and yellow plots). Each white plot contained a unique accession from Table S2-1.

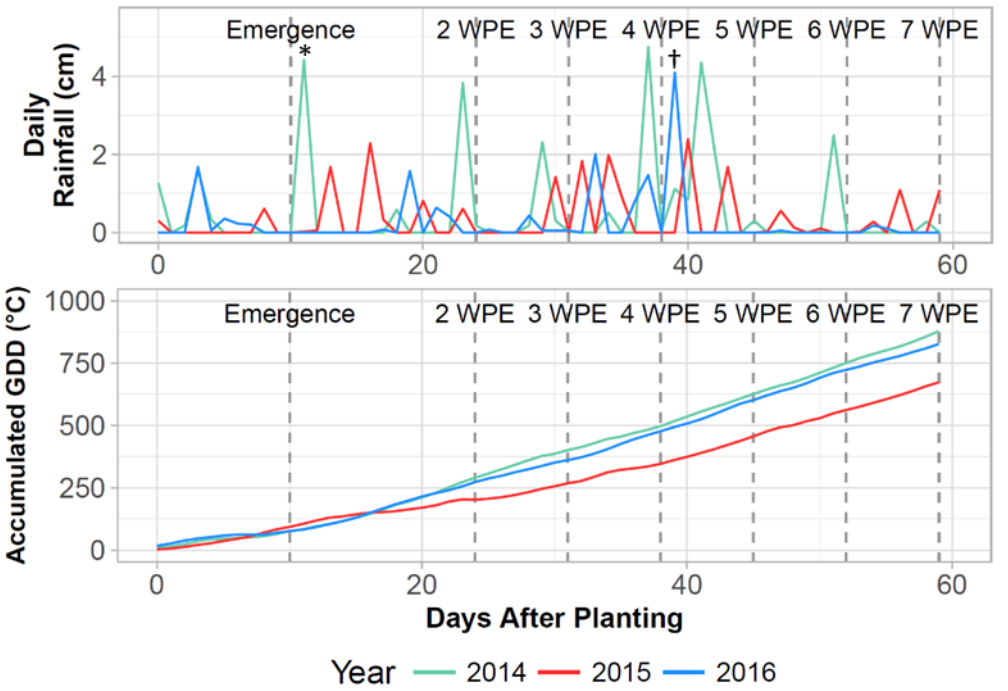

Supplementary Figure 2-2. Daily precipitation and accumulated growing degree days (GDD) from planting to seven weeks past-emergence (WPE) in 2014, 2015, and 2016. The (*) indicates heavy rainfall (4.4 cm) that occurred one day after emergence in 2014, and the (†) indicates heavy rainfall (4.1 cm) that occurred one day after the 4WPE time point in 2016, after which very little additional rain fell.

A

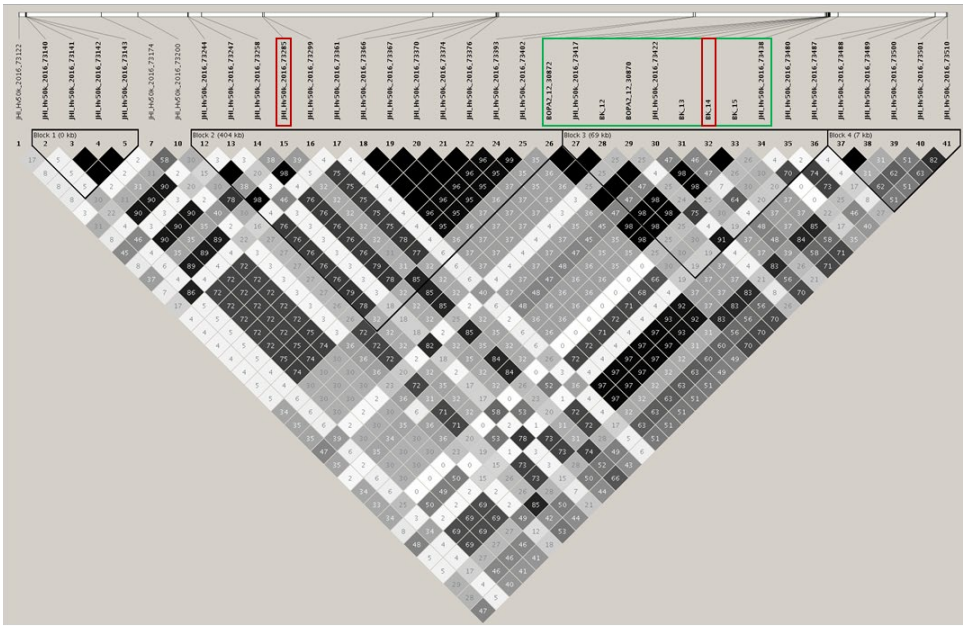

B

Supplementary Figure 2-3. LD analysis of SNPs in and around Photoperiod-H1 (Ppd-H1). A) LD Plot showing R2 values between all SNPs in and flanking the Ppd-H1 coding sequence. BK_14 was used in this study to distinguish Ppd-H1 and ppd-H1 alleles, and SNP22, the causative SNP described in Turner et al. (2005), is located between BK_14 and BK_15, which were in complete LD. The two most significant SNPs detected by genome-wide association mapping in the Ppd-H1 QTL for all lines in 2014 and 2015 are in red boxes (D′ between JHI-Hv50k-2016-73285 and BK_14 is 0.95). Note: not all SNPs shown in the LD plot were included in GWAS because they were represented by Tagged SNPs. All SNPs in the Ppd-H1 gene (2H 29123785-29127889 bp) are in a green box. LD blocks (in black triangles) were based on confidence intervals (Haploview, Version 4.1). B) Haplotypes of SNPs shown in LD plot with a frequency of at least 5%. The two most significant SNPs, JHI-Hv50k-2016-73285 and BK_14, are shown in red.

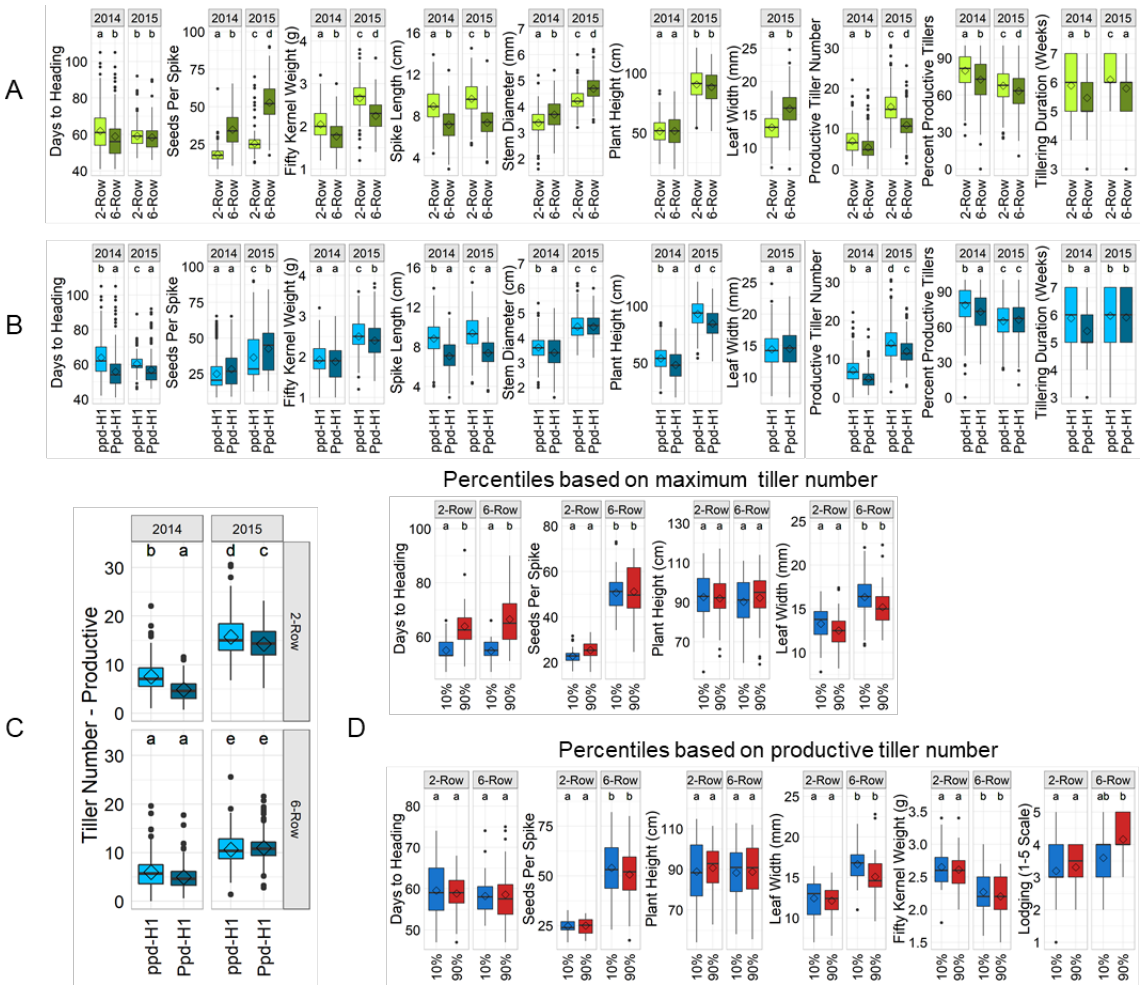

Supplementary Figure 2-4. Box plots summarizing additional traits in various groups. A) Box plots summarizing traits in 2-rows and 6-rows in 2014 and 2015. Diamonds represent mean trait values, and letters indicate whether groups were significantly different (Tukey Test, FDR p-value < 0.01). B) Box plots summarizing traits in lines containing *Ppd-H1* or *ppd-H1* alleles grown in 2014 and 2015. C) Box plots comparing productive tiller number between 2-rows containing either *Ppd-H1* or *ppd-H1* alleles and between 6-rows containing either *Ppd-H1* or *ppd-H1* alleles. D) Box plots summarizing traits in percentiles based on maximum and productive tiller number that were not included in Fig. 3.

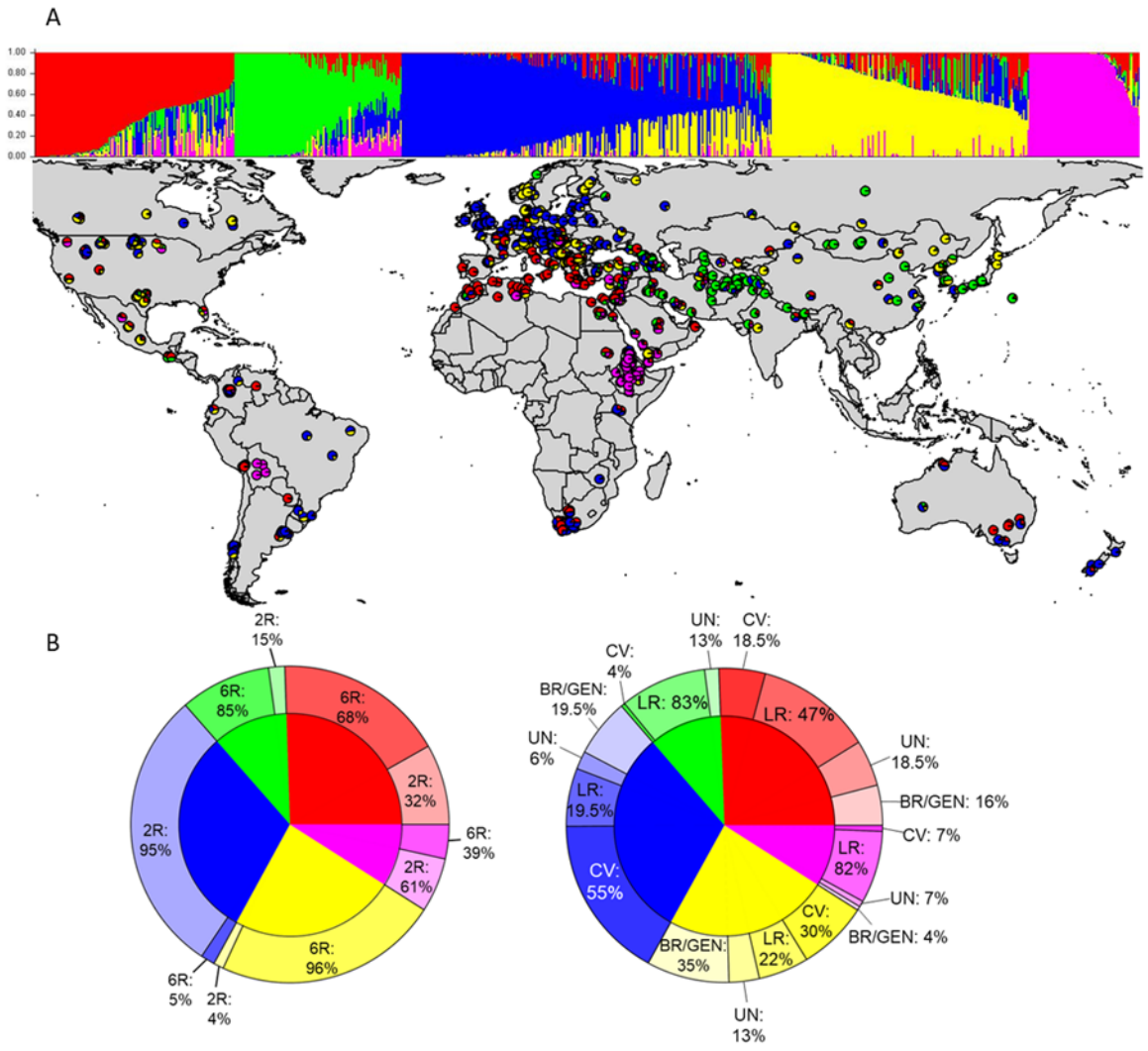

Supplementary Figure 2-5. Population structure analysis of mapping panel. A) Bar graph (top) showing assignments of lines to the five STRUCTURE subpopulations, and a map (bottom) showing collection locations of individual lines, each represented by a pie chart showing the proportion of assignment to the five STRUCTURE subpopulations. B) Pie charts showing proportion of spike row-type (left) and improvement status (right) in each subpopulation. Abbreviations in pie charts: 2-row (2R), 6-row (6R), cultivar (CV), landrace (LR), breeding line or genetic stock (BR/GEN), unknown (UN).

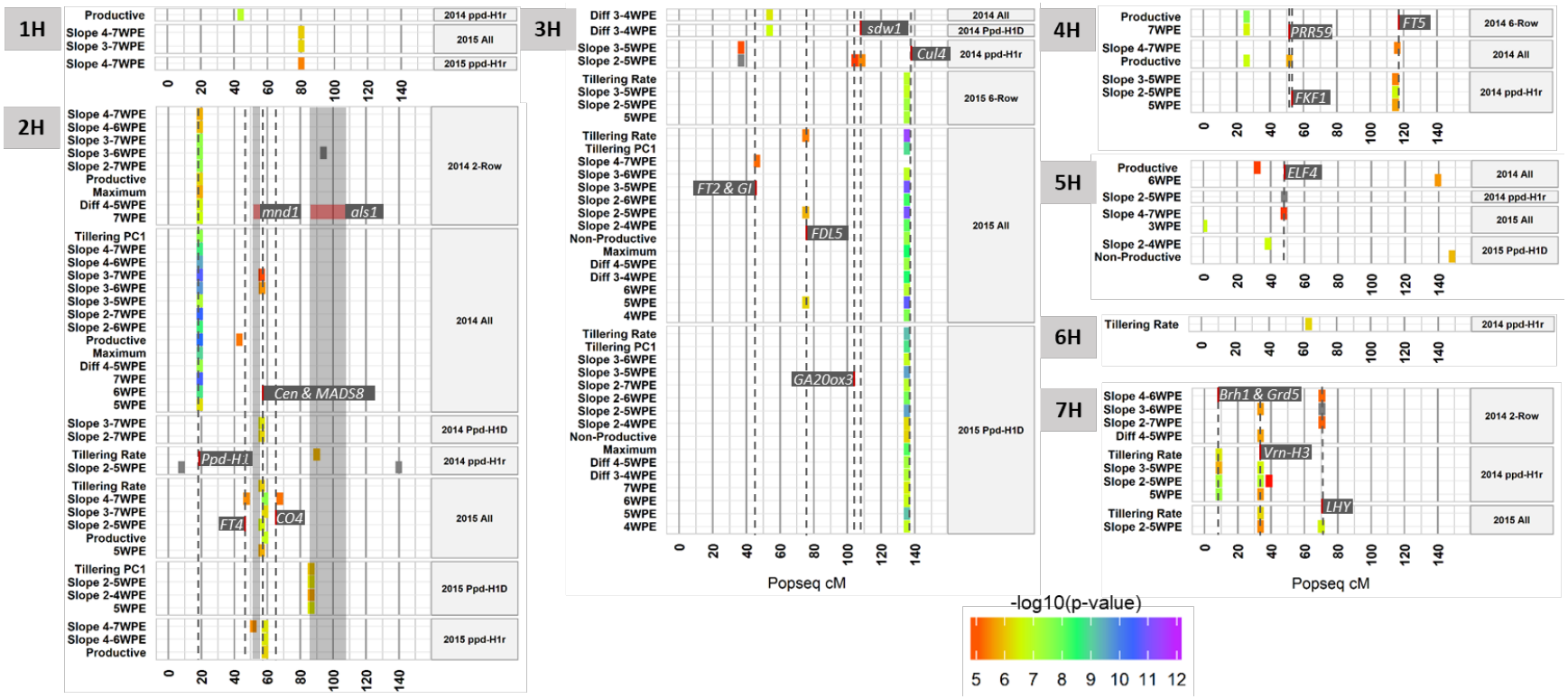

Supplementary Figure 2-6. Genomic positions and significance of all quantitative trait loci (QTL) associated with tiller development (tillering). Colored bars show genetic positions of SNPs (+/- 2 cM) associated with all tillering traits: weekly tiller number from 2-7 weeks past emergence (e.g. 5WPE), maximum and productive tiller number, difference between two consecutive weeks (e.g. Diff 4-5WPE), slope between at least three consecutive weeks (e.g. Slope 4-6WPE), tillering rate (maximum tillers/duration of tillering in weeks), or tillering PC1 (calculated using weekly and productive tiller counts). Colors of bars indicate -log10(p-value) of the most significant SNP in each QTL interval. Gray dotted lines and shaded regions show positions of genes and mutant introgressions previously implicated in control of heading time, inflorescence morphology, or tiller number (summarized in Table 1-1).

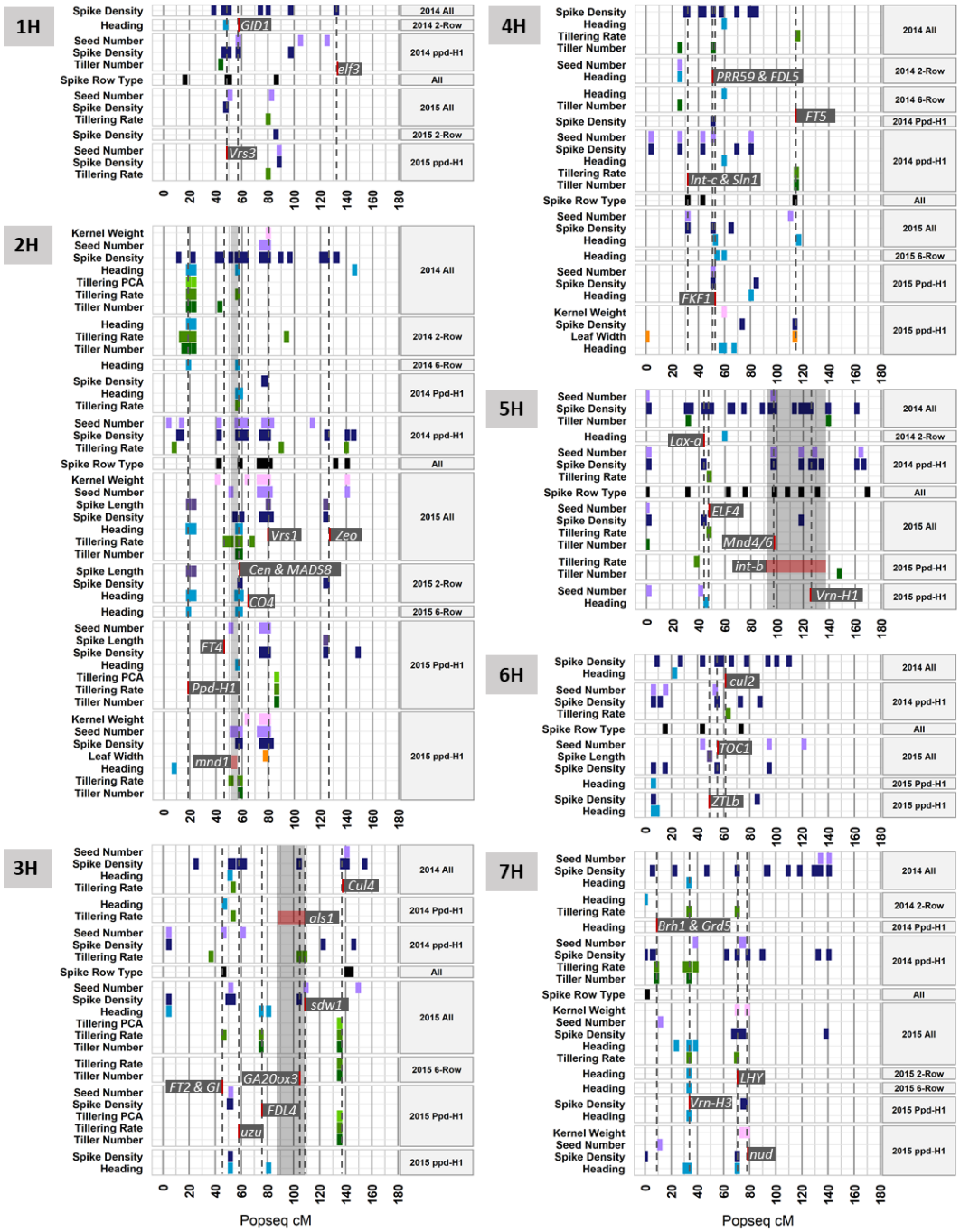

Supplementary Figure 2-7. Quantitative trait loci (QTL) associated with tiller development (tillering) and all other traits. Colored bars show genetic positions of significant SNPs (+/- 2 cM) associated with tillering, days to heading (heading), leaf width, and various inflorescence related traits (spike row-type, seeds per spike, spike density, and spike length). Gray dotted lines and shaded regions show positions of genes and mutant introgressions previously implicated in control of heading time, inflorescence morphology, or tiller number (summarized in Table 1-1).

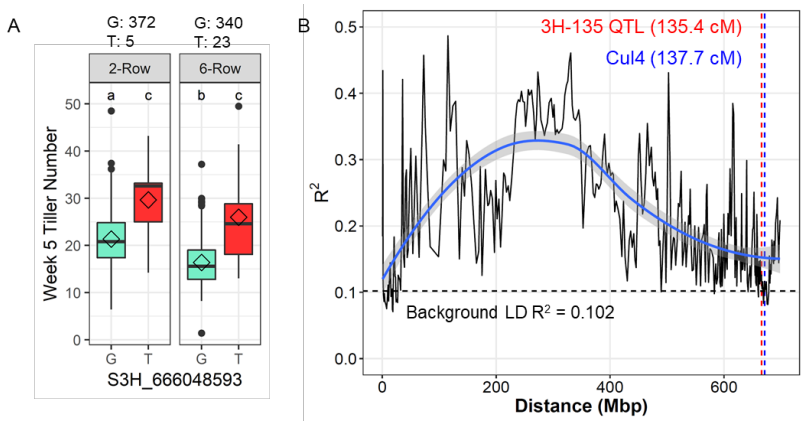

Supplementary Figure 2-8. Cul4 is not a likely candidate gene for the tiller number QTL 3H-135. A. SNP S3H_666048593 in QTL 3H-135 was associated with tiller number in 2015 in all lines and 6-rows. Although tiller number was significantly different in 2-rows with the different alleles, minor allele frequency was too low (1.3%) for QTL identification, as the minor allele cutoff used for association mapping was 5%. B. Linkage disequilibrium (LD) decays below background LD levels between QTL 3H-135 (red dotted line) and the known tillering gene *Uniculme 4* (*Cul4*) (blue dotted line), making *Cul4* an unlikely candidate gene. The solid blue line was fit by local regression (LOESS) to show average LD across the chromosome, and gray shading represents 95% confidence intervals. The black dotted line represents background LD, which was calculated as the 95th percentile of significant (pDiseq < 0.01) R^2 values for all SNP pairs >= 50 cM apart on 3H.

Chapter 3. Comparative transcriptomics of meristems reveals gene expression patterns underlying early lateral branch development in barley

Synopsis

In barley, modified lateral branches called tillers develop from axillary meristems (AXM) and are a defining characteristic of shoot architecture in barley. However, little is known about gene expression patterns underlying AXM and tiller development. In this study, amplified RNA was sequenced from laser microdissected shoot apical meristems (SAM), from which main shoots develop, and AXM at different seedling stages from two cultivars, Bowman and Morex. From genes differentially expressed between individual meristems and non-meristem tissues (e.g. leaves), we identified a set of 43 genes expressed in nearly all meristems, regardless of type (SAM or AXM), morphological stage (e.g. vegetative or early inflorescence), or genotype. Based on broad meristem expression and homology to meristem genes characterized in other species, like *CLAVATA1*, *CUP SHAPED COTYLEDON2*, and *KNOTTED1*, it is likely that this set of genes is important for general meristem maintenance and function. Furthermore, we found that gene expression profiles were primarily distinguished by genotype and meristem type, but profiles of different meristem types tended to be more similar if morphological stages were similar. Although morphologically similar SAM and AXM had similar expression profiles, we identified some genes that were identified in SAM but not AXM and vice versa, and clustering based on expression in all meristems identified genes that are likely important for tiller development as some, like *UNICULME4* and

INTERMEDIUM-C (*TEOSINTE BRANCHED1* ortholog), have been previously shown to influence tiller outgrowth. Finally, expression of some genes in AXM and ligule suggest, as in other species, dual function in AXM and leaf development.

Introduction

The shoot apical meristem (SAM) is an organ that forms during plant embryonic development and gives rise to all aboveground tissues including the main shoot and lateral organs like leaves and axillary meristems (AXM). Lateral branches in barley called tillers develop from AXM that form in coleoptile and leaf axils of the main stem and are an important component of shoot architecture and grain yield. Four major steps are required for lateral branch development: 1) establishment of axil identity, 2) initiation of an AXM in the axil, 3) transition of an AXM into a vegetative axillary bud (AXB), and 4) internode elongation in the AXB to form a lateral branch. Key genes involved in lateral branching have been identified and characterized in *Arabidopsis thaliana*, and these four major steps can be distinguished by expression of specific genes or genetic pathways (Reviewed in McSteen and Leyser, 2005; Schmitz and Theres, 2005). However, little is known about gene expression patterns underlying AXM initiation and development and lateral branching in barley.

Most of what we know about genetic control of tiller development in barley comes from studies using high and low tillering mutants. In barley, low tillering mutants, like *uniculm2* (*cul2*), *absent lower laterals* (*als1*), *low number of tillers 1* (*lnt1*), and *uniculme 4* (*cul4*), are epistatic to high tillering mutants, like *many noded dwarf 1* (*mnd1*) and *granum-a* (*gra-a*), as indicated by low tillering phenotypes in double mutant combinations of low and high tillering alleles. It is likely that this epistatic effect is due to inability of low tillering mutants to initiate or maintain AXM (Babb and Muehlbauer, 2003; Dabbert et al., 2009, 2010; Tavakol et al., 2015). Transcriptomic analyses of

seedling crown tissue, which contains SAM and AXM, from *als*, *cul2*, and *cul4* mutants revealed that many genes involved in stress response and defense were upregulated compared to non-mutants, and some genes involved in calcium signaling were also upregulated in *cul2* mutants, suggesting that these signaling pathways may play a role in tiller development (Okagaki et al., 2013; Tavakol et al., 2015).

Two genes have been identified and characterized in low tillering mutants. The *cul4* mutant phenotype is caused by loss of function of a gene encoding a BROAD COMPLEX, TRAMTRACK, BRIC-À-BRAC (BTB)-ankyrin domain containing protein homologous to *Arabidopsis thaliana BLADE-ON-PETIOLE 1* (*BOP1*) and *BOP2* (Tavakol et al., 2015). The *Cul4* gene is expressed in leaf axils at the site of AXM initiation and in newly formed AXM, and *cul4* mutants form very few primary tillers and no secondary tillers. Low tiller number is caused by reduced initiation of AXM in leaf axils, but tiller development is also affected, as the internodes of some lateral branches do not elongate and leafy outgrowths are observed instead of tillers (Tavakol et al., 2015). The *lnt1* mutant phenotype is caused by loss of function of a Three Amino Acid Loop Extension (TALE) homeobox protein, encoded by a gene called *JuBel2*, which is homologous to Arabidopsis *BEL1* (Dabbert et al., 2010; Müller et al., 2001). JuBel2 and JuBel1, another BEL1 homolog, have been shown to interact with three class 1 KNOTTED-like homeobox (KNOX) proteins in barley in a yeast two-hybrid screen: KNOX1, KNOX3 (mutated in the barley mutant *hooded*), and KNOX7; and expression domains of *JuBel1*, *JuBel2*, *KNOX1*, *KNOX3*, and *KNOX7* overlap completely in embryos. Furthermore, Arabidopsis overexpressing barley *JuBel2* had more lateral

branches than wild-types, indicating a role in lateral branch development (Müller et al., 2001). Redundant BEL1 paralogs in Arabidopsis, PENNYWISE (PNY) and POUND-FOOLISH (PNF), have been shown to form heterodimers in-vivo with class 1 KNOX proteins SHOOT MERISTEMLESS (STM) and BREVIPEDICELLUS (BP) to regulate specification and patterning of inflorescence and vegetative branches (Kanrar et al., 2006).

In addition to having defects in tiller development, some low tillering mutants also have defects in inflorescence and/or leaf development. Inflorescences of *als*, *lnt1*, *cul2*, and *intermedium-b* (*int-b*) mutants are abnormal, having reduced spikelet number or size or irregular phyllotaxic arrangement of spikelets (Babb and Muehlbauer, 2003; Dabbert et al., 2009, 2010). These phenotypes suggest that some of the same genes or genetic pathways in barley regulate spikelet meristem initiation and patterning and vegetative AXM initiation and AXB outgrowth. Interestingly, some low tillering mutants have abnormal leaf development, specifically at the blade-sheath boundary. For example, *CUL4* is expressed in ligules, epidermal outgrowths that form on the adaxial leaf surface at the blade-sheath boundary, and *cul4* mutant leaves do not form ligules (Tavakol et al., 2015). Another mutant, *eligulum-A* (*eli-A*), was identified as a partial suppressor of the *cul2* mutant phenotype (Okagaki et al., 2018). Typically, *cul2* mutants do not produce any tillers, but when crossed with plants carrying strong *eli-a* mutant alleles (*eli-a.18*), they produced one or two. In addition, *eli-a.18* mutants did not form ligules, a structure that consists of a band of cells at the blade-sheath boundary, and had very reduced auricles, tissue flaps that grow from the leaf margin at the blade-sheath boundary and

wrap around the stem (Okagaki et al., 2018). Despite their ability to enhance tillering in *cul2* mutants, single *eli-a.18* mutants in a Bowman background developed about half as many tillers as Bowman, and, although a specific model has not been developed to explain these mutant phenotypes, it is postulated that defects in auxin transport may be the underlying cause (Okagaki et al., 2018).

Genes that influence axillary meristem initiation and development and either leaf patterning or inflorescence development are fairly common in plants, probably due to their wider role in organ boundary specification, primordia initiation, or outgrowth. These developmental processes are all influenced by auxin transport; therefore, gene mutations that modify auxin transport often result in complex phenotypes. For example, mutations in genes that specify organ boundaries, like *CUP-SHAPED COTYLEDON* (*CUC*) genes in Arabidopsis, perturb polar auxin transport and can result in reduced branching, loss of leaf serration, and abnormal inflorescences (Bilsborough et al., 2011; Nikovics et al., 2006; Raman et al., 2008; Vroemen et al., 2003). Vegetative and reproductive axillary meristem formation is also inhibited in three maize mutants with impaired polar auxin transport: *barren stalk 1* (*ba1*), *Barren inflorescence 1* (*Bif1*), and *bif2* (Gallavotti et al., 2008; McSteen et al., 2007). Several lines of evidence from Arabidopsis and other species suggest that the diverse phenotypes resulting from reduced or ectopic expression of class 1 *KNOX* genes is due to increased or decreased polar auxin transport, respectively (reviewed in Hay and Tsiantis, 2010). Arabidopsis *bp* mutants exhibited increased lateral branching, reduced height, and abnormal phyllotaxic arrangement of

siliques in inflorescences (Byrne, 2003); while ectopic expression of *BP* in *35S::BP* lines resulted in abnormal patterning of leaf margins (Lincoln et al., 1994).

After AXM develop into AXB, they either remain dormant or grow into lateral branches. AXB outgrowth is influenced by environmental cues that are relayed through various signaling pathways (reviewed in Beveridge, 2006 and Dun et al., 2009). The hormone auxin is synthesized in the shoot apex and moves downward through the plant, where it promotes synthesis of hormones called strigolactones (SL) in roots, which travel upwards and enter AXB to prevent outgrowth. Conversely auxin inhibits hormones called cytokinins (CK), which can be synthesized locally or enter AXB through xylem to promote outgrowth (reviewed in Kieber and Schaller, 2014). Three proteins in rice are involved in SL signaling: DWARF14 (D14), an α/β hydrolase; DWARF3 (D3), an F-box protein; and DWARF53 (D53) a P-loop containing nucleoside triphosphate hydrolase (Jiang et al., 2013; Yao et al., 2018; Yoshida et al., 2012). A complex containing D14 and D3 senses SL and mediates degradation of D53, an inhibitor of SL signaling. In rice, *D14* mRNA is expressed in leaves and vasculature, and the protein is transported through phloem to axillary buds where it acts as a receptor to sense SL (Kameoka et al., 2016). The TB1/CYCLOIDEA (CYC)/PROLIFERATING CELL NUCLEAR ANTIGEN FACTOR1,2 (TCP) family transcription factor TEOSINTE BRANCHED 1 (and orthologs in other species) acts downstream of SL to inhibit lateral branching.

No studies to date have compared transcriptome data from shoot apical meristems and vegetative axillary meristems in grasses. Ohtsu et al. (2007) characterized gene expression in maize SAM, and a later study in maize characterized gene expression in

SAM throughout development and in AXM from which ear inflorescences develop (Takacs et al., 2012). A more recent study in barley compared transcriptome data from barley SAM transitioning from vegetative to inflorescence meristems (Digel et al., 2015). Comparing gene expression profiles in SAM and vegetative AXM from which tillers are derived will further our understanding of genetic control underlying tiller development in barley. The main stem in barley and other grasses elongates shortly after germination, but whether or not tillers develop depends on environmental conditions. However, the main stem and tillers are virtually indistinguishable in maturing plants. Therefore, we expect that AXM will have distinctive gene expression patterns earlier in development for sensing and responding to growth stimuli, but that gene expression in more developed SAM and AXM will converge. This study resulted in an increase in the current body of knowledge regarding gene expression underlying development of vegetative AXM and tillers in barley. Moreover, by comparing genes expressed in ligules and meristems, we identified additional genes that may regulate lateral branch development and leaf patterning.

Materials and Methods

Growing Conditions

A 2-row cultivar, Bowman, and a 6-row cultivar, Morex, were independently grown for seedling tissue. Four Bowman seeds were planted in Propagation Mix (Sun Gro, Agawam, MA) in 5.25 inch square pots. Forty-eight pots total were grown in three replicates in a growth chamber at 20 °C with 16 hours of light. Crown tissue was

harvested at four and seven days after planting (DAP) at 9:00 am USA Central Time Zone from each replicate, and all tissue was harvested within one hour of starting. Most seedlings harvested at four DAP were stage GRO:0007057 (“leaf just at coleoptile tip”), but they ranged from GRO:0007056 (“coleoptile emerged from seed”) to GRO:0007059 (“first leaf through coleoptile”) (gramene.org/db/ontology). All seedlings harvested at seven DAP were GRO:0007060 (“first leaf unfolded”). For each stage and replicate, four pots were randomly selected and the 16 individual plants in each pot were prepared for laser microdissection and RNA sequencing as described below. Three pots were also randomly selected from each replicate and all seedlings were prepared for RNA in-situ hybridizations as described below. Single Morex seeds were planted in propagation mix in individual Cone-tainers (SC10 Super, diameter 3.8 cm, depth 21 cm, Ray Leach, Tangent, OR), and Cone-tainers were placed into six racks (RL98, Ray Leach, Tangent, OR), with two racks corresponding to a single replicate (196 seeds per replicate). Racks containing cone-tainers were covered in plastic to keep the soil moist and put into a dark cold room for four days. Then they were moved into a growth chamber at 20°C with 16 hours of light. After coleoptiles emerged, 2 g of Osmocote Plus (Scotts Miracle-Gro, Marysville, OH) was added to the soil surface of each cone-tainer. Crown tissue from individual seedlings was harvested within one hour, starting at 9:00 am USA Central Time Zone, at three seedling stages: GRO:0007059 (“first leaf through coleoptile”), GRO:007060 (“first leaf unfolded”), and GRO:0007061 (“two leaves unfolded”). Twenty seedlings were randomly selected from each replicate at each stage and prepared for laser microdissection and RNA sequencing as described below.

Laser microdissection and RNA sequencing

Crown tissue (1 cm of stem above the roots) from cv. Bowman and Morex seedlings was collected at the stages described above and prepared for paraffin embedding according to a protocol developed by Scanlon et al. (2009). Ten micron median sections through meristems of individual plants were mounted on PEN membrane glass slides (Leica Microsystems, Buffalo Grove, IL). Instructions from the manufacturer (memo from Leica Microsystems) were followed to make slides RNase free before application of tissue sections. First, PEN membrane slides were soaked in RNase Zap (Thermo Fisher, Waltham, MA) for 15 seconds, followed by two rinses in molecular grade water. Then slides were air-dried and irradiated in a UV cross-linker for 30 minutes. Sections were prepared for laser microdissection according to Scanlon et al. (2009). Meristem tissue from six median sections through individual meristems was laser microdissected using a Leica LMD6500 laser dissection microscope (University Imaging Centers, Minneapolis, MN) and pooled into a single biological replicate with three replicates per stage. Leaf tissue and ligule tissues were laser microdissected from shoot apical meristem (SAM) median sections.

RNA was extracted from laser microdissected tissue using a PicoPure RNA Isolation Kit (Thermo Fisher) and amplified using an Arcturus RiboAmp HS Plus RNA Amplification Kit (Thermo Fisher). Amplified RNA was submitted to the University of Minnesota Genomics Center (UMGC, Saint Paul, MN) for quality testing, library preparation, and sequencing. Amplified RNA was quantified using a RiboGreen assay, and quality was assessed by capillary electrophoresis using an Agilent BioAnalyzer 2100.

Libraries were prepared using a TruSeq Stranded Total RNA Library Prep Kit (Illumina, San Diego, CA), omitting the size selection step (based on personal communication with Michael J. Scanlon). Libraries were sequenced using an Illumina HiSeq 2500 system to generate 125 bp, paired reads.

Transcriptome data generated by the International Barley Genome Sequencing Consortium (IBGSC) was downloaded from the European Nucleotide Archive (accession PRJEB14349, www.ebi.ac.uk/ena). RNA sequencing data from the following tissues that do not contain meristems were selected and included in a pool of "non-meristem" transcriptome data to identify meristem-specific genes: palea, lemma, epidermis, and senescing leaves (Supplementary Table 3.4 in Mascher et al., 2017).

Cutadapt (v 1.18) was used to trim low quality bases from 3' ends (Illumina Q Score < 20) and filter short reads (< 30 bases) from all reads, including IBGSC data. Sequencing adaptors and poly-A tails were removed from reads generated in this experiment using Cutadapt, and quality of all reads was assessed before and after trimming and filtering using FastQC (v 0.11.6). Paired reads were aligned to the IBGSC Morex reference genome assembly using Tophat (v 2.1.1) (Beier et al., 2017; Mascher et al., 2017), and the percentage of reads aligned are summarized in Table S3-1. Gene counts for uniquely, concordantly aligned read pairs were generated using HTSeq (v 0.11.0) and an annotation file for high confidence gene models (Hv_IBSC_PGSB_r1_HighConf.gtf).

Identification of differentially expressed genes and gene clusters

To identify meristem-specific genes, individual meristems (based on genotype, seedling stage, and type) were compared to non-meristem tissues (IBSC tissues plus laser microdissected seedling leaf tissue) to identify differentially expressed (DE) genes with an FDR-adjusted p-value < 0.01 and log2-fold change > 2 using two different R packages, DESeq2 and EdgeR (Love et al., 2014; Robinson et al., 2010). DE genes were identified with DESeq2 using a negative binomial general linear model with Wald significance tests, and DE genes were identified with EdgeR using a generalized log-linear model and likelihood ratio tests. The set of 43 core meristem genes (Fig. 3-2, Table S3-2), included genes that were upregulated in more than half of all individual meristems compared to non-meristem tissues in both genotypes.

To identify genes expressed only in shoot apical meristems or axillary meristems (Fig. 3-3), individual axillary meristems were first compared to the shoot apical meristem that was the most similar morphologically to identify genes that were upregulated in SAM or AXM. For example, AXM classified as vegetative (V AXM) were compared to V SAM to identify DE genes. For AXM stages that were between SAM stages, AXM were compared to both the more developed and less developed SAM. For example, late vegetative (LV) AXM were compared to V SAM and SAM that were transitioning from vegetative to inflorescence meristems (T SAM). DE genes were identified using DESeq2 and EdgeR. Genes with a log2-fold change > 2 in AXM compared to SAM were considered upregulated in AXM (FDR-adjusted p-value < 0.01), and Genes with a log2-fold change > 2 in SAM compared to AXM were considered upregulated in SAM (FDR-adjusted p-value < 0.01). Three criteria had to be met for a gene to be considered

expressed in AXM but not SAM: total counts in SAM <= 5, total counts in SAM < 5% of average counts for AXM, and average counts for AXM >= 5. The criteria were the same for considering genes to be expressed in SAM but not AXM, with tissue types reversed.

Clustering based on gene expression in meristem tissues (Fig. 3-4) was performed using the R package MBCluster.Seq (version 1, Si et al., 2014) on a set of 1,477 genes that were differentially expressed between SAM and AXM. The 1,477 differentially expressed genes were identified by both DESeq2 and EdgeR (FDR-adjusted p-value < 0.01, log2 fold-change >2) as being upregulated in either AXM or SAM. Each individual AXM (based on stage, leaf axil, and genotype) was compared to the SAM of the same genotype that was most similar based on morphology. For example, the AXM forming in the coleoptile axil (T_0 AXM) at GRO:0007059 was classified as a vegetative AXM and was compared to SAM at GRO:0007059, which was classified as a vegetative SAM. Classifications of all meristem stages based morphology are included in Table 3-1. In some cases, AXM fell between two SAM stages based on morphology. For example, the T_0 AXM at GRO:0007060 was classified as late vegetative AXM and was compared to vegetative SAM at GRO:0007059 and transitioning SAM at GRO:0007060.

Clustering of 146 genes with higher expression in ligules compared to leaves at the same stage in Morex was performed using MBCluster.Seq (DESeq2 and EdgeR, log2 fold-change >2, FDR-adjusted p-value < 0.01), and was based on expression in leaf, ligule, and all meristems in Morex.

Gene Ontology (GO) term and UniProt domain identifiers were previously assigned to all genes in the annotation file from the Morex reference genome assembly

(Beier et al., 2017). Fisher's Exact Tests in R were used in this study to compare all high confidence genes and genes in clusters to identify GO terms and UniProt domains that were enriched in clusters. All plots included in figures were generated using the ggplot2 R package (version 3.0.0) or gplots R package (version 3.0.1).

RNA in-situ hybridizations

Crown tissue from cv. Bowman seedlings was collected at four days after planting and seven days after planting and prepared for paraffin embedding according to Javelle et al. (2011). Riboprobe plasmids were cloned by amplifying a 300-500 bp portion of the coding sequence or 3' UTR of the genes of interest from Bowman genomic DNA (Table S3-3) and inserting it into a pGEM-T vector using a pGEM-T Easy Vector System (Promega, Madison, WI). The insert plus flanking T7 and SP6 RNA polymerase sites was amplified from the riboprobe plasmid using M13 primers, and the resulting PCR product was Sanger sequenced with the M13 forward primer to validate the sequence and determine the orientation of the insert in relation to the RNA polymerase sites. Digoxigenin labeled probes were generated by in-vitro transcription from the purified, M13 PCR product using a DIG RNA Labeling Kit (Roche Diagnostics, Indianapolis, IN). RNA probes were hybridized to ten micron-thick, median sections through the SAM, T_0 AXM, and the AXM that formed in the first leaf axil (T_1 AXM) of each seedling.

Results

Factors differentiating meristem gene expression

Shoot apical meristem and axillary meristem tissues from median meristem sections were captured by laser microdissection from different seedling stages in Bowman and Morex. Stage 1 (S1) in Bowman ranged from GRO:0007056 (coleoptile emerged) to GRO:0007059 (first leaf emerged from coleoptile), with most being GRO:0007057 (first leaf at coleoptile tip); and S1 in Morex were all GRO:0007059 (Table 3-1, Fig. 3-1A). S2 in Bowman and Morex were GRO:0007060 (one leaf unfolded), and S3 in Morex was GRO:0007061 (two leaves unfolded; Table 3-1, Fig. 3-1A). Tissue captures from median meristem sections were pooled, and RNA was extracted and amplified. Libraries were created from amplified RNA and sequenced (UMGC), and read pairs were aligned to the Morex reference genome assembly (Beier et al., 2017; Mascher et al., 2017). Alignments were used to generate normalized gene counts. For clustering and identification of differentially expressed genes, meristems were classified based on meristem type (SAM or AXM), and morphological stage (early vegetative, vegetative, late vegetative, transitioning, and early inflorescence – double-ridge stage), as described in Materials and Methods and in Table 3-1.

One goal of this study was to identify the primary factors that differentiated meristem transcriptomes. Principal coordinates analysis (PCoA) of a dissimilarity matrix calculated using normalized log2 counts-per-million (CPM) of all genes in all Morex meristem samples was performed, and the first two principal coordinate (PCo) values for all samples were plotted to visualize similarity of meristem transcriptomes (Fig. 3-1B). PCo1, which explained 23% of the total variance, separated meristem samples primarily by meristem type, with SAM clustering more to the left and AXM clustering more to the

right of the plot. However, meristems that were more similar morphologically, tended to cluster more closely together along PCo1. For example, S1 SAM was a vegetative meristem, and it clustered more closely in the MDS plot with vegetative AXM tissues, like Stage 3 T_3AXM and Stage 2 T_1AXM, than it did with transitioning or double-ridge SAM stages (S2 and S3 SAM, respectively) (Fig. 3-1B). PCo2 only explained 7% of the total variance, and separation based on a single variable was not clear (Fig. 3-1B). PCoA using data from Bowman and Morex yielded similar results, but PCo1, which explained 24% of the total variance, clearly separated samples by genotype and PCo2, which explained 22% of the total variance, separated samples primarily by meristem type and morphological stage (Fig. S3-4).

Two meristems, S1 T_0AXM and S2 T_3AXM, clustered furthest from the others along PCo1 and PCo2 (Fig. 3-1B). Interestingly, even though S1 T_0AXM appeared to be a vegetative axillary meristem, its transcriptome was distinct from other vegetative axillary meristems, as indicated by greater separation (Fig. 3-1B). Based on morphology, S2 T_0AXM appeared to be slightly more advanced developmentally than S2 T_1AXM, which was not surprising considering that T_0AXM develop first (Fig. 3-1A). However, by S3, T_1AXM appeared to have surpassed T_0AXM developmentally based on morphology and location in the PCoA plot. By S3, T_0AXM samples clustered closely with late vegetative and transitioning AXM (S3 T_2AXM and S3 T_1AXM) and with later stage SAM tissues, indicating that gene expression profiles of AXM become more similar to SAM as they develop.

Identification of core meristem genes in barley

Despite differences in gene expression profiles based on genotype, meristem type and morphological stage, some genes were more highly expressed in nearly all meristems compared to tissues that did not contain meristems (non-meristem tissues). Non-meristem tissues included epidermis, senescing leaf, palea and lemma (bracts that enclose florets in grasses), and seedling leaf tissue that was laser-microdissected from Bowman and Morex median SAM sections (Fig. S3-5). All replicates of individual meristems were compared to non-meristem tissues to identify genes upregulated in meristems. Genes were considered for further analysis if they were expressed in more than one individual meristem and if they were upregulated in both genotypes, unless they were specifically upregulated in two or more meristem tissue types that were not harvested from Bowman, as some meristem tissue types were only harvested from Morex. Based on these criteria, we identified 142 genes upregulated in meristems compared to non-meristem tissues (Fig. S3-6). Only two biological process GO terms were enriched in this set of 142 genes: DNA-dependent regulation of transcription (GO:0006355) and multicellular organismal development (GO:0007275). More than half of the 24 enriched InterPro domains are found in transcription factors (e.g. homeobox, B3, TCP domains), and, not surprisingly, the two most significantly enriched were both KNOX domains (IPR005540 and IPR005541). Nine of the 24 enriched domains are typically found in proteins involved in post-transcriptional gene silencing and protein degradation pathways (e.g. Argonaute and ubiquitin domains) (Table S3-4).

Of the 142 genes upregulated in meristems compared to non-meristem tissues, only nine were upregulated in all meristems regardless of genotype, meristem type, or

morphological stage (Fig. S3-6, marked by pink bar). Homologs of all nine genes have been characterized in meristems of other species and are likely important for meristem maintenance and function. For example, a gene encoding a NAC domain transcription factor homologous to *CUC2* was upregulated at least seven-fold log2 CPM higher in meristems than non-meristem tissues (Fig. 3-2). In addition to these nine genes, 34 genes were upregulated in most meristems (Fig. 3-2), and many of them have also been characterized in meristems of other species, indicating that these 43 genes are generally important for meristem maintenance or function. For example, a gene encoding a CLV1-like receptor kinase homologous to THICK TASSEL DWARF 1 (TD1) in maize was upregulated in both genotypes and all but three individual meristems (Fig. 3-2). Interestingly, a gene that was upregulated in all but one meristem (S2 T3 AXM – early vegetative AXM) and that had the highest average expression in meristems, encoded a protein with unknown function that is specific to the Triticeae tribe (identified in barley, *Triticum aestivum*, and *Aegilops taushii* by BLAST against non-redundant protein sequences and the nucleotide collection in NCBI). Based on expression in all but the least-developed meristem, it is possible that this gene is involved specifically in inflorescence development in barley and other Triticeae.

Identification of shoot apical meristem and axillary meristem specific genes

Our analyses indicated that meristems that are less morphologically similar tend to have less similar gene expression profiles and that gene expression profiles appear to converge as meristems begin transitioning into late vegetative and inflorescence meristems. We also identified genes that are likely important for function and

maintenance of all meristems. However, we wanted to examine whether any genes were uniquely expressed only in SAM or AXM. To be considered in the SAM but not AXM, a gene needed to have <=5 counts in AXM, >=5 counts in SAM, and the total counts in AXM had to be less than 5% of the average counts in SAM. The criteria were the same for identifying genes expressed in AXM but not SAM, with tissues reversed.

Overall, few genes fit these criteria. Only six genes were found to be expressed in SAM but not AXM (Fig. 3-3A, Table S3-2). Functions of two of these genes are uncharacterized. One gene encodes a protein homologous to Arabidopsis LIGHT-RESPONSE BTB 2 (LRB2), which is an important component in red light sensing (Christians et al., 2012). Another encodes a protein homologous to DNA-directed RNA polymerase II subunit 1 (NRPB1), part of an RNA polymerase II complex that transcribes DNA into mRNA, and another encodes a SWI-INDEPENDENT3 (SIN3)-Like protein that negatively regulates transcription by binding histone deacetylases (Wang et al., 2016). The last encodes an F-Box protein, which are involved in protein-protein interactions and in some cases protein ubiquitination (reviewed in Kipreos and Pagano, 2000).

Thirty-two genes were expressed only in AXM (Fig. 3-3A, Table S3-2). Ten of these 32 genes encoded transcription factors, four of which contained HD-ZIP domains and three of which contained TCP domains, including *INT-C*, the barley ortholog of *TB1*. Three proteins were annotated as Early Nodulin-like (ENODL). The ENODL protein family has not been well characterized, but it is likely that some have a role in defense and carbohydrate transport (Denancé et al., 2014). Several proteins with wound-inducible

domains were identified as being upregulated in AXM compared to SAM, but only one fit the criteria for being expressed only in AXM. RNA in-situ hybridization of an ENODL protein and the wound-induced protein confirmed that these genes were expressed specifically in AXM (Fig. 3-3B).

Genes differentially expressed between SAM and AXM

To identify genes that may be important for AXM and/or tiller development, individual AXM were compared to SAM that were the most similar morphologically to identify genes upregulated in AXM. If AXM appeared to fall between two SAM stages developmentally based on morphology, it was compared to both SAM stages. For example, S2 T_0AXM was classified as a late vegetative AXM and was compared to S1 SAM (vegetative) and S2 SAM (transitioning). In total, 490 genes were upregulated in AXM compared to SAM with log2 CPM fold-change higher than two and FDR-adjusted p-value less than 0.01, and 213 of them (43%) were identified in more than one SAM-AXM comparison (Table S3-2). All 32 of the genes that were expressed in AXM but not SAM (Fig. 3-3A) were also identified in this set of 490 genes. Only 12 genes were significantly upregulated in at least half of all AXM in SAM-AXM comparisons, and of these 12, three were expressed only in AXM and not SAM and encoded a TCP transcription factor, an ENODL protein, and an uncharacterized protein. The gene encoding the TCP transcription factor (HORVU2Hr1G003020), which is homologous to *INT-C*/*TB1*, was upregulated in AXM in more SAM-AXM comparisons than any other gene. Three of the 12 genes encoded ENOD proteins, and another three encoded proteins

with wound-inducible domains, indicating that these families may be important for AXM or tiller development.

Genes upregulated in SAM versus AXM were identified in the same SAM-AXM comparisons with the same criteria. In total, 465 genes were identified as being upregulated in SAM versus AXM, and 158 of them (34%) were identified in more than one SAM-AXM comparison. Only six genes were significantly upregulated in at least half of all SAM in SAM-AXM comparisons, and of these six, only one, the gene encoding NRPB1 (HORVU2Hr1G126750), was only expressed in SAM and not AXM. Fifty-three genes were identified in the 490 genes upregulated in AXM and in the 465 genes upregulated in SAM, indicating that they are expressed at different stages of meristem development but are not SAM or AXM-specific (Table S3-2).

Expression patterns of genes upregulated in axillary meristems

The following five sets of DE genes were included in a clustering analysis to identify clusters that were upregulated in AXM compared to SAM: 1) genes upregulated in meristems versus non-meristem tissues, 2) genes upregulated in AXM versus SAM, 3) genes upregulated in SAM versus AXM, 4) genes differentially expressed between the same AXM at different stages (e.g. S1 T_0AXM and S2 T_0AXM), and 5) genes differentially expressed between the same SAM at different stages. After removing duplicates from all gene sets, 1477 unique genes remained, and before clustering, meristems were grouped based on meristem type (SAM or AXM), morphological stage, and relative expression of *Int-C*/*Tb1* (AXM only), which encodes an inhibitor of vegetative AXM outgrowth (Table 3-1, Fig. S3-7). Clustering was initially performed

using different numbers of clusters, and six clusters were included in the final clustering because adding more resulted in clusters with the same overall expression pattern.

Two of the six clusters contained genes that were most highly expressed in double-ridge early inflorescence meristems (DR INF) and transitioning SAM and AXM, so they are likely involved in transition from vegetative to inflorescence meristems or floral organ development (Fig. S3-7). Genes in a third cluster were more highly expressed in vegetative SAM and AXM, and the remaining three clusters contained genes that were expressed higher in AXM than SAM (Fig. S3-7). Not surprisingly, all 32 genes that were expressed in AXM but not SAM were in these three clusters, supporting a role for these gene clusters specifically in AXM development or AXB outgrowth. The first cluster contained 11 of the 32 genes, the second cluster contained 19 genes, and the third cluster contained the remaining two genes. Interestingly, no clusters were identified that were expressed higher specifically in SAM, indicating that few genes may be required specifically for SAM development (Fig. S3-7).

The first of the three clusters upregulated in AXM contained 260 genes that were more highly expressed in early vegetative (EV) AXM specifically and included three genes known to influence tillering in barley: *Cul4*, *JuBel2*, *Int-C* (Fig. 3-4A, Table S3-5). This cluster also contained a gene homologous to Arabidopsis *EXCESSIVE BRANCHES 1* (*EXB1*) (Fig. 3-4A), which encodes a WRKY transcription factor that affects AXM initiation and AXB outgrowth (Guo et al., 2015). Transcriptional regulation and phosphorylation were the only two Gene Ontology (GO) biological processes enriched in this cluster (Fig. 3-4B, Table S3-4). Four of the five InterPro domains enriched in Cluster

1 (e.g. Homeobox and AP2/ERF) are transcription factor domains, and the fifth domain is a histidine-kinase related domain, likely involved in phosphorylation and signal transduction (Fig. 3-4B, Table S3-4).

The second cluster contained 106 genes specifically upregulated in vegetative and late vegetative AXM compared to other meristems (Fig. 3-4A, Table S3-5). Based on expression, it is possible that these genes are important for transition from an early vegetative AXM to a vegetative meristem, or they could be important for AXB outgrowth. Oxidation-reduction was the only GO biological process significantly enriched, and ENOD and wound-induced family proteins were the only significantly enriched InterPro domains (Fig. 3-4B, Table S3-4). This cluster contained six genes encoding proteins annotated as ENOD and six genes encoding proteins annotated as wound-induced, suggesting that these families may be important for AXM development or AXM outgrowth.

The third cluster contained 179 genes that were expressed highest in DR INF, V AXM, and LV AXM (Fig. 3-4A, Table S3-5). The only enriched GO biological process was enriched defense response, and the only enriched InterPro domains were Thionin family members, TCP transcription factors, and wound-induced (Wun1-like) family members (Fig. 3-4B). Thionins are small, cysteine rich peptides generally involved in defense or stress responses (Westermann and Craik, 2010), and as previously mentioned, wound-induced proteins accumulate at sites of wounding but could be involved more generally in stress responses.

Expression patterns of genes upregulated in ligules

As previously discussed, some genes in plants have broad roles in development and influence development and patterning of several different organs. Some genes in barley influence development of axillary meristems and leaves, specifically organs called ligules that form at the blade-sheath boundary; therefore, we were interested in examining meristem expression patterns of genes upregulated in ligules to potentially identify genes involved more broadly in development. First, Morex ligule tissue was compared to leaf tissue at the same stage to identify genes that were upregulated with a log2 CPM fold-change higher than two and FDR-adjusted p-value less than 0.01 (Fig. 3-5A). In total, 146 genes were identified as being upregulated in ligule compared to leaf, and most were upregulated only in the earliest ligule stage compared to leaf, indicating that gene expression in ligule and leaf become more similar as they develop (Fig. 3-5B). Only six genes were upregulated in ligule compared to leaf at all stages (Fig. 3-5B), and one of these genes, *Cul4* (HORVU3Hr1G106880) has been shown to influence ligule as well as AXM development (Tavakol et al., 2015). A heatmap was used to visualize relative expression of the 146 genes in ligule, leaf, and meristem tissues (Fig. S3-8).

The 146 genes that were upregulated in ligules compared to leaves were included in a clustering analysis based on expression in Morex leaf, ligule, and meristem tissues. As with the previous clustering analysis, meristems were grouped based on morphological stage, and two clusters were identified as being upregulated in ligules and meristems. The first cluster contained genes that were expressed fairly evenly across all ligules and meristems (Fig. 3-5C), suggesting that they be generally important for various developmental processes. Two of the genes identified in the first cluster were also

identified as being upregulated in meristems compared to non-meristem tissues, one encoding an ALOG domain-containing protein and the other a heterogeneous nuclear riboprotein (Fig. 3-5C). The third gene indicated in the cluster encodes a gene homologous to *BEL1*. BEL1 proteins have been shown to interact with KNOX proteins to regulate various developmental processes (reviewed in Hay and Tsiantis, 2010). The second cluster contained genes more highly expressed in axillary meristems, especially EV and V AXM, and in DR INF (Fig. 3-5C). Two of these genes, *Cul4* and *EXB1*-like, were also identified in Cluster 1 in Fig. 3-4A, suggesting the possibility that these two genes may interact and be important for both AXM and ligule development.

Discussion

In this study, we examined the gene expression patterns underlying shoot apical and axillary meristem development in barley. Our primary objectives were (1) to develop an atlas of gene expression in the barley SAM and AXM; (2) to examine the similarity in gene expression in the SAM and AXM; (3) to identify genes that are specific to the AXM; and (4) to identify genes that are expressed in the ligule and AXM. To gauge the similarity of the SAM and AXM, we examined transcriptomes at various stages of development and observed that AXM at earlier developmental stages have different gene expression profiles than SAM, but gene expression profiles of late vegetative and transitioning AXM appeared to be very similar to SAM. Despite differences between SAM and less developed AXM, we identified a set of genes that are likely important for general meristem maintenance and function, as they are broadly expressed in meristems and many have been characterized in meristems of other species. We also identified

genes that may be important at different stages of AXM development through identification of differentially expressed genes and clustering based on expression across meristem types and stages. Last, we identified clusters of genes expressed in ligules and meristems that may be important for leaf and meristem development.

Genes likely important for meristem function in barley

Many of the 43 genes expressed higher in meristems compared to non-meristem tissues have been previously characterized in meristems of other species, and more than half (24/43) encoded putative transcription factors (TFs). For example, the transcripts encoding homeobox domain containing proteins are most homologous to the maize *KNOTTED1*, *ROUGH SHEATH 2*, and *LIGULELESS3* genes. A gene homologous to *MONOCULM1* (*MOC1*), which is required for lateral branching in rice, was also identified.

Some of the 43 genes identified encode proteins involved in hormone signaling, which is important for meristem function. For example, five genes encode B3 domain-containing proteins in the ABSCISIC-ACID INSENSTIVE 3-VIVIPAROUS1 (ABI3-VP1) family of TFs, which are important for abscisic acid (ABA) signaling (Giraudat et al., 1992; McCarty et al., 1991), and another gene homologous to maize *VP8* regulates ABA accumulation in meristems (Suzuki et al., 2008). ABA response and maintenance of ABA levels are important for meristem development. For example, Arabidopsis *abi3* mutant embryos had SAMs with precocious development of vasculature and leaf primordia more similar to seedling SAMs (Nambara et al., 1995), and maize *vp8* mutants did not survive past embryogenesis and had abnormal SAMs with enlarged cells and

lacking leaf primordia (Suzuki et al., 2008). Maintaining low levels of bioactive gibberellin (GA) is also important for maintenance of meristematic function, and another gene identified in nearly all meristems encodes a GA-inactivating enzyme, GA2-oxidase, that restricts bioactive GA to developing organ primordia in rice and Arabidopsis (reviewed in Shani et al., 2006).

Differences in gene expression between SAM and AXM

To our knowledge, transcriptomic comparison of SAM and vegetative AXM has not been described in grasses prior to this study, and besides a study in pea that compared gene expression of SAM to dormant AXM using an oligonucleotide array representing 7610 genes (Liang et al., 2009), this comparison has also not been described in dicots. Liang and coauthors (2009) identified 27 genes that were differentially expressed at least 2-fold between SAM and AXM, but they concluded that gene expression in SAM and AXM were very similar overall compared to other tissues, such as root apical meristem, leaf, and stem. Using PCoA analysis to compare overall gene expression in SAM and AXM at various stages, we observed that less developed AXM tended to cluster further from SAM tissues but that expression profiles of SAM and AXM converged as AXM development progressed. Not including genes with expression that fluctuated by stage, for example, genes involved in transition to inflorescence meristems, we hypothesized that differences in expression profiles between SAM and less developed AXM would be due to expression of genes that are important for sensing and responding to signaling pathways that regulate lateral branching.

Not surprisingly, very few genes were identified in SAM tissues that were not identified in AXM tissues, indicating that most of the genes expressed in SAM are required for meristem development in general. One of the six genes expressed in SAM but not AXM encoded a protein homologous to LIGHT-RESPONSE BTB 2 (LRB2), which is a strong regulator of photomorphogenesis in Arabidopsis (Christians et al., 2012). LRB2 acts downstream of phytochrome B (phyB) and phyD, possibly by mediating degradation of phyB/D after exposure to high levels of red light. This finding suggests that the SAM has more control of photomorphogenic responses than AXM. Sorghum mutants deficient in phyB do not develop any tillers during vegetative growth but begin developing tillers after flowering, suggesting that photomorphogenic regulation of tiller development only occurs during the vegetative growth period (Kebrom and Mullet, 2016). The LRB2-like gene identified in our study was expressed highest in transitioning SAM and was no longer expressed in SAM that had progressed to a DR INF, suggesting that it regulates flowering time (Fig. 3-2A), but it could potentially be involved in photomorphogenic regulation of tiller development as well.

More genes were identified as being expressed in AXM but not SAM, but it was still a relatively short list (32 genes), indicating that most differences between gene expression in SAM and AXM are probably due to differences in developmental stage. As expected, *Int-C*/*TB1*, which specifically regulates AXB outgrowth, was one of the genes in this list, and two other TCP TFs were also in this list. It is possible that they could function redundantly, as with the TB1 homologs BRANCHED 1 (BRC1) and BRC2 in

Arabidopsis (Aguilar-Martínez et al., 2007), or they could be serving a different role, as TCP TFs have various functions in growth and development.

Six genes encoding wound-induced proteins were part of the cluster containing genes expressed higher in V and LV AXM than other meristems (Cluster 2, Table S3-5), and one was identified as being expressed in AXM but not SAM (Figure 3). Several jasmonate-induced proteins, which are also involved in wound responses, were upregulated in AXMs as well (two in Cluster 1 and three in Cluster 3, Table S3-5). Proteins with wound inducible domains accumulate at sites of wounding and are involved in protecting wounded tissue from pathogen infection (reviewed in Savatin et al., 2014), so it is possible that they have a role in protecting axillary buds from infection. However, it is also possible that they function in developmental regulation as well. For example, oligogalacturonides are signaling molecules involved in both wounding response and cell wall remodeling associated with development, so proteins in signaling pathways associated with these molecules could also be involved in both processes (reviewed in Ferrari et al., 2013). No studies, to our knowledge, have reported any direct links between wound-induced or jasmonate-induced proteins and AXM or lateral branch development, though a few have reported links between changes in gene expression or protein localization and mechanical stress, like stretching or compressing cells or tissues. For example, one study reported that gene expression is impacted by mechanical stress of embryo and endosperm expanding against a sensitive cell layer in the seed coat (Creff et al., 2015), and another study proposed that polarization of the auxin efflux carrier PIN-FORMED1 (PIN1) is regulated by mechanical stress in the SAM (Nakayama et al.,

2012). It is likely that AXM undergo mechanical stress as they push through layers of tissue to grow and develop, whereas the SAM resides in a less constrictive region, so it is possible that overexpression of these genes is merely a byproduct of this increased mechanical stress and does not serve any specific function in AXM development or AXB outgrowth. However, several other studies, besides the two examples above, have reported a link between mechanical stress and development, so it is possible that mechanical stress and expression of genes related to mechanical stress could be important for AXM development or internode elongation.

Six early nodulin-like (ENODL) proteins were identified in the cluster containing genes expressed higher in V and LV AXM than other meristems (Cluster 2, Table S3-5), and three of them were expressed in AXM but not SAM. ENODL proteins have not been characterized much outside of their role in nodulation, though they are expressed in non-nodulating species and are likely involved in transport of hormones, carbohydrates, and other molecules (Denancé et al., 2014). Homozygous T-DNA insertion in an Arabidopsis gene encoding an ENODL protein that localized to phloem resulted in a major reduction in number and size of siliques and a possible reduction in lateral branch number (Khan et al., 2007). In another study, Kebrom and Mullet (2016) reported that ENOD93 expression decreased following growth arrest of AXB in phyB deficient plants, so they postulated that ENOD93 is required for AXB to escape dormancy.

Many genes involved in hypoxic (low oxygen) response and glycolysis were also more highly expressed in V and LV AXM. For example, genes encoding several key glycolysis enzymes were identified in Clusters 2 and 3 (Table S3-5), such as

phosphoenolpyruvate carboxykinase, triosephosphate isomerase, pyruvate kinase, and pyruvate decarboxylase-2. Two genes encoded hypoxia-responsive proteins, and one gene encoded a cysteine oxidase, which acts as an oxygen sensor and regulates stability of group VII ethylene response factors in hypoxic environments in Arabidopsis (Giuntoli and Perata, 2018; White et al., 2018). Increased expression of genes involved in hypoxic response indicates that V and LV AXM reside in hypoxic environments; therefore, glycolysis, which can occur in anaerobic environments, is probably necessary to generate enough ATP for survival and growth. However, glycolysis in hypoxic environments is also important for reducing levels of reactive oxygen species that "leak" from the electron transport chain under hypoxic conditions (reviewed in Loscalzo, 2016). Oxidation-reduction is an integral component of glycolysis and hypoxic response and was the only enriched GO biological process in Cluster 2 (Fig. 4). As with wound-induced genes, hypoxia and enhanced expression of genes related to hypoxia in AXM compared to SAM could be a byproduct of location within the plant, but it is also possible that these genes are important for AXM development. In maize for example, Kelliher and Walbot (2012) showed that a hypoxic environment induces germ cell formation in maize, indicating that hypoxic conditions are important for normal development in some tissues.

Expression patterns of genes known to influence lateral branching in barley

Interestingly, of the five known barley tillering genes isolated to-date, four were identified in this study either as genes differentially expressed in AXM compared to SAM or meristems compared to non-meristem tissues. The fifth known tillering gene,

ELI-A, is classified as a low confidence transposable element and would not have been identified in this study, as only high confidence gene models were used for alignments. As previously mentioned, *INT-C*, the ortholog of maize *TB1*, was not expressed in SAM and was highly expressed in EV AXM (Cluster 1, Figure 4), with expression decreasing as development progressed. No or very low *INT-C* expression in LV and T AXM suggests that they are no longer dormant, as TB1 is a known inhibitor of AXB outgrowth and its expression has been shown to decrease in non-dormant axillary buds in sorghum (Kebrom et al., 2006). Loss-of-function mutations in *CUL4* and *JUBEL2* result in low tillering with reduced AXM initiation, and both genes were expressed highest in EV AXM (Cluster 1, Figure 4). Identification of these known tillering genes suggests that other genes in Cluster 1 may also be involved in AXM initiation or dormancy release. Loss-of-function mutations in *MND* result in the high tillering *mnd4*/*mnd6* mutants. *MND* was expressed in all meristems but was more highly expressed in vegetative SAM than other tissues. *MND* encodes a CYP78A cytochrome P450 homologous to rice *PLASTOCHRON1* (*PLA1*), and *pla1* mutants are phenotypically similar to *mnd4*/*mnd6* mutants, suggesting that it regulates vegetative growth rate (Mascher et al., 2014).

Genes upregulated in ligules and AXM may function broadly in plant development

CUL4 has been shown to influence development of ligules and AXM, and RNA in-situ hybridization has shown that it is specifically expressed in leaf axils, EV AXM, and ligules (Tavakol et al., 2015). Not surprisingly, *CUL4* was identified in this study in a cluster with higher expression in EV AXM compared to other meristems (Cluster 1, Figure 4) and in another cluster with higher expression in ligules and EV AXM (Cluster

2, Figure 5) compared to leaf tissue. Another gene that encodes a WRKY TF (HORVU3Hr1G060500) homologous to *EXCESSIVE BRANCHES 1* (*EXB1*) in Arabidopsis was identified in the same two clusters as *CUL4*, so it is possible that this gene also influences development of both organs. Like *CUL4*, *EXB1* is expressed in leaf axils in Arabidopsis and loss of expression results in a low-branching phenotype (Guo et al., 2015). Similar expression patterns and mutant phenotypes suggests the possibility that CUL4 and this EXB1-like protein may be involved in the same signaling pathway. Besides *CUL4* and the *EXB1*-like gene, six other genes were also identified in Fig. 4 Cluster 1 in Fig. 5 Cluster 2 that may be important for development of AXM and ligule (Table S3-5).

Our study and others suggest that genes expressed in boundary regions, such as leaf axils where AXM develop, regions between meristematic tissue and organ primordia in meristems, and blade-sheath boundary in leaves, may be important for development of AXM and leaf. For example, previous work showed that maize genes expressed more highly in pre-ligular tissue than blade or sheath tissue were also expressed in leaf axils, and some have a known role in development of different organs, like AXM, leaf primordia, and ligules (Johnston et al., 2014). These authors identified a gene expressed in pre-ligules and leaf axils that encodes a BOP1/2-like protein homologous to *CUL4*, and they also identified a gene homologous to *EXB1* (GRMZM5G812272) that was expressed more highly in pre-ligule than blade (log fold-change 4.68) or sheath (log fold-change 7.31), though there was no information about expression in leaf axils. Two genes identified in the cluster of genes expressed in ligules and all meristems (Cluster 1, Table

S3-5), were homologous to an Arabidopsis gene in the *ALOG* family called *LIGHT-DEPENDENT SHORT HYPOCOTYLS 3* (LSH3), which is highly expressed in boundary regions (Tian et al., 2014). This provides further evidence that genes with higher expression in meristems and ligules may have boundary-specific expression patterns, but further experiments will be necessary to verify these expression patterns and determine whether they are important for development of leaves and meristems.

In summary, we presented evidence that SAM and AXM are generally very similar and that most of the differences in gene expression are likely due to differences in morphological stage. However, we did identify a small number of genes that are specifically expressed in either SAM or AXM, indicating that there are differences between the two meristem types, and identification of known tillering genes upregulated in AXM compared to SAM supports the idea that genes identified in this study may be important for tiller development. We also identified multiple members of some gene families expressed higher in AXM than SAM that have no known role in AXM or lateral branch development, like wound-induced and ENOD families, that could be important for tiller development. Finally, identification of genes known to influence ligule and AXM development also supports that genes in another cluster we identified may be important for development of multiple organ types. Overall, results of this study will enhance our understanding of gene expression underlying development of meristems and ligules in barley and may ultimately highlight new genes and genetic pathways underlying regulation of tiller development in grasses.

Table 3-1. Description of meristem tissues laser microdissected from Bowman and Morex.

Genotype	Seedling Stage (gramene.org)	Stage in Figures	Meristem Type	Meristem Morphological Stage	Relative INT-C/TB1 Expression
Bowman	GRO:0007056-59	Stage 1	SAM	Vegetative SAM	None
Bowman	GRO:0007056-59	Stage 1	T_0 AXM	Vegetative AXM	Moderate
Bowman	GRO:0007060	Stage 2	SAM	Transitioning SAM	None
Bowman	GRO:0007060	Stage 2	T_0 AXM	Late vegetative AXM	Low
Bowman	GRO:0007060	Stage 2	T_1 AXM	Vegetative AXM	Moderate
Morex	GRO:0007059	Stage 1	SAM	Vegetative SAM	None
Morex	GRO:0007059	Stage 1	T_0 AXM	Vegetative AXM	High
Morex	GRO:0007060	Stage 2	SAM	Transitioning SAM	None
Morex	GRO:0007060	Stage 2	T_0 AXM	Late vegetative AXM	None
Morex	GRO:0007060	Stage 2	T_1 AXM	Vegetative AXM	Moderate
Morex	GRO:0007060	Stage 2	T_2 AXM	Early vegetative AXM	Very high
Morex	GRO:0007060	Stage 2	T_3 AXM	Early vegetative AXM	Very high
Morex	GRO:0007061	Stage 3	SAM	Double ridge IM	Very low
Morex	GRO:0007061	Stage 3	T_0 AXM	Transitioning AXM	None
Morex	GRO:0007061	Stage 3	T1 AXM	Transitioning AXM	None
Morex	GRO:0007061	Stage 3	T2 AXM	Late vegetative AXM	None
Morex	GRO:0007061	Stage 3	T3 AXM	Vegetative AXM	High

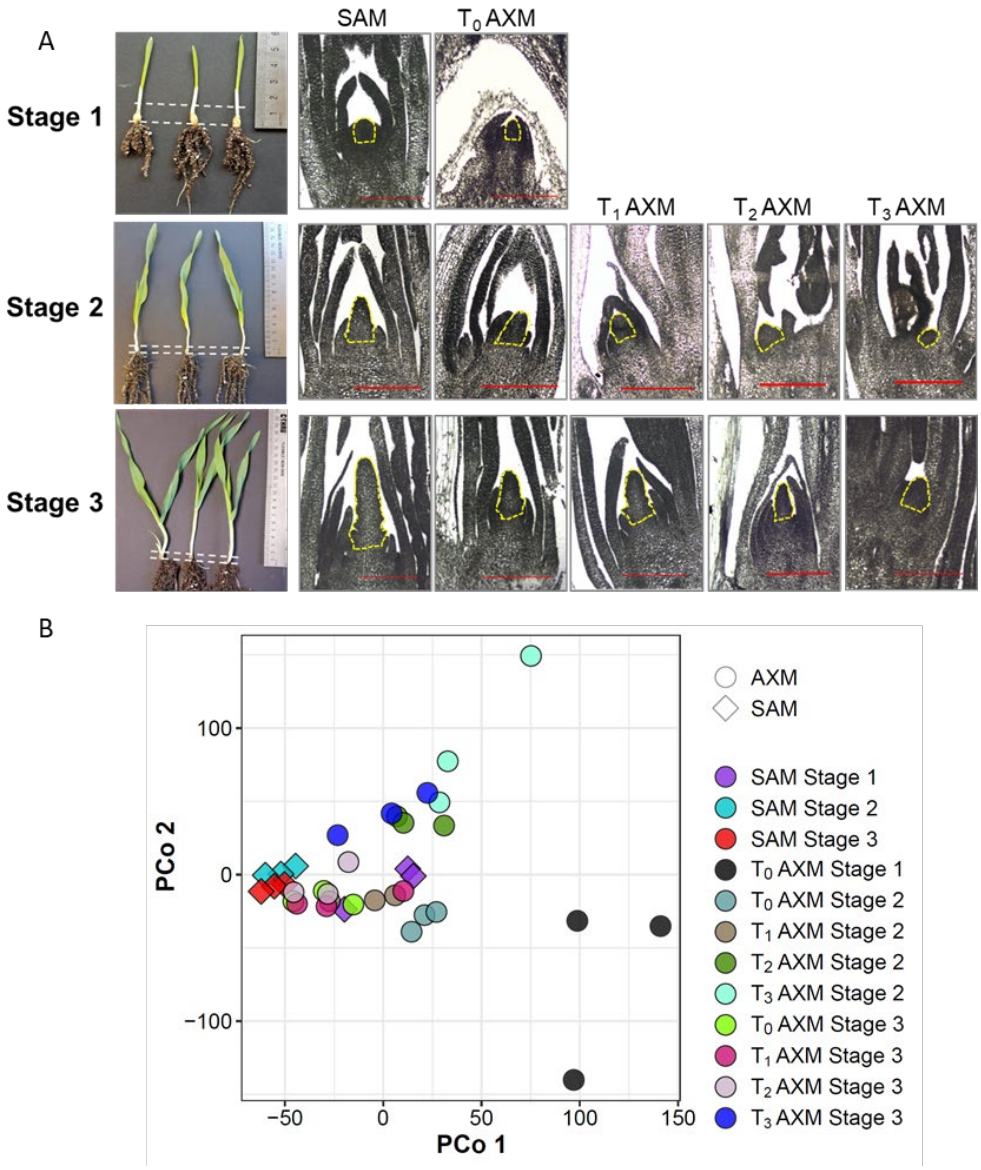

Figure 3-1. Meristem gene expression profiles were differentiated by meristem type and morphology. A) Representative images of Morex seedlings and median sections through meristems at three stages: Stage 1 - GRO:0007059, Stage 2 - GRO:0007060, and Stage 3 - GRO:0007061. White dotted lines on seedlings show crown region that was dissected for meristem tissue, and yellow dotted lines on sections show meristems that were microdissected. Scale bars are 400 μm. B) RNA was extracted from meristem tissue, amplified, and sequenced. Multidimensional scaling was performed using a dissimilarity matrix of normalized log2 counts-per-million for all genes. The first principal coordinate (PCo1) separated meristems by meristem type, shoot apical meristem (SAM) or axillary meristem (AXM), and PCo2 separated meristems primarily by morphology. T_0-T_3 indicates the leaf or coleoptile axil in which the AXM is located (T_0: coleoptile, T_1: first leaf, etc.).

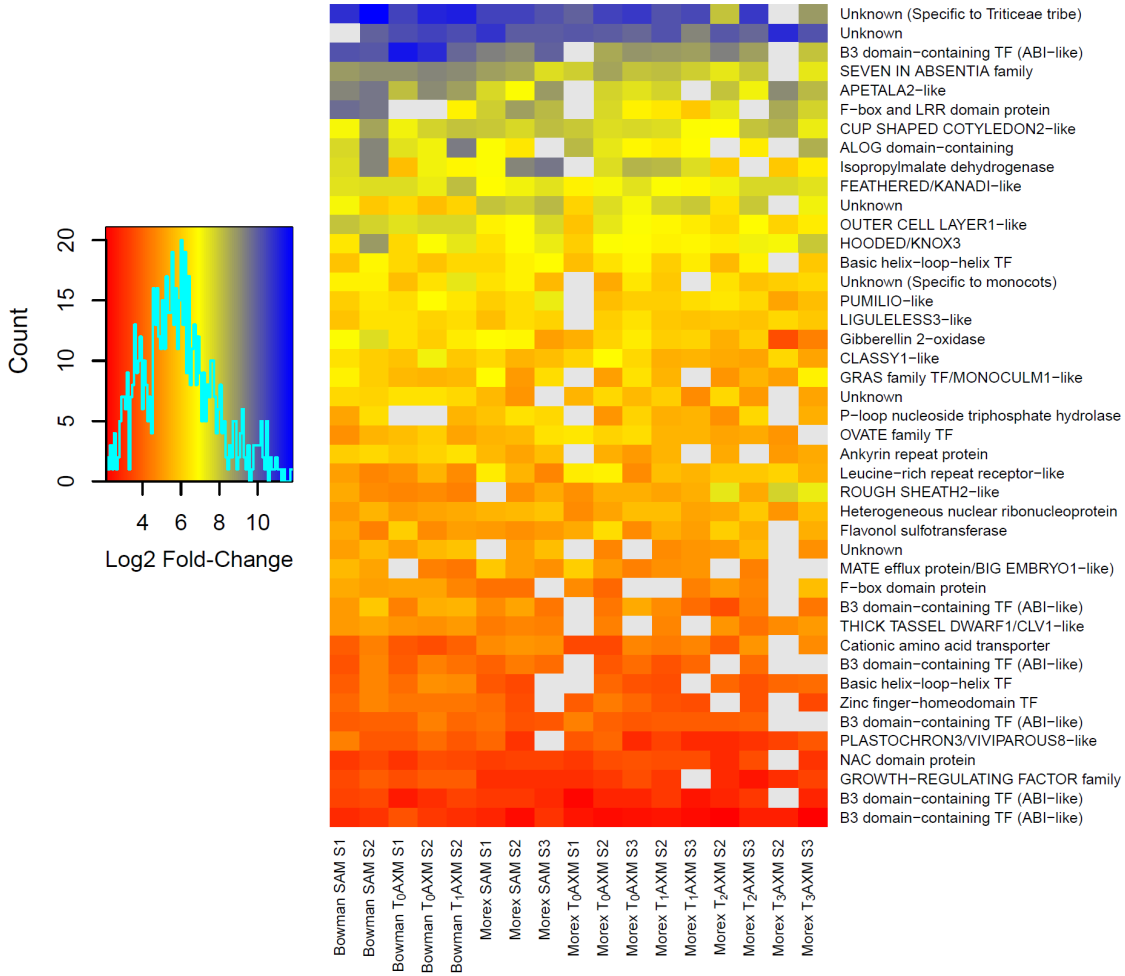

Figure 3-2. Core meristem genes in barley. Meristem-specific genes were identified by comparing individual meristems to non-meristem tissues, and 43 genes that are likely important for meristem maintenance or function were expressed in nearly all meristems regardless of genotype, stage, or whether they were a shoot apical meristem (SAM) or axillary meristem (AXM). Fold-change of normalized log2 counts-per-million for meristems versus non-meristem tissues is shown, and gray boxes indicate genes were not significantly upregulated in that particular meristem. T_0-T_3 indicates the leaf or coleoptile axil in which the AXM is located (T_0: coleoptile, T_1: first leaf, etc.). Abbreviations for protein annotations: transcription factor (TF); abscisic acid insensitive (ABI); leucine-rich repeat (LRR); Arabidopsis LIGHT SENSITIVE HYPOCOTYL1 and Oryza G1 (ALOG); knotted-like Homeobox-like (KNOX); GIBERELLIC-ACID INSENSITIVE, REPRESSOR of GAI, and SCARECROW (GRAS); multi-antimicrobial extrusion (MATE); CLAVATA1 (CLV1); NO APICAL MERISTEM, *Arabidopsis thaliana* activating factor 1/2, CUP SHAPED COTYLEDON 2 (NAC).

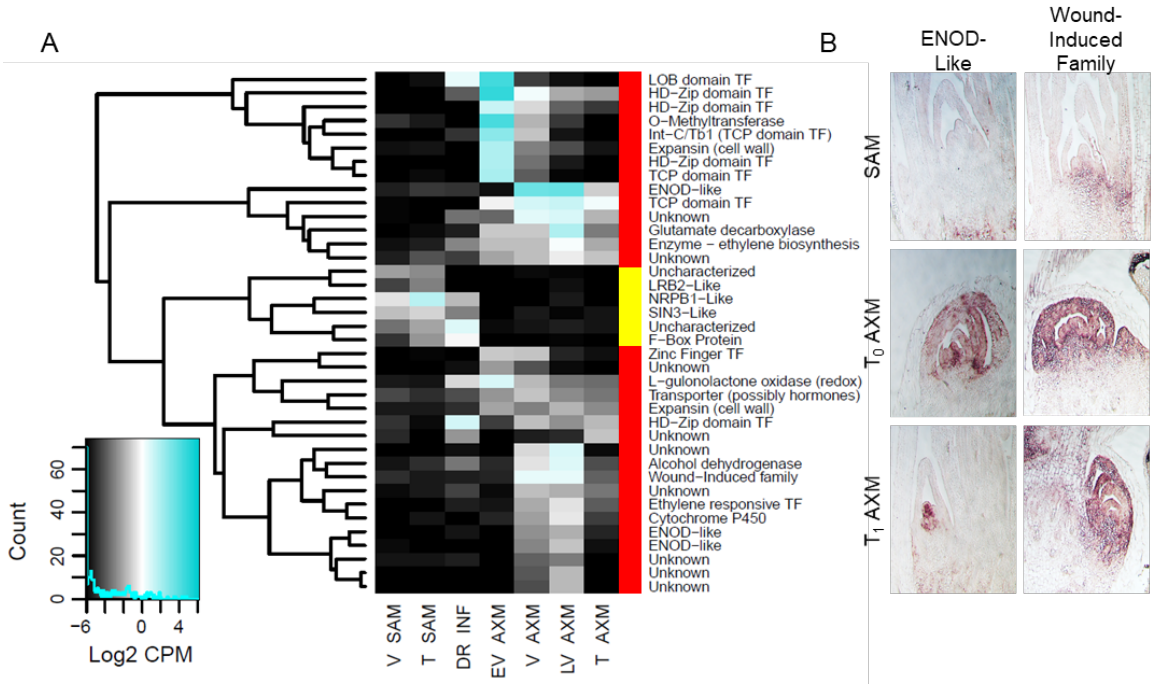

Figure 3-3. Genes expressed only in shoot apical (SAM) or axillary meristems (AXM). A) Normalized counts from Bowman and Morex were used to identify genes that were expressed only in SAM, indicated in the heatmap by a yellow bar, or AXM, indicated by red bars. The criteria for a gene to be considered expressed in AXM but not SAM were as follows: total counts in SAM <= 5, total counts in SAM < 5% of average counts for AXM, and average counts for AXM >= 5. The criteria were the same for considering genes to be expressed in SAM but not AXM, with tissue types reversed. B) RNA in-situ hybridizations in Bowman at Stage 2 (GRO:0007060) of two genes identified as being expressed in AXM but not SAM. One encodes a protein with a wound-inducible domain (HORVU2Hr1G116740), and the other encodes an early nodulin (ENOD)-like protein (HORVU3Hr1G026540).

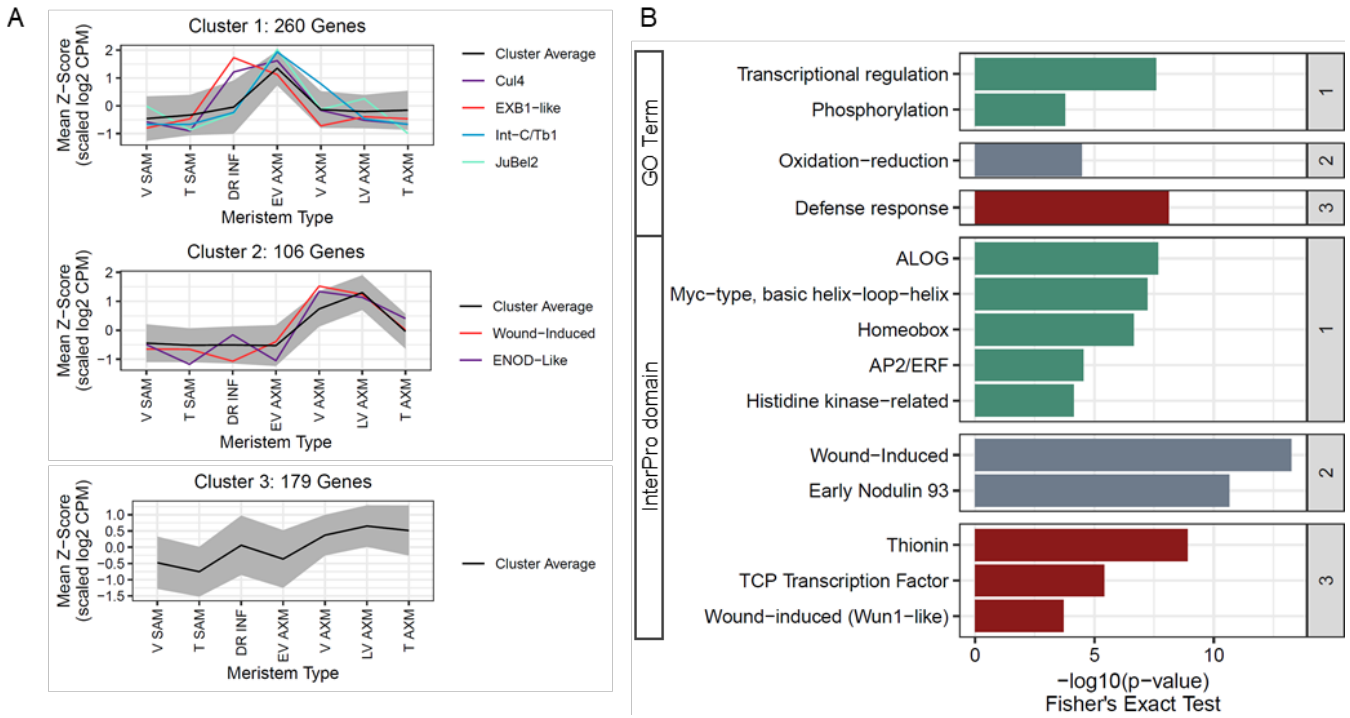

Figure 3-4. Expression clusters containing genes specifically upregulated during early or late axillary meristem (AXM) development. A) Genes were clustered based on scaled, normalized log2 counts-per-million for all meristems laser microdissected from Bowman and Morex, and three clusters were identified in which AXM expression was higher than shoot apical meristem (SAM) expression. Cluster 1 contained genes more highly expressed in early vegetative (EV) AXM compared to other tissues, and three genes in this cluster, *Uniculme 4* (*Cul4*); *Intermedium-C* (*Int-C*), *JuBel2*, have been previously shown to influence tiller development. Cluster 2 contained genes that were more highly expressed in vegetative (V) and late vegetative (LV) AXM, including several genes annotated as wound-induced proteins or early nodulin (ENOD)-like proteins. Cluster 3 contained genes that were more highly expressed in V and LV AXM and double ridge inflorescence meristem (DR INF). B) Gene Ontology (GO) biological processes (top) and InterPro domains (bottom) enriched (FDR-adjusted p-value < 0.01) in Clusters 1 (green bars), 2 (gray bars), and 3 (red bars). Abbreviations: transitioning (T); TB1, CYCLOIDEA (CYC), PROLIFERATING CELL NUCLEAR ANTIGEN FACTOR1 (PCF1) and PCF2 (TCP); EXCESSIVE BRANCHES 1 (EXB1).

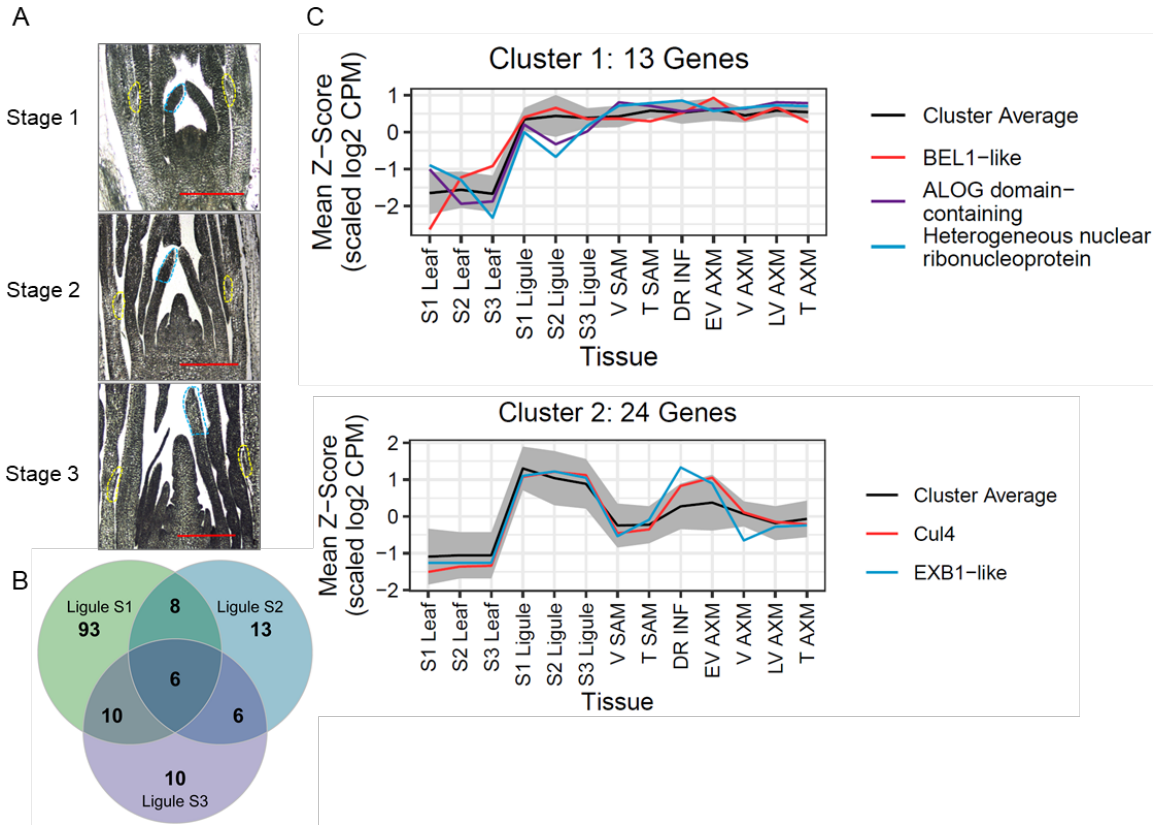

Figure 3-5. Some genes upregulated in ligules compared to leaves have distinct expression patterns in meristems. A) Representative images of median sections through shoot apical meristems (SAM) from which leaf (outlined in blue) and ligule (outlined in yellow) tissue were laser microdissected for RNA sequencing at three stages: Stage (S) 1 - GRO:0007059, S2 - GRO:0007060, and S3 - GRO:0007061. B) Venn diagram shows overlap of genes more highly expressed in ligules than leaves between the three stages. C) Genes more highly expressed in ligules than leaves were clustered based on expression in seedling leaf, ligule, and meristems. Genes in Cluster 1 were expressed similarly in all ligules and meristems, and two genes shown were also in the list of core meristem genes. Genes in Cluster 2 were expressed in all ligules and were more highly expressed in early vegetative axillary meristems. The two genes shown were also part of Cluster 1 from Fig. 3. Abbreviations: Arabidopsis LIGHT SENSITIVE HYPOCOTYL1 and Oryza G1 (ALOG), *Uniculme 4* (*Cul4*).

Supplementary Figure 3-1. Example images and descriptions of stages used to harvest tissue for meristem sections. Morex seedlings are shown. Waddington's (W) stages for shoot apical meristem corresponding to each seedling stage are also shown. For dissections at all stages, roots were cut off, the grain was removed (scutellum was left intact at stage 1), and the bottom 1 cm of shoot tissue was cut off and put immediately into ice-cold acetone for fixing.

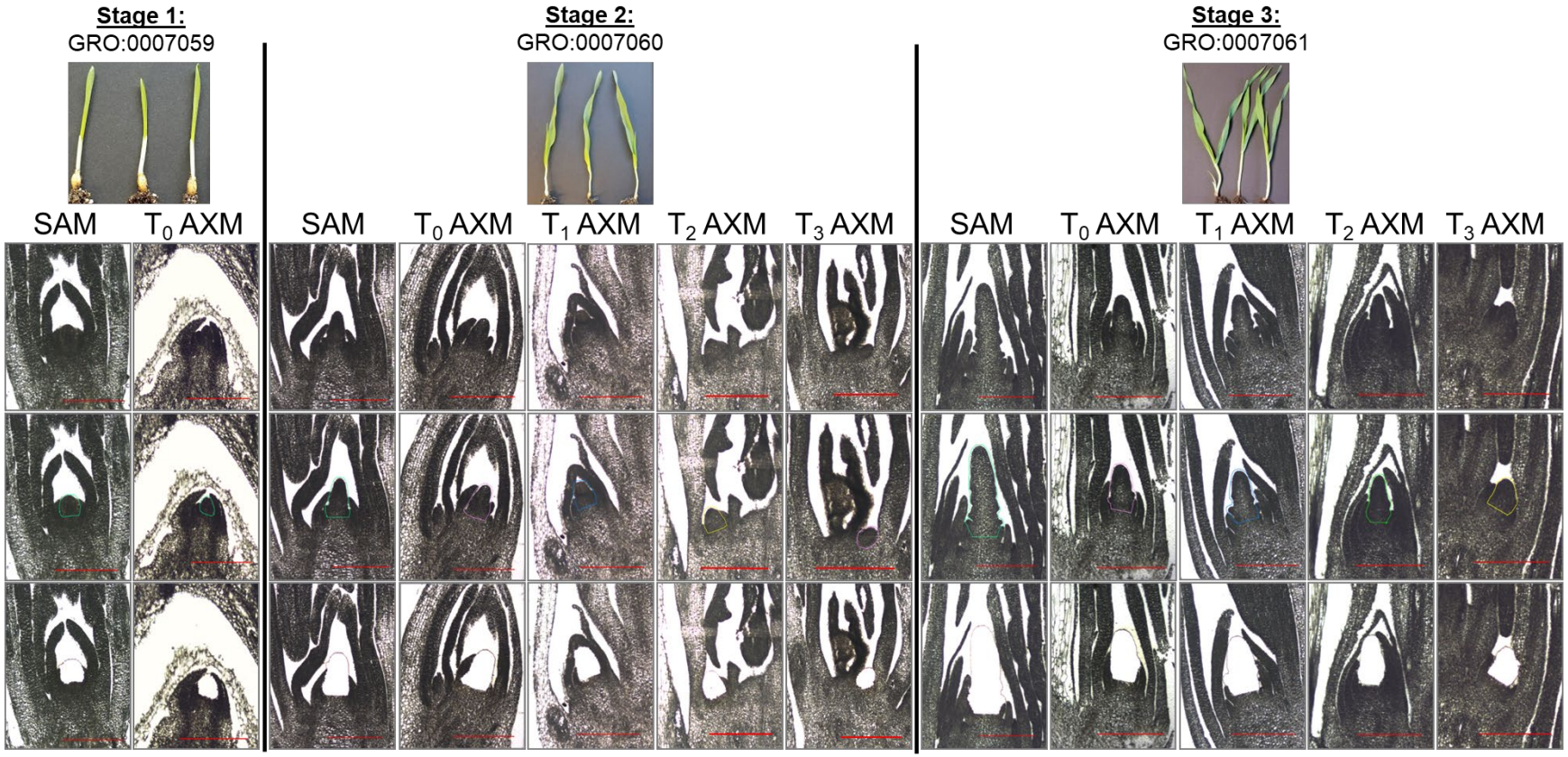

Supplementary Figure 3-2. Representative images of median meristem sections from which meristem tissue was laser microdissected. Top and center images are before laser capture, and center images show outlines indicating the region that was cut. Bottom images are after laser microdissection of meristem tissue.

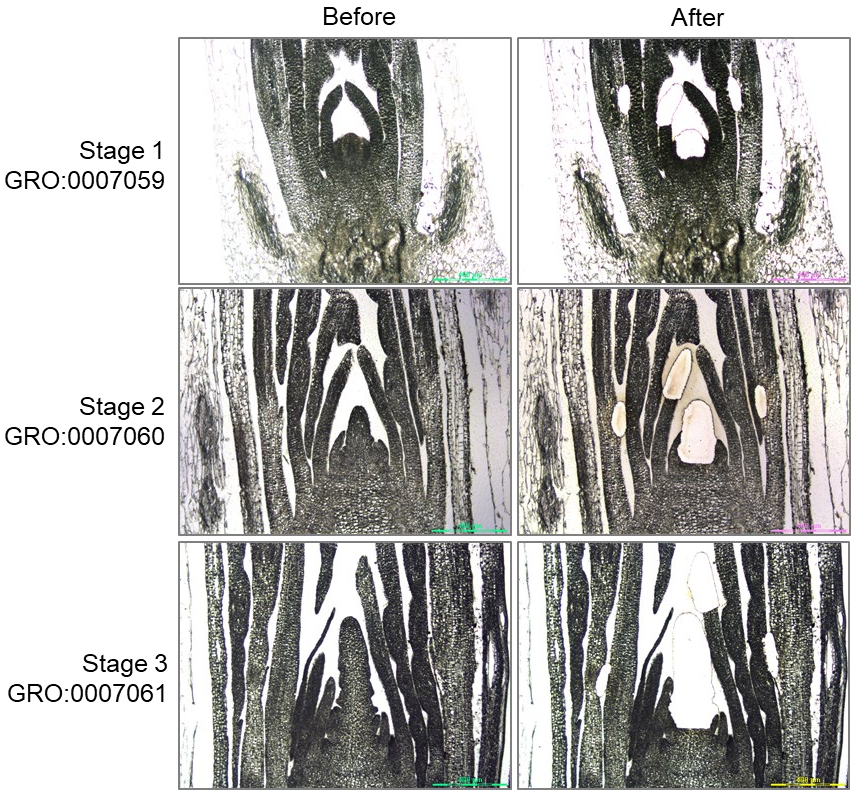

Supplementary Figure 3-3. Before and after images of median meristem sections from which leaf and ligule tissue was laser microdissected. Leaf and ligule tissues were harvested from Morex at three seedling stages.

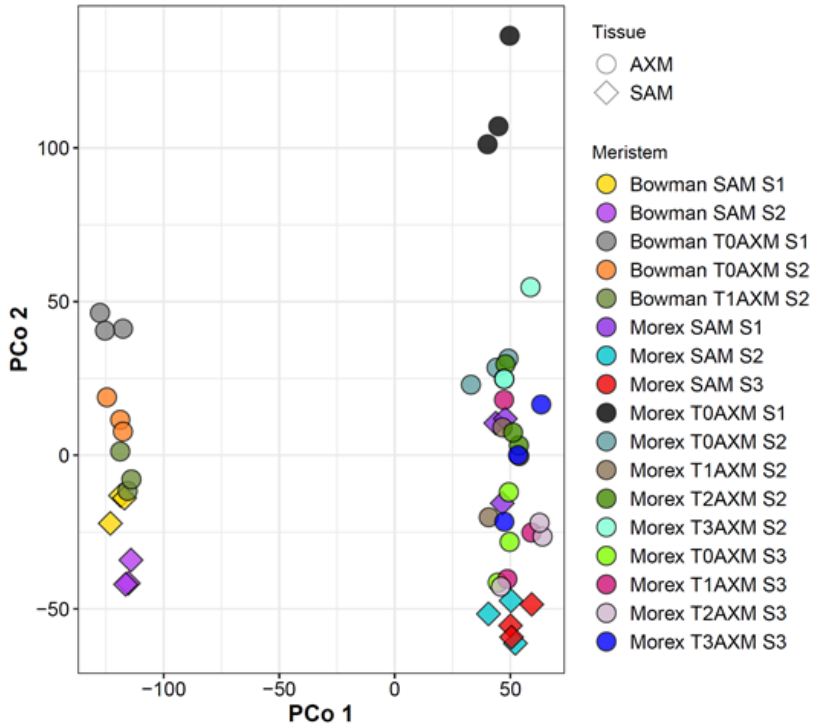

Supplementary Figure 3-4. Meristem gene expression profiles were differentiated primarily by genotype. RNA was extracted from Bowman and Morex meristem tissue, amplified, and sequenced. Multidimensional scaling was performed using a dissimilarity matrix of normalized log2 counts-per-million for all genes. The first principal coordinate (PCo1) separated meristems by genotype. T_0-T_3 indicates the leaf or coleoptile axil in which the AXM is located (T_0: coleoptile, T_1: first leaf, etc.).

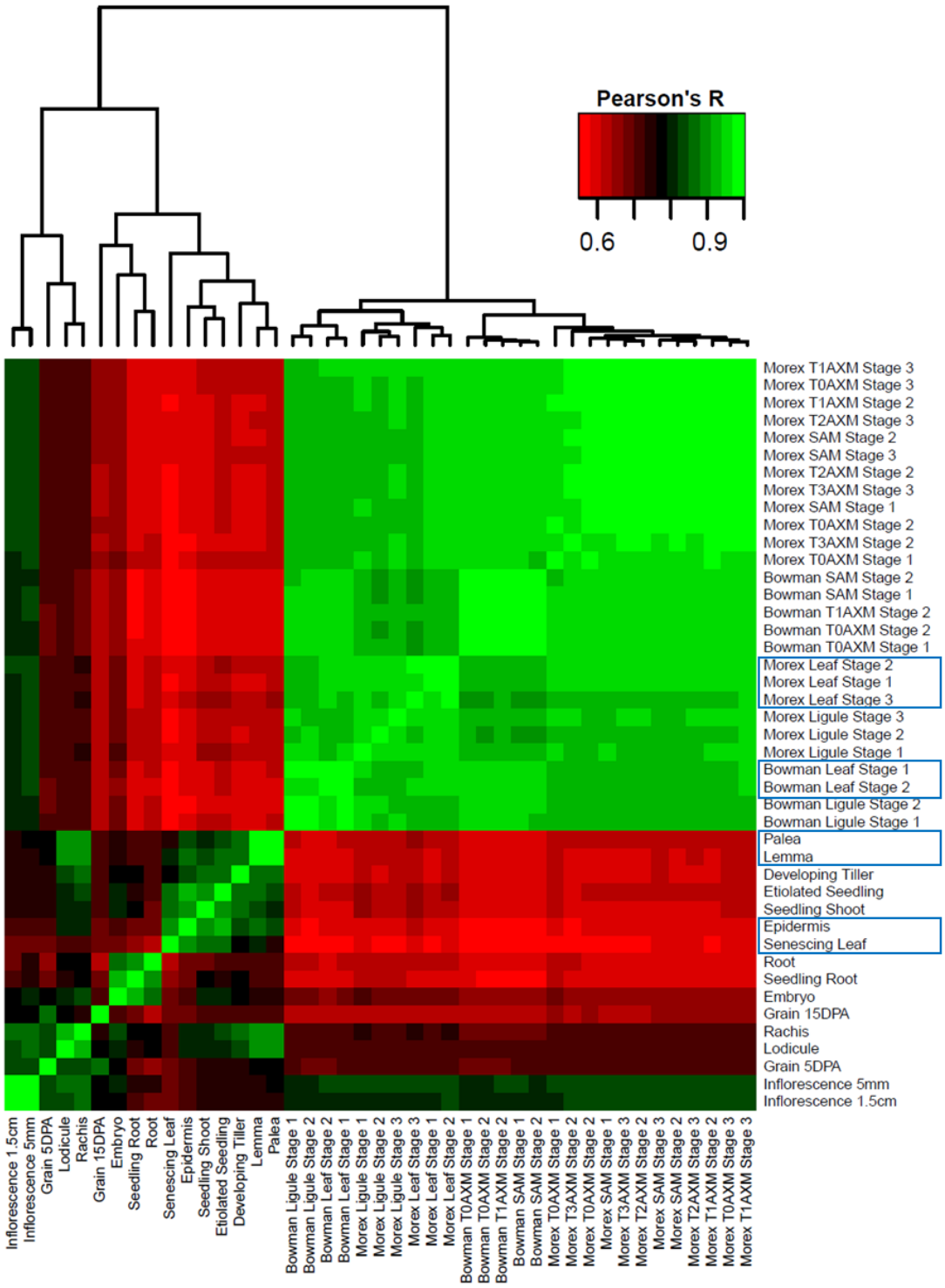

Supplementary Figure 3-5. Correlation of tissue types by expression of all genes. Tissues include laser-microdissected Bowman and Morex seedling tissues and transcriptome data from the Morex Reference Genome. Blue boxes indicate tissues included in pool of non-meristem tissues.

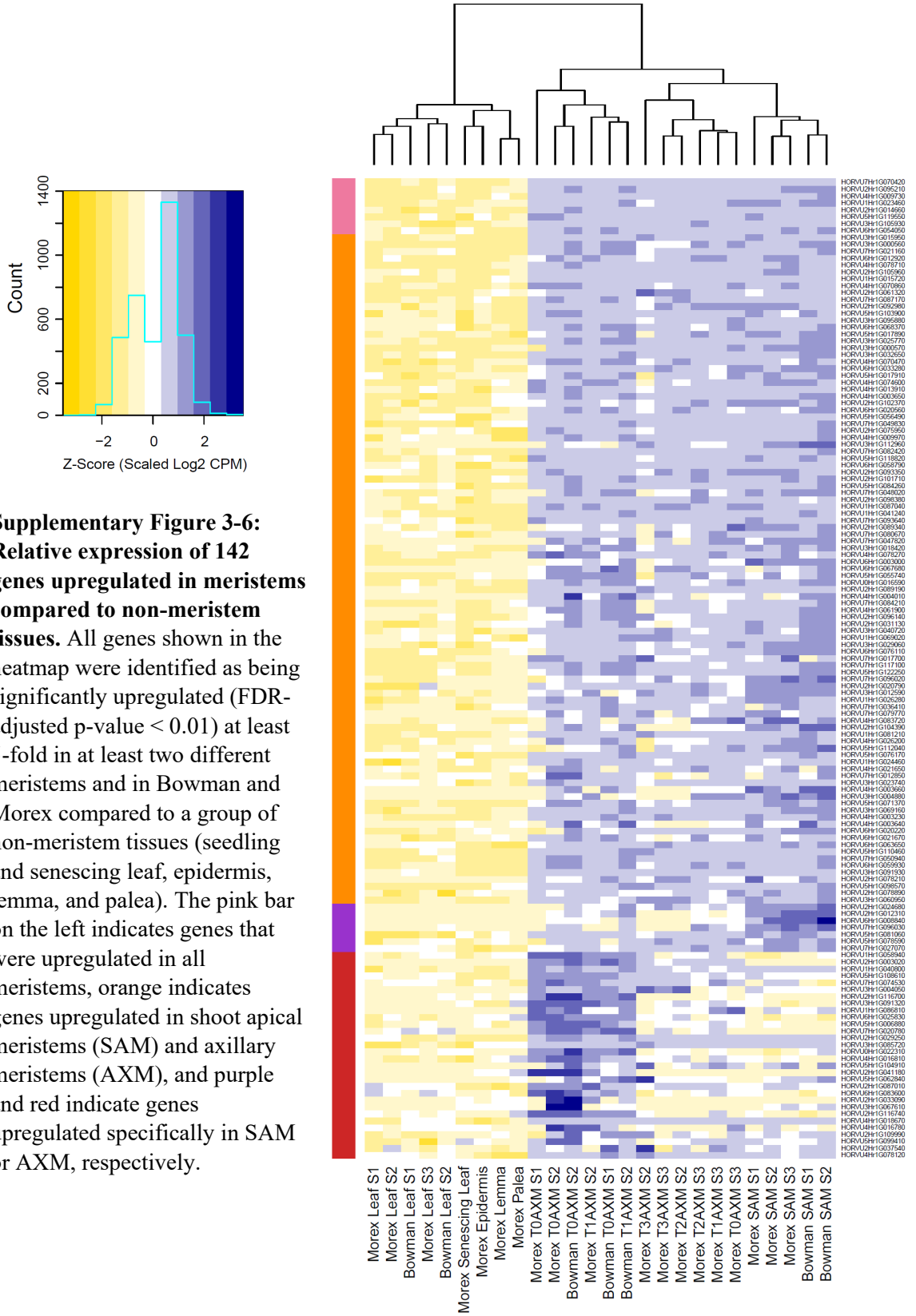

Supplementary Figure 3-6: Relative expression of 142 genes upregulated in meristems compared to non-meristem tissues. All genes shown in the heatmap were identified as being significantly upregulated (FDR-adjusted p-value < 0.01) at least 5-fold in at least two different meristems and in Bowman and Morex compared to a group of non-meristem tissues (seedling and senescing leaf, epidermis, lemma, and palea). The pink bar on the left indicates genes that were upregulated in all meristems, orange indicates genes upregulated in shoot apical meristems (SAM) and axillary meristems (AXM), and purple and red indicate genes upregulated specifically in SAM or AXM, respectively.

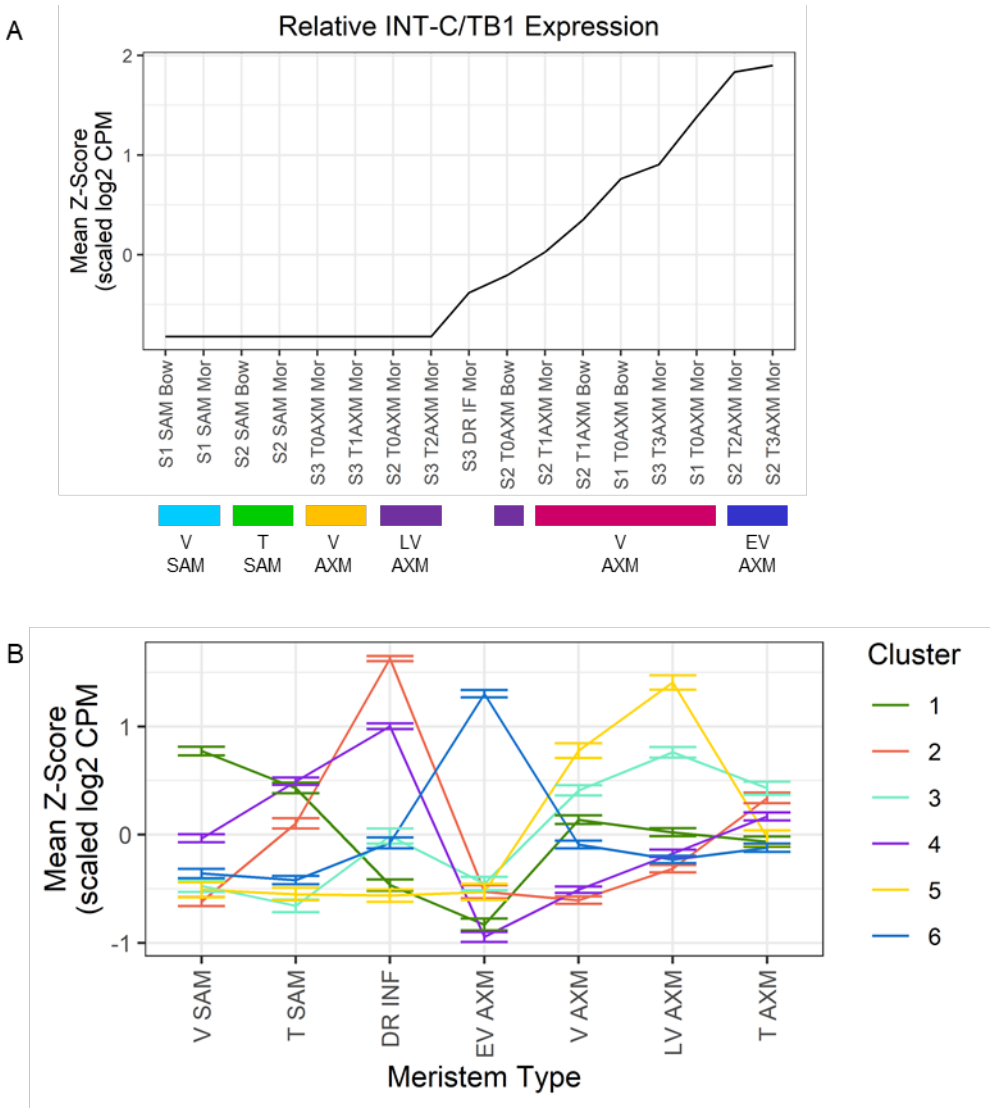

Supplementary Figure 3-7. Clustering of 1477 genes that were differentially expressed between meristems in Bowman and Morex grouped by morphology and relative expression of Int-C/TB1. A) Meristems were grouped visually based on morphology and by relative expression of *Intermedium-C*/*TEOSINTE BRANCHED 1* (*Int-C*/*TB1*), which encodes an inhibitor of vegetative axillary meristem (V AXM) outgrowth. B) Clusters 1 and 2 were expressed highest in double ridge inflorescence meristem (DR INF) and lowest in V and early vegetative (EV) meristems, indicating a possible role in inflorescence development or transition from vegetative to inflorescence meristem. Cluster 1 was expressed highest in vegetative (V), late vegetative (LV), and transitioning (T) meristems. Cluster 3 was expressed highest in V to T AXM. Clusters 3 and 5 were expressed highest in AXM and are the two clusters included in Fig. 4. Cluster 3 (Cluster 2 in Fig. 4) was expressed highest in V and LV AXM, and Cluster 6 (Cluster 1 in Fig. 4) was highly expressed in EV AXM and low in other meristems.

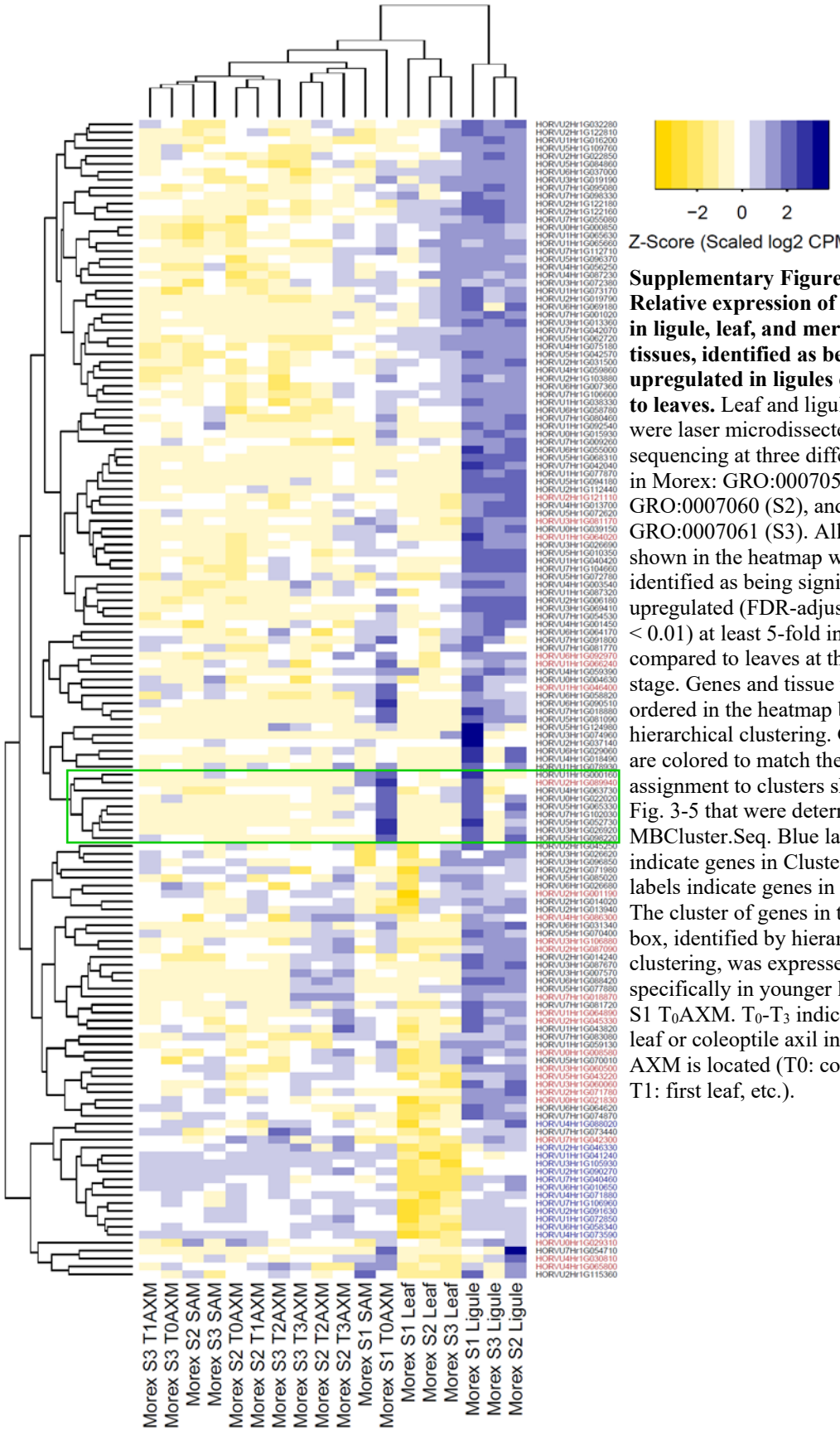

Supplementary Figure 3-8: Relative expression of 146 genes in ligule, leaf, and meristem tissues, identified as being upregulated in ligules compared to leaves. Leaf and ligule tissue were laser microdissected for RNA sequencing at three different stages in Morex: GRO:0007059 (S1), GRO:0007060 (S2), and GRO:0007061 (S3). All genes shown in the heatmap were identified as being significantly upregulated (FDR-adjusted p-value < 0.01) at least 5-fold in ligules compared to leaves at the same stage. Genes and tissue types were ordered in the heatmap based on hierarchical clustering. Gene labels are colored to match their assignment to clusters shown in Fig. 3-5 that were determined using MBCluster.Seq. Blue labels indicate genes in Cluster 1 and red labels indicate genes in Cluster 2. The cluster of genes in the green box, identified by hierarchical clustering, was expressed highest specifically in younger ligules and S1 T_0AXM. T_0-T_3 indicates the leaf or coleoptile axil in which the AXM is located (T0: coleoptile, T1: first leaf, etc.).

References

Aguilar-Martínez, J.A., Poza-Carrión, C., and Cubas, P. (2007). Arabidopsis BRANCHED1 acts as an integrator of branching signals within axillary buds. The Plant Cell *19*, 458–472.

Aida, M., Ishida, T., Fukaki, H., Fujisawa, H., and Tasaka, M. (1997). Genes involved in organ separation in Arabidopsis: an analysis of the *cup-shaped cotyledon* mutant. The Plant Cell *9*, 841–857.

Aida, M., Ishida, T., and Tasaka, M. (1999). Shoot apical meristem and cotyledon formation during Arabidopsis embryogenesis: interaction among the *CUP-SHAPED COTYLEDON* and *SHOOT MERISTEMLESS* genes. Development *126*, 1563–1570.

Alqudah, A.M., and Schnurbusch, T. (2014). Awn primordium to tipping is the most decisive developmental phase for spikelet survival in barley. Functional Plant Biol. *41*, 424–436.

Alqudah, A.M., and Schnurbusch, T. (2015). Barley Leaf Area and Leaf Growth Rates Are Maximized during the Pre-Anthesis Phase. Agronomy *5*, 107–129.

Alqudah, A.M., Koppolu, R., Wolde, G.M., Graner, A., and Schnurbusch, T. (2016). The Genetic Architecture of Barley Plant Stature. Front. Genet. *7*.

Anderson, P., Oelke, A.E., and Simmons, S.R. (2013). Growth and Development Guide for Spring Barley (Regents of the University of Minnesota).

Andrés, F., and Coupland, G. (2012). The genetic basis of flowering responses to seasonal cues. Nat Rev Genet *13*, 627–639.

Aspinall, D. (1961). The control of tillering in the barley plant 1. The pattern of tillering and its relation to nutrient supply. Australian Journal of Biological Sciences *14*, 493–505.

Aspinall, D. (1963). The control of tillering in the barley plant II. The control of tiller-bud growth during ear development. Australian Journal of Biological Sciences *16*, 285–304.

Aspinall, D., Nicholls, P., and May, L. (1964). The effects of soil moisture stress on the growth of barley. I. Vegetative development and grain yield. Australian Journal of Agricultural Research *15*, 729–729.

Babb, S., and Muehlbauer, G.J. (2003). Genetic and morphological characterization of the barley *uniculm2* (*cul2*) mutant. TAG. Theoretical and Applied Genetics. Theoretische Und Angewandte Genetik *106*, 846–857.

Balla, J., Kalousek, P., Reinöhl, V., Friml, J., and Procházka, S. (2011). Competitive canalization of PIN-dependent auxin flow from axillary buds controls pea bud outgrowth. The Plant Journal : For Cell and Molecular Biology *65*, 571–577.

Barley, R., and Waites, R. (2002). Plant Meristems: The Interplay of KNOX and Gibberellins. Current Biology *12*, R696–R698.

Barrett, J.C., Fry, B., Maller, J., and Daly, M.J. (2005). Haploview: analysis and visualization of LD and haplotype maps. Bioinformatics *21*, 263–265.

Barton, M.K. (2010). Twenty years on: The inner workings of the shoot apical meristem, a developmental dynamo. Developmental Biology *341*, 95–113.

Bayer, M.M., Rapazote-Flores, P., Ganal, M., Hedley, P.E., Macaulay, M., Plieske, J., Ramsay, L., Russell, J., Shaw, P.D., Thomas, W., et al. (2017). Development and Evaluation of a Barley 50k iSelect SNP Array. Frontiers in Plant Science *8*, e1792.

Beier, S., Himmelbach, A., Colmsee, C., Zhang, X.-Q., Barrero, R.A., Zhang, Q., Li, L., Bayer, M., Bolser, D., Taudien, S., et al. (2017). Construction of a map-based reference genome sequence for barley, *Hordeum vulgare* L. Scientific Data *4*, 170044.

Benbelkacem, A., Mekni, M.S., and Rasmussen, D.C. (1984). Breeding for high tiller number and yield in barley. Crop Science *24*.

Bennett, T., Sieberer, T., Willett, B., Booker, J., Luschnig, C., and Leyser, O. (2006). The *Arabidopsis MAX* pathway controls shoot branching by regulating auxin transport. Current Biology : CB *16*, 553–563.

Berger, Y., Harpaz-Saad, S., Brand, A., Melnik, H., Sirding, N., Alvarez, J.P., Zinder, M., Samach, A., Eshed, Y., and Ori, N. (2009). The NAC-domain transcription factor GOBLET specifies leaflet boundaries in compound tomato leaves. Development *136*, 823–832.

Beveridge, C.A. (2006). Axillary bud outgrowth: sending a message. Current Opinion in Plant Biology *9*, 35–40.

Beveridge, C.A., Mathesius, U., Rose, R.J., and Gresshoff, P.M. (2007). Common regulatory themes in meristem development and whole-plant homeostasis. Current Opinion in Plant Biology *10*, 44–51.

Bilsborough, G.D., Runions, A., Barkoulas, M., Jenkins, H.W., Hasson, A., Galinha, C., Laufs, P., Hay, A., Prusinkiewicz, P., and Tsiantis, M. (2011). Model for the regulation of *Arabidopsis thaliana* leaf margin development. PNAS *108*, 3424–3429.

Blein, T., Pulido, A., Vialette-Guiraud, A., Nikovics, K., Morin, H., Hay, A., Johansen, I.E., Tsiantis, M., and Laufs, P. (2008). A Conserved Molecular Framework for Compound Leaf Development. Science *322*, 1835–1839.

Boden, S.A., Weiss, D., Ross, J.J., Davies, N.W., Trevaskis, B., Chandler, P.M., and Swain, S.M. (2014). EARLY FLOWERING3 Regulates Flowering in Spring Barley by Mediating Gibberellin Production and *FLOWERING LOCUS T* Expression. The Plant Cell *26*, 1557–1569.

Bolduc, N., and Hake, S. (2009). The Maize Transcription Factor KNOTTED1 Directly Regulates the Gibberellin Catabolism Gene *ga2ox1*. Plant Cell *21*, 1647–1658.

Bonnett, O.T. Inflorescences of Maize, Wheat, Rye, Barley, and Oats: Their Initiation and Development. Journal of Agricultural Research *60*, 25–38.

Bradbury, P.J., Zhang, Z., Kroon, D.E., Casstevens, T.M., Ramdoss, Y., and Buckler, E.S. (2007). TASSEL: software for association mapping of complex traits in diverse samples. Bioinformatics *23*, 2633–2635.

Bull, H., Casao, M.C., Zwirek, M., Flavell, A.J., Thomas, W.T.B., Guo, W., Zhang, R., Rapazote-Flores, P., Kyriakidis, S., Russell, J., et al. (2017). Barley *SIX-ROWED SPIKE3* encodes a putative Jumonji C-type H3K9me2/me3 demethylase that represses lateral spikelet fertility. Nature Communications *8*, 936.

Byrne, M.E. (2003). Phyllotactic pattern and stem cell fate are determined by the Arabidopsis homeobox gene *BELLRINGER*. Development *130*, 3941–3950.

Calixto, C.P.G., Waugh, R., and Brown, J.W.S. (2015). Evolutionary Relationships Among Barley and Arabidopsis Core Circadian Clock and Clock-Associated Genes. J Mol Evol *80*, 108–119.

Campoli, C., Shtaya, M., Davis, S.J., and von Korff, M. (2012a). Expression conservation within the circadian clock of a monocot: natural variation at barley *Ppd-H1* affects circadian expression of flowering time genes, but not clock orthologs. BMC Plant Biology *12*, 97.

Campoli, C., Drosse, B., Searle, I., Coupland, G., and von Korff, M. (2012b). Functional characterisation of *HvCO1*, the barley (*Hordeum vulgare*) flowering time ortholog of *CONSTANS*. Plant J. *69*, 868–880.

Campoli, C., Pankin, A., Drosse, B., Casao, C.M., Davis, S.J., and von Korff, M. (2013). *HvLUX1* is a candidate gene underlying the early maturity 10 locus in barley: phylogeny, diversity, and interactions with the circadian clock and photoperiodic pathways. New Phytol *199*, 1045–1059.

Chandler, P.M., Marion-Poll, A., Ellis, M., and Gubler, F. (2002). Mutants at the *Slender1* Locus of Barley cv Himalaya. Molecular and Physiological Characterization. Plant Physiol *129*, 181–190.

Chandler, P.M., Harding, C.A., Ashton, A.R., Mulcair, M.D., Dixon, N.E., and Mander, L.N. (2008). Characterization of Gibberellin Receptor Mutants of Barley (*Hordeum vulgare* L.). Molecular Plant *1*, 285–294.

Chono, M., Honda, I., Zeniya, H., Yoneyama, K., Saisho, D., Takeda, K., Takatsuto, S., Hoshino, T., and Watanabe, Y. (2003). A semidwarf phenotype of barley *uzu* results from a nucleotide substitution in the gene encoding a putative brassinosteroid receptor. Plant Physiology *133*, 1209–1219.

Christians, M.J., Gingerich, D.J., Hua, Z., Lauer, T.D., and Vierstra, R.D. (2012). The Light-Response BTB1 and BTB2 Proteins Assemble Nuclear Ubiquitin Ligases That Modify Phytochrome B and D Signaling in Arabidopsis. Plant Physiology *160*, 118–134.

Comadran, J., Kilian, B., Russell, J., Ramsay, L., Stein, N., Ganal, M., Shaw, P., Bayer, M., Thomas, W., Marshall, D., et al. (2012). Natural variation in a homolog of Antirrhinum *CENTRORADIALIS* contributed to spring growth habit and environmental adaptation in cultivated barley. Nat Genet *44*, 1388–1392.

Creff, A., Brocard, L., and Ingram, G. (2015). A mechanically sensitive cell layer regulates the physical properties of the Arabidopsis seed coat. Nature Communications *6*, 6382.

Dabbert, T., Okagaki, R.J., Cho, S., Boddu, J., and Muehlbauer, G.J. (2009). The genetics of barley low-tillering mutants: *absent lower laterals* (*als*). TAG. Theoretical and Applied Genetics. Theoretische Und Angewandte Genetik *118*, 1351–1360.

Dabbert, T., Okagaki, R.J., Cho, S., Heinen, S., Boddu, J., and Muehlbauer, G.J. (2010). The genetics of barley low-tillering mutants: *low number of tillers-1* (*lnt1*). TAG. Theoretical and Applied Genetics. Theoretische Und Angewandte Genetik *121*, 705–715.

Davis, M.H., and Simmons, S.R. (1994). Tillering response of barley to shifts in light quality caused by neighboring plants. Crop Science *34*, 1604–1604.

Denancé, N., Szurek, B., and Noël, L.D. (2014). Emerging functions of nodulin-like proteins in non-nodulating plant species. Plant Cell Physiol. *55*, 469–474.

Digel, B., Pankin, A., and von Korff, M. (2015). Global Transcriptome Profiling of Developing Leaf and Shoot Apices Reveals Distinct Genetic and Environmental Control of Floral Transition and Inflorescence Development in Barley. The Plant Cell tpc.15.00203.

Digel, B., Tavakol, E., Verderio, G., Tondelli, A., Xu, X., Cattivelli, L., Rossini, L., and Korff, M. von (2016). Photoperiod-H1 (Ppd-H1) Controls Leaf Size. Plant Physiology *172*, 405–415.

Doebley, J., Stec, A., and Gustus, C. (1995). *teosinte branched1* and the origin of maize: evidence for epistasis and the evolution of dominance. Genetics *141*, 333–346.

Döring, H.-P., Lin, J., Uhrig, H., and Salamini, F. (1999). Clonal analysis of the development of the barley (*Hordeum vulgare* L.) leaf using periclinal chlorophyll chimeras. Planta *207*, 335–342.

Druka, A., Franckowiak, J., Lundqvist, U., Bonar, N., Alexander, J., Houston, K., Radovic, S., Shahinnia, F., Vendramin, V., Morgante, M., et al. (2011). Genetic Dissection of Barley Morphology and Development. Plant Physiol. *155*, 617–627.

Dun, E.A., Brewer, P.B., and Beveridge, C.A. (2009). Strigolactones: discovery of the elusive shoot branching hormone. Trends in Plant Science *14*, 364–372.

Earl, D.A., and vonHoldt, B.M. (2012). STRUCTURE HARVESTER: a website and program for visualizing STRUCTURE output and implementing the Evanno method. Conservation Genet Resour *4*, 359–361.

van Esse, G.W., Walla, A., Finke, A., Koornneef, M., Pecinka, A., and von Korff, M. (2017). *Six-rowed spike 3* (*VRS3*) is a histone demethylase that controls lateral spikelet development in barley. Plant Physiology pp.00108.2017.

Evanno, G., Regnaut, S., and Goudet, J. (2005). Detecting the number of clusters of individuals using the software STRUCTURE: a simulation study. Mol. Ecol. *14*, 2611–2620.

Faure, S., Higgins, J., Turner, A., and Laurie, D.A. (2007). The *FLOWERING LOCUS T-Like* Gene Family in Barley (*Hordeum vulgare*). Genetics *176*, 599–609.

Ferrari, S., Savatin, D.V., Sicilia, F., Gramegna, G., Cervone, F., and De Lorenzo, G. (2013). Oligogalacturonides: plant damage-associated molecular patterns and regulators of growth and development. Front. Plant Sci. *4*.

Finlayson, S.A. (2007). Arabidopsis Teosinte Branched1-like 1 regulates axillary bud outgrowth and is homologous to monocot Teosinte Branched1. Plant & Cell Physiology *48*, 667–677.

Fletcher, G.M., and Dale, J.E. (1974). Growth of Tiller Buds in Barley: Effects of Shade Treatment and Mineral Nutrition. Ann. Bot. *38*, 63–76.

Flintham, J.E., Börner, A., Worland, A.J., and Gale, M.D. (1997). Optimizing wheat grain yield: effects of *Rht* (gibberellin-insensitive) dwarfing genes. The Journal of Agricultural Science *128*, 11–25.

Ford, B., Deng, W., Clausen, J., Oliver, S., Boden, S., Hemming, M., and Trevaskis, B. (2016). Barley (*Hordeum vulgare*) circadian clock genes can respond rapidly to temperature in an EARLY FLOWERING 3-dependent manner. J Exp Bot *67*, 5517–5528.

Forster, B.P., Franckowiak, J.D., Lundqvist, U., Lyon, J., Pitkethly, I., and Thomas, W.T.B. (2007). The Barley Phytomer. Ann Bot *100*, 725–733.

Friml, J., Yang, X., Michniewicz, M., Weijers, D., Quint, A., Tietz, O., Benjamins, R., Ouwerkerk, P.B.F., Ljung, K., Sandberg, G., et al. (2004). A PINOID-Dependent Binary Switch in Apical-Basal PIN Polar Targeting Directs Auxin Efflux. Science *306*, 862–865.

Fu, D., Szűcs, P., Yan, L., Helguera, M., Skinner, J.S., Zitzewitz, J. von, Hayes, P.M., and Dubcovsky, J. (2005). Large deletions within the first intron in *VRN-1* are associated with spring growth habit in barley and wheat. Mol Genet Genomics *273*, 54–65.

Gallavotti, A., Zhao, Q., Kyozuka, J., Meeley, R.B., Ritter, M.K., Doebley, J.F., Pè, M.E., and Schmidt, R.J. (2004). The role of *barren stalk1* in the architecture of maize. Nature *432*, 630–635.

Gallavotti, A., Yang, Y., Schmidt, R.J., and Jackson, D. (2008). The Relationship between auxin transport and maize branching. Plant Physiology *147*, 1913–1923.

Gälweiler, L. (1998). Regulation of Polar Auxin Transport by AtPIN1 in Arabidopsis Vascular Tissue. Science *282*, 2226–2230.

García del Moral, M.B., and García del Moral, L.F. (1995). Tiller production and survival in relation to grain yield in winter and spring barley. Field Crops Research *44*, 85–93.

Giraudat, J., Hauge, B.M., Valon, C., Smalle, J., Parcy, F., and Goodman, H.M. (1992). Isolation of the Arabidopsis *ABI3* gene by positional cloning. Plant Cell *4*, 1251–1261.

Giuntoli, B., and Perata, P. (2018). Group VII Ethylene Response Factors in Arabidopsis: Regulation and Physiological Roles. Plant Physiology *176*, 1143–1155.

Gomez-Roldan, V., Fermas, S., Brewer, P.B., Puech-Pagès, V., Dun, E.A., Pillot, J.-P., Letisse, F., Matusova, R., Danoun, S., Portais, J.-C., et al. (2008). Strigolactone inhibition of shoot branching. Nature *455*, 189–194.

Greb, T., Clarenz, O., Schafer, E., Muller, D., Herrero, R., Schmitz, G., and Theres, K. (2003). Molecular analysis of the *LATERAL SUPPRESSOR* gene in Arabidopsis reveals a

conserved control mechanism for axillary meristem formation. Genes & Development *17*, 1175–1187.

Griffiths, S., Dunford, R.P., Coupland, G., and Laurie, D.A. (2003). The Evolution of *CONSTANS-Like* Gene Families in Barley, Rice, and Arabidopsis. Plant Physiology *131*, 1855–1867.

Guitard, A.A. (1960). The Influence of Variety, Temperature, and Stage of Growth on the Response of Spring Barley to Photoperiod. Can. J. Plant Sci. *40*, 65–80.

Guo, D., Zhang, J., Wang, X., Han, X., Wei, B., Wang, J., Li, B., Yu, H., Huang, Q., Gu, H., et al. (2015). The WRKY Transcription Factor WRKY71/EXB1 Controls Shoot Branching by Transcriptionally Regulating *RAX* Genes in Arabidopsis. The Plant Cell *27*, 3112–3127.

Hake, S., Smith, H.M.S., Holtan, H., Magnani, E., Mele, G., and Ramirez, J. (2004). The Role of *Knox* Genes in Plant Development. Annual Review of Cell and Developmental Biology *20*, 125–151.

Hay, A., and Tsiantis, M. (2010). *KNOX* genes: versatile regulators of plant development and diversity. Development *137*, 3153–3165.

Hay, A., Kaur, H., Phillips, A., Hedden, P., Hake, S., and Tsiantis, M. (2002). The Gibberellin Pathway Mediates KNOTTED1-Type Homeobox Function in Plants with Different Body Plans. Current Biology *12*, 1557–1565.

Helliwell, C.A., Chandler, P.M., Poole, A., Dennis, E.S., and Peacock, W.J. (2001). The CYP88A cytochrome P450, ent-kaurenoic acid oxidase, catalyzes three steps of the gibberellin biosynthesis pathway. PNAS *98*, 2065–2070.

Heng, Y., Wu, C., Long, Y., Luo, S., Ma, J., Chen, J., Liu, J., Zhang, H., Ren, Y., Wang, M., et al. (2018). OsALMT7 Maintains Panicle Size and Grain Yield in Rice by Mediating Malate Transport. The Plant Cell tpc.00998.2017.

Hill, W.G., and Weir, B.S. (1988). Variances and covariances of squared linkage disequilibria in finite populations. Theoretical Population Biology *33*, 54–78.

Honsdorf, N., March, T.J., Berger, B., Tester, M., and Pillen, K. (2014). High-Throughput Phenotyping to Detect Drought Tolerance QTL in Wild Barley Introgression Lines. PLOS ONE *9*, e97047.

Houston, K., McKim, S.M., Comadran, J., Bonar, N., Druka, I., Uzrek, N., Cirillo, E., Guzy-Wrobelska, J., Collins, N.C., Halpin, C., et al. (2013). Variation in the interaction between alleles of *HvAPETALA2* and microRNA172 determines the density of grains on the barley inflorescence. Proc Natl Acad Sci U S A *110*, 16675–16680.

Huang, X., Qian, Q., Liu, Z., Sun, H., He, S., Luo, D., Xia, G., Chu, C., Li, J., and Fu, X. (2009). Natural variation at the *DEP1* locus enhances grain yield in rice. Nature Genetics *41*, 494–497.

Ito, A., Yasuda, A., Yamaoka, K., Ueda, M., Nakayama, A., Takatsuto, S., and Honda, I. (2017). *Brachytic 1* of barley (Hordeum vulgare L.) encodes the α subunit of heterotrimeric G protein. Journal of Plant Physiology *213*, 209–215.

Jackson, D., Veit, B., and Hake, S. (1994). Expression of maize *KNOTTED1* related homeobox genes in the shoot apical meristem predicts patterns of morphogenesis in the vegetative shoot. Development *120*, 405–413.

Jasinski, S., Piazza, P., Craft, J., Hay, A., Woolley, L., Rieu, I., Phillips, A., Hedden, P., and Tsiantis, M. (2005). KNOX Action in Arabidopsis Is Mediated by Coordinate Regulation of Cytokinin and Gibberellin Activities. Current Biology *15*, 1560–1565.

Javelle, M., Marco, C.F., and Timmermans, M. (2011). In Situ Hybridization for the Precise Localization of Transcripts in Plants. Journal of Visualized Experiments *57*, e3328.

Jia, Q., Li, C., Shang, Y., Zhu, J., Hua, W., Wang, J., Yang, J., and Zhang, G. (2015). Molecular characterization and functional analysis of barley semi-dwarf mutant Riso no. 9265. BMC Genomics *16*, 927.

Jiang, L., Liu, X., Xiong, G., Liu, H., Chen, F., Wang, L., Meng, X., Liu, G., Yu, H., Yuan, Y., et al. (2013). DWARF 53 acts as a repressor of strigolactone signalling in rice. Nature *504*, 401–405.

Johnston, R., Wang, M., Sun, Q., Sylvester, A.W., Hake, S., and Scanlon, M.J. (2014). Transcriptomic Analyses Indicate That Maize Ligule Development Recapitulates Gene Expression Patterns That Occur during Lateral Organ Initiation. Plant Cell *26*, 4718–4732.

Jones, B., Gunnerås, S.A., Petersson, S.V., Tarkowski, P., Graham, N., May, S., Dolezal, K., Sandberg, G., and Ljung, K. (2010). Cytokinin Regulation of Auxin Synthesis in Arabidopsis Involves a Homeostatic Feedback Loop Regulated via Auxin and Cytokinin Signal Transduction. The Plant Cell *22*, 2956–2969.

Jost, M., Taketa, S., Mascher, M., Himmelbach, A., Yuo, T., Shahinnia, F., Rutten, T., Druka, A., Schmutzer, T., Steuernagel, B., et al. (2016). A Homolog of Blade-On-Petiole 1 and 2 (BOP1/2) Controls Internode Length and Homeotic Changes of the Barley Inflorescence. Plant Physiol *171*, 1113–1127.

Kameoka, H., Dun, E.A., Lopez-Obando, M., Brewer, P.B., Germain, A. de S., Rameau, C., Beveridge, C.A., and Kyozuka, J. (2016). Phloem Transport of the Receptor

DWARF14 Protein Is Required for Full Function of Strigolactones. Plant Physiology *172*, 1844–1852.

Kanrar, S., Onguka, O., and Smith, H.M.S. (2006). Arabidopsis inflorescence architecture requires the activities of KNOX-BELL homeodomain heterodimers. Planta *224*, 1163–1173.

Karsai, I., Mészáros, K., Hayes, P.M., and Bedő, Z. (1997). Effects of loci on chromosomes 2 (2H) and 7 (5H) on developmental patterns in barley (*Hordeum vulgare* L.) under different photoperiod regimes. Theor Appl Genet *94*, 612–618.

Karsai, I., Mészáros, K., Szücs, P., Hayes, P.M., Láng, L., and Bedö, Z. (1999). Effects of loci determining photoperiod sensitivity (*Ppd-H1*) and vernalization response (*Sh2*) on agronomic traits in the 'Dicktoo'×'Morex' barley mapping population. Plant Breeding *118*, 399–403.

Kawakatsu, T., Taramino, G., Itoh, J.-I., Allen, J., Sato, Y., Hong, S.-K., Yule, R., Nagasawa, N., Kojima, M., Kusaba, M., et al. (2009). *PLASTOCHRON3/GOLIATH* encodes a glutamate carboxypeptidase required for proper development in rice. The Plant Journal *58*, 1028–1040.

Kebrom, T.H., and Mullet, J.E. (2016). Transcriptome Profiling of Tiller Buds Provides New Insights into PhyB Regulation of Tillering and Indeterminate Growth in Sorghum. Plant Physiology *170*, 2232–2250.

Kebrom, T.H., Burson, B.L., and Finlayson, S.A. (2006). Phytochrome B represses *Teosinte Branched1* expression and induces sorghum axillary bud outgrowth in response to light signals. Plant Physiology *140*, 1109–1117.

Kebrom, T.H., Chandler, P.M., Swain, S.M., King, R.W., Richards, R.A., and Spielmeyer, W. (2012). Inhibition of Tiller Bud Outgrowth in the *tin* Mutant of Wheat Is Associated with Precocious Internode Development. Plant Physiology *160*, 308–318.

Kelliher, T., and Walbot, V. (2012). Hypoxia Triggers Meiotic Fate Acquisition in Maize. Science *337*, 345–348.

Kerstetter, R., Laudencia-Chingcuanco, D., Smith, L., and Hake, S. (1997). Loss-of-function mutations in the maize homeobox gene, *knotted1*, are defective in shoot meristem maintenance. Development *124*, 3045–3054.

Khan, J.A., Wang, Q., Sjölund, R.D., Schulz, A., and Thompson, G.A. (2007). An Early Nodulin-Like Protein Accumulates in the Sieve Element Plasma Membrane of Arabidopsis. Plant Physiol *143*, 1576–1589.

Khan, M., Xu, M., Murmu, J., Tabb, P., Liu, Y., Storey, K., McKim, S.M., Douglas, C.J., and Hepworth, S.R. (2012). Antagonistic interaction of BLADE-ON-PETIOLE1 and 2

with BREVIPEDICELLUS and PENNYWISE regulates Arabidopsis inflorescence architecture. Plant Physiology *158*, 946–960.

Kieber, J.J., and Schaller, G.E. (2014). Cytokinins. Arabidopsis Book *12*.

Kipreos, E.T., and Pagano, M. (2000). The F-box protein family. Genome Biology *1*, reviews3002.1.

Kirby, E.J.M., and Applegate, M. (1981). Cereal development guide (Kenilworth, England: Cereal Unit, National Agricultural Centre).

Kirby, E.J.M., and Eisenberg, B.E. (1966). Some Effects of Photoperiod on Barley. J Exp Bot *17*, 204–213.

Kirby, E.J.M., and Faris, D.G. (1972). The effect of plant density on tiller growth and morphology in barley. The Journal of Agricultural Science *78*, 281–288.

Kirby, E.J.M., and Riggs, T.J. (1978). Developmental consequences of two-row and six-row ear type in spring barley: 2. Shoot apex, leaf and tiller development. The Journal of Agricultural Science *91*, 207–216.

Kobayashi, K., Yasuno, N., Sato, Y., Yoda, M., Yamazaki, R., Kimizu, M., Yoshida, H., Nagamura, Y., and Kyozuka, J. (2012). Inflorescence meristem identity in rice is specified by overlapping functions of three *AP1/FUL*-like MADS box genes and *PAP2*, a *SEPALLATA* MADS box gene. Plant Cell *24*, 1848–1859.

Komatsu, K., Maekawa, M., Ujiie, S., Satake, Y., Furutani, I., Okamoto, H., Shimamoto, K., and Kyozuka, J. (2003). LAX and SPA: major regulators of shoot branching in rice. Proceedings of the National Academy of Sciences of the United States of America *100*, 11765–11770.

Komatsuda, T., Pourkheirandish, M., He, C., Azhaguvel, P., Kanamori, H., Perovic, D., Stein, N., Graner, A., Wicker, T., Tagiri, A., et al. (2007). Six-rowed barley originated from a mutation in a homeodomain-leucine zipper I-class homeobox gene. PNAS *104*, 1424–1429.

Koppolu, R., Anwar, N., Sakuma, S., Tagiri, A., Lundqvist, U., Pourkheirandish, M., Rutten, T., Seiler, C., Himmelbach, A., Ariyadasa, R., et al. (2013). *Six-rowed spike4* (*Vrs4*) controls spikelet determinacy and row-type in barley. Proc Natl Acad Sci U S A *110*, 13198–13203.

Laurie, D.A., Pratchett, N., Bezant, J.H., and Snape, J.W. (1994). Genetic analysis of a photoperiod response gene on the short arm of chromosome 2(2H) of *Hordeum vulgare* (barley). Heredity *72*, 619–627.

Laurie, D.A., Pratchett, N., Snape, J.W., and Bezant, J.H. (1995). RFLP mapping of five major genes and eight quantitative trait loci controlling flowering time in a winter × spring barley (*Hordeum vulgare* L.) cross. Genome *38*, 575–585.

Li, C., and Bangerth, F. (2003). Stimulatory effect of cytokinins and interaction with IAA on the release of lateral buds of pea plants from apical dominance. Journal of Plant Physiology *160*, 1059–1063.

Li, C., Lin, H., and Dubcovsky, J. (2015). Factorial Combinations of Protein Interactions Generate a Multiplicity of Florigen Activation Complexes in Wheat and Barley. Plant J *84*, 70–82.

Li, X., Qian, Q., Fu, Z., Wang, Y., Xiong, G., Zeng, D., Wang, X., Liu, X., Teng, S., Hiroshi, F., et al. (2003). Control of tillering in rice. Nature *422*, 618–621.

Liang, D., Wong, C.E., Singh, M.B., Beveridge, C.A., Phipson, B., Smyth, G.K., and Bhalla, P.L. (2009). Molecular dissection of the pea shoot apical meristem. J Exp Bot *60*, 4201–4213.

Liller, C.B., Neuhaus, R., Korff, M. von, Koornneef, M., and Esse, W. van (2015). Mutations in Barley Row Type Genes Have Pleiotropic Effects on Shoot Branching. PLOS ONE *10*, e0140246.

Lin, C.S., and Poushinsky, G. (1983). A Modified Augmented Design for an Early Stage of Plant Selection Involving a Large Number of Test Lines without Replication. Biometrics *39*, 553–561.

Lin, C.-S., and Poushinsky, G. (1985). A modified augmented design (type 2) for rectangular plots. Can. J. Plant Sci. *65*, 743–749.

Lin, C.S., Poushinsky, G., and Jui, P.Y. (1983). Simulation study of three adjustment methods for the modified augmented design and comparison with the balanced lattice square design. The Journal of Agricultural Science *100*, 527–534.

Lincoln, C., Long, J., Yamaguchi, J., Serikawa, K., and Hake, S. (1994). A *Knotted1*-like homeobox gene in Arabidopsis is expressed in the vegetative meristem and dramatically alters leaf morphology when overexpressed in transgenic plants. The Plant Cell *6*, 1859–1876.

Lipka, A.E., Tian, F., Wang, Q., Peiffer, J., Li, M., Bradbury, P.J., Gore, M.A., Buckler, E.S., and Zhang, Z. (2012). GAPIT: genome association and prediction integrated tool. Bioinformatics *28*, 2397–2399.

Long, J.A., Moan, E.I., Medford, J.I., and Barton, M.K. (1996). A member of the KNOTTED class of homeodomain proteins encoded by the *STM* gene of Arabidopsis. Nature *379*, 66–69.

Loscalzo, J. (2016). Adaptions to Hypoxia and Redox Stress: Essential Concepts Confounded by Misleading Terminology. Circ Res *119*, 511–513.

Loscos, J., Igartua, E., Contreras-Moreira, B., Gracia, M.P., and Casas, A.M. (2014). *HvFT1* polymorphism and effect—survey of barley germplasm and expression analysis. Front Plant Sci *5*.

Love, M.I., Huber, W., and Anders, S. (2014). Moderated estimation of fold change and dispersion for RNA-seq data with DESeq2. Genome Biology *15*, 550.

Lundqvist, U., and Lundqvist, A. (1988). Induced intermedium mutants in barley: origin, morphology and inheritance. Hereditas *108*, 13–26.

Marroni, F., Pinosio, S., Zaina, G., Fogolari, F., Felice, N., Cattonaro, F., and Morgante, M. (2011). Nucleotide diversity and linkage disequilibrium in *Populus nigra cinnamyl alcohol dehydrogenase* (*CAD4*) gene. Tree Genetics & Genomes *7*, 1011–1023.

Mascher, M., Muehlbauer, G.J., Rokhsar, D.S., Chapman, J., Schmutz, J., Barry, K., Muñoz-Amatriaín, M., Close, T.J., Wise, R.P., Schulman, A.H., et al. (2013). Anchoring and ordering NGS contig assemblies by population sequencing (POPSEQ). Plant J *76*, 718–727.

Mascher, M., Jost, M., Kuon, J.-E., Himmelbach, A., Aßfalg, A., Beier, S., Scholz, U., Graner, A., and Stein, N. (2014). Mapping-by-sequencing accelerates forward genetics in barley. Genome Biology *15*, R78.

Mascher, M., Gundlach, H., Himmelbach, A., Beier, S., Twardziok, S.O., Wicker, T., Radchuk, V., Dockter, C., Hedley, P.E., Russell, J., et al. (2017). A chromosome conformation capture ordered sequence of the barley genome. Nature *544*, 427–433.

May, K.W., Kozub, G.C., and Schaalje, G.B. (1989). Field evaluation of a modified augmented design (type 2) for screening barley lines. Can. J. Plant Sci. *69*, 9–15.

McCarty, D.R., Hattori, T., Carson, C.B., Vasil, V., Lazar, M., and Vasil, I.K. (1991). The *Viviparous-1* developmental gene of maize encodes a novel transcriptional activator. Cell *66*, 895–905.

McSteen, P., and Hake, S. (2001). *barren inflorescence2* regulates axillary meristem development in the maize inflorescence. Development *128*, 2881–2891.

McSteen, P., and Leyser, O. (2005). Shoot Branching. Annual Review of Plant Biology *56*, 353–374.

McSteen, P., Malcomber, S., Skirpan, A., Lunde, C., Wu, X., Kellogg, E., and Hake, S. (2007). *barren inflorescence2* encodes a co-ortholog of the PINOID serine/threonine

kinase and is required for organogenesis during inflorescence and vegetative development in maize. Plant Physiology *144*, 1000–1011.

Meyerowitz, E.M. (1997). Genetic Control of Cell Division Patterns in Developing Plants. Cell *88*, 299–308.

Mickelson, H.R., and Rasmusson, D.C. (1994). Genes for Short Stature in Barley. Crop Science *34*, 1180–1183.

Minakuchi, K., Kameoka, H., Yasuno, N., Umehara, M., Luo, L., Kobayashi, K., Hanada, A., Ueno, K., Asami, T., Yamaguchi, S., et al. (2010). FINE CULM1 (FC1) works downstream of strigolactones to inhibit the outgrowth of axillary buds in rice. Plant & Cell Physiology *51*, 1127–1135.

Miralles, D. (2000). Responses of Leaf and Tiller Emergence and Primordium Initiation in Wheat and Barley to Interchanged Photoperiod. Annals of Botany *85*, 655–663.

Miralles, D., and Richards, R.A. (2000). Responses of Leaf and Tiller Emergence and Primordium Initiation in Wheat and Barley to Interchanged Photoperiod. Annals of Botany *85*, 655–663.

Mulki, M.A., and von Korff, M. (2016). CONSTANS Controls Floral Repression by Up-Regulating *VERNALIZATION2* (*VRN-H2*) in Barley. Plant Physiology *170*, 325–337.

Müller, D., and Leyser, O. (2011). Auxin, cytokinin and the control of shoot branching. Annals of Botany *107*, 1203–1212.

Müller, J., Wang, Y., Franzen, R., Santi, L., Salamini, F., and Rohde, W. (2001). In vitro interactions between barley TALE homeodomain proteins suggest a role for protein–protein associations in the regulation of *Knox* gene function. The Plant Journal *27*, 13–23.

Müller, K.J., Romano, N., Gerstner, O., Garcia-Marotot, F., Pozzi, C., Salamini, F., and Rohde, W. (1995). The barley *Hooded* mutation caused by a duplication in a homeobox gene intron. Nature *374*, 727–730.

Muñoz-Amatriaín, M., Cuesta-Marcos, A., Endelman, J.B., Comadran, J., Bonman, J.M., Bockelman, H.E., Chao, S., Russell, J., Waugh, R., Hayes, P.M., et al. (2014). The USDA Barley Core Collection: Genetic Diversity, Population Structure, and Potential for Genome-Wide Association Studies. PLoS ONE *9*, e94688.

Nakayama, N., Smith, R.S., Mandel, T., Robinson, S., Kimura, S., Boudaoud, A., and Kuhlemeier, C. (2012). Mechanical Regulation of Auxin-Mediated Growth. Current Biology *22*, 1468–1476.

Nambara, E., Nambara, E., McCourt, P., and Naito, S. (1995). A regulatory role for the *ABI3* gene in the establishment of embryo maturation in Arabidopsis thaliana. Development *121*, 629–636.

Nan Su San, Ootsuki, Y., Adachi, S., Yamamoto, T., Ueda, T., Tanabata, T., Motobayashi, T., Ookawa, T., and Hirasawa, T. (2018). A near-isogenic rice line carrying a QTL for larger leaf inclination angle yields heavier biomass and grain. Field Crops Research *219*, 131–138.

Nardmann, J., and Werr, W. (2006). The Shoot Stem Cell Niche in Angiosperms: Expression Patterns of WUS Orthologues in Rice and Maize Imply Major Modifications in the Course of Mono- and Dicot Evolution. Mol Biol Evol *23*, 2492–2504.

Naz, A.A., Arifuzzaman, M., Muzammil, S., Pillen, K., and Léon, J. (2014). Wild barley introgression lines revealed novel QTL alleles for root and related shoot traits in the cultivated barley (*Hordeum vulgare* L.). BMC Genetics *15*, 107.

Nice, L.M., Steffenson, B.J., Blake, T., Horsley, R., Smith, K., and Muehlbauer, G.J. (2017). Mapping Agronomic Traits in a Wild Barley Advanced Backcross–Nested Association Mapping Population. Crop Science *57*, 1199–1210.

Nikovics, K., Blein, T., Peaucelle, A., Ishida, T., Morin, H., Aida, M., and Laufs, P. (2006). The Balance between the MIR164A and *CUC2* Genes Controls Leaf Margin Serration in Arabidopsis. The Plant Cell *18*, 2929–2945.

Ohmori, Y., Tanaka, W., Kojima, M., Sakakibara, H., and Hirano, H.-Y. (2013). WUSCHEL-RELATED HOMEOBOX4 Is Involved in Meristem Maintenance and Is Negatively Regulated by the CLE Gene *FCP1* in Rice. Plant Cell *25*, 229–241.

Ohtsu, K., Smith, M.B., Emrich, S.J., Borsuk, L.A., Zhou, R., Chen, T., Zhang, X., Timmermans, M.C.P., Beck, J., Buckner, B., et al. (2007). Global gene expression analysis of the shoot apical meristem of maize (*Zea mays* L.). The Plant Journal : For Cell and Molecular Biology *52*, 391–404.

Oikawa, T., and Kyozuka, J. (2009). Two-Step Regulation of LAX PANICLE1 Protein Accumulation in Axillary Meristem Formation in Rice. The Plant Cell *21*, 1095–1108.

Okagaki, R.J., Cho, S., Kruger, W.M., Xu, W.W., Heinen, S., and Muehlbauer, G.J. (2013). The barley *UNICULM2* gene resides in a centromeric region and may be associated with signaling and stress responses. Functional & Integrative Genomics *13*, 33–41.

Okagaki, R.J., Haaning, A., Bilgic, H., Heinen, S., Druka, A., Bayer, M., Waugh, R., and Muehlbauer, G.J. (2018). ELIGULUM-A regulates lateral branch and leaf development in barley. Plant Physiology pp.01459.2017.

Ori, N., Eshed, Y., Chuck, G., Bowman, J.L., and Hake, S. (2000). Mechanisms that control *knox* gene expression in the Arabidopsis shoot. Development *127*, 5523–5532.

Pasam, R.K., Sharma, R., Malosetti, M., Eeuwijk, F.A. van, Haseneyer, G., Kilian, B., and Graner, A. (2012). Genome-wide association studies for agronomical traits in a world wide spring barley collection. BMC Plant Biology *12*, 16.

Pautler, M., Tanaka, W., Hirano, H.-Y., and Jackson, D. (2013). Grass meristems I: shoot apical meristem maintenance, axillary meristem determinacy and the floral transition. Plant & Cell Physiology *54*, 302–312.

Poland, J.A., Brown, P.J., Sorrells, M.E., and Jannink, J.-L. (2012). Development of High-Density Genetic Maps for Barley and Wheat Using a Novel Two-Enzyme Genotyping-by-Sequencing Approach. PLoS ONE *7*, e32253.

Pritchard, J.K., Stephens, M., and Donnelly, P. (2000). Inference of population structure using multilocus genotype data. Genetics *155*, 945–959.

Prusinkiewicz, P., Crawford, S., Smith, R.S., Ljung, K., Bennett, T., Ongaro, V., and Leyser, O. (2009). Control of bud activation by an auxin transport switch. Proceedings of the National Academy of Sciences of the United States of America *106*, 17431–17436.

R Core Team (2017). R: A language and environment for statistical computing. (Vienna, Austria: R Foundation for Statistical Computing).

Raman, S., Greb, T., Peaucelle, A., Blein, T., Laufs, P., and Theres, K. (2008). Interplay of miR164, *CUP-SHAPED COTYLEDON* genes and LATERAL SUPPRESSOR controls axillary meristem formation in Arabidopsis thaliana. The Plant Journal : For Cell and Molecular Biology *55*, 65–76.

Ramsay, L., Comadran, J., Druka, A., Marshall, D.F., Thomas, W.T.B., Macaulay, M., MacKenzie, K., Simpson, C., Fuller, J., Bonar, N., et al. (2011). *INTERMEDIUM-C*, a modifier of lateral spikelet fertility in barley, is an ortholog of the maize domestication gene *TEOSINTE BRANCHED 1*. Nature Genetics *43*, 169–172.

Rebetzke, G.J., and Richards, R.A. (2000). Gibberellic acid-sensitive dwarfing genes reduce plant height to increase kernel number and grain yield of wheat. Aust. J. Agric. Res. *51*, 235–246.

Ritter, M.K., Padilla, C.M., and Schmidt, R.J. (2002). The maize mutant *barren stalk1* is defective in axillary meristem development. American Journal of Botany *89*, 203–210.

Robinson, M.D., McCarthy, D.J., and Smyth, G.K. (2010). edgeR: a Bioconductor package for differential expression analysis of digital gene expression data. Bioinformatics *26*, 139–140.

Russell, J., Mascher, M., Dawson, I.K., Kyriakidis, S., Calixto, C., Freund, F., Bayer, M., Milne, I., Marshall-Griffiths, T., Heinen, S., et al. (2016). Exome sequencing of geographically diverse barley landraces and wild relatives gives insights into environmental adaptation. Nature Genetics *48*, 1024–1030.

Saisho, D., Tanno, K., Chono, M., Honda, I., Kitano, H., and Takeda, K. (2004). Spontaneous Brassinolide-insensitive Barley Mutants '*uzu*' Adapted to East Asia. Breeding Science *54*, 409–416.

Sakamoto, T., Kamiya, N., Ueguchi-Tanaka, M., Iwahori, S., and Matsuoka, M. (2001). KNOX homeodomain protein directly suppresses the expression of a gibberellin biosynthetic gene in the tobacco shoot apical meristem. Genes Dev. *15*, 581–590.

Sakamoto, T., Morinaka, Y., Ohnishi, T., Sunohara, H., Fujioka, S., Ueguchi-Tanaka, M., Mizutani, M., Sakata, K., Takatsuto, S., Yoshida, S., et al. (2006). Erect leaves caused by brassinosteroid deficiency increase biomass production and grain yield in rice. Nature Biotechnology *24*, 105–109.

Sakuma, S., Lundqvist, U., Kakei, Y., Thirulogachandar, V., Suzuki, T., Hori, K., Wu, J., Tagiri, A., Rutten, T., Koppolu, R., et al. (2017). Extreme Suppression of Lateral Floret Development by a Single Amino Acid Change in the VRS1 Transcription Factor. Plant Physiology *175*, 1720–1731.

de San Celedonio, R.P., Abeledo, L.G., and Miralles, D.J. (2014). Identifying the critical period for waterlogging on yield and its components in wheat and barley. Plant Soil *378*, 265–277.

Sasaki, A., Ashikari, M., Ueguchi-Tanaka, M., Itoh, H., Nishimura, A., Swapan, D., Ishiyama, K., Saito, T., Kobayashi, M., Khush, G.S., et al. (2002). Green revolution: A mutant gibberellin-synthesis gene in rice. Nature *416*, 701–702.

Sato, Y., Hong, S.K., Tagiri, A., Kitano, H., Yamamoto, N., Nagato, Y., and Matsuoka, M. (1996). A rice homeobox gene, *OSH1*, is expressed before organ differentiation in a specific region during early embryogenesis. PNAS *93*, 8117–8122.

Sato, Y., Sentoku, N., Miura, Y., Hirochika, H., Kitano, H., and Matsuoka, M. (1999). Loss-of-function mutations in the rice homeobox gene *OSH15* affect the architecture of internodes resulting in dwarf plants. EMBO J *18*, 992–1002.

Sauer, M., Balla, J., Luschnig, C., Wisniewska, J., Reinöhl, V., Friml, J., and Benková, E. (2006). Canalization of auxin flow by Aux/IAA-ARF-dependent feedback regulation of PIN polarity. Genes & Development *20*, 2902–2911.

Savatin, D.V., Gramegna, G., Modesti, V., and Cervone, F. (2014). Wounding in the plant tissue: the defense of a dangerous passage. Front. Plant Sci. *5*.

Scanlon, M.J., Ohtsu, K., Timmermans, M.C.P., and Schnable, P.S. (2009). Laser Microdissection-Mediated Isolation and In Vitro Transcriptional Amplification of Plant RNA. Current Protocols in Molecular Biology *87*, 25A.3.1-25A.3.15.

Schmitz, G., and Theres, K. (2005). Shoot and inflorescence branching. Current Opinion in Plant Biology *8*, 506–511.

Schmitz, J., Franzen, R., Ngyuen, T.H., Garcia-Maroto, F., Pozzi, C., Salamini, F., and Rohde, W. (2000). Cloning, mapping and expression analysis of barley *MADS-box* genes. Plant Mol Biol *42*, 899–913.

Schoof, H., Lenhard, M., Haecker, A., Mayer, K.F.X., Jürgens, G., and Laux, T. (2000). The Stem Cell Population of Arabidopsis Shoot Meristems Is Maintained by a Regulatory Loop between the *CLAVATA* and *WUSCHEL* Genes. Cell *100*, 635–644.

Schumacher, K., Schmitt, T., Rossberg, M., Schmitz, G., and Theres, K. (1999). The *Lateral suppressor* gene of tomato encodes a new member of the VHIID protein family. Proceedings of the National Academy of Sciences *96*, 290–295.

Shani, E., Yanai, O., and Ori, N. (2006). The role of hormones in shoot apical meristem function. Current Opinion in Plant Biology *9*, 484–489.

Shinohara, N., Taylor, C., and Leyser, O. (2013). Strigolactone can promote or inhibit shoot branching by triggering rapid depletion of the auxin efflux protein PIN1 from the plasma membrane. PLoS Biology *11*, e1001474–e1001474.

Si, Y., Liu, P., Li, P., and Brutnell, T.P. (2014). Model-based clustering for RNA-seq data. Bioinformatics *30*, 197–205.

Simmons, S.R., Rasmusson, D.C., and Wiersma, J.V. (1982). Tillering in barley: genotype, row spacing, and seedling rate effects. Crop Science *22*, 801–805.

Skinner, R.H., and Simmons, S.R. (1993). Modulation of leaf elongation, tiller appearance and tiller senescence in spring barley by far-red light. Plant, Cell and Environment *16*, 555–562.

Skirpan, A., Wu, X., and McSteen, P. (2008). Genetic and physical interaction suggest that BARREN STALK 1 is a target of BARREN INFLORESCENCE2 in maize inflorescence development. The Plant Journal : For Cell and Molecular Biology *55*, 787–797.

Skirpan, A., Culler, A.H., Gallavotti, A., Jackson, D., Cohen, J.D., and McSteen, P. (2009). BARREN INFLORESCENCE2 interaction with ZmPIN1a suggests a role in auxin transport during maize inflorescence development. Plant & Cell Physiology *50*, 652–657.

Somssich, M., Je, B.I., Simon, R., and Jackson, D. (2016). CLAVATA-WUSCHEL signaling in the shoot meristem. Development *143*, 3238–3248.

Spielmeyer, W., Ellis, M.H., and Chandler, P.M. (2002). Semidwarf (*sd-1*), "green revolution" rice, contains a defective gibberellin 20-oxidase gene. PNAS *99*, 9043–9048.

Stoskopf, N.C., and Reinbergs, E. (1966). Breeding for yield in spring cereals. Can. J. Plant Sci. *46*, 513–519.

Sussex, I.M. (1989). Developmental programming of the shoot meristem. Cell *56*, 225–229.

Suzuki, M., Latshaw, S., Sato, Y., Settles, A.M., Koch, K.E., Hannah, L.C., Kojima, M., Sakakibara, H., and McCarty, D.R. (2008). The Maize *Viviparous8* Locus, Encoding a Putative ALTERED MERISTEM PROGRAM1-Like Peptidase, Regulates Abscisic Acid Accumulation and Coordinates Embryo and Endosperm Development. Plant Physiology *146*, 1193–1206.

Takacs, E.M., Li, J., Du, C., Ponnala, L., Janick-Buckner, D., Yu, J., Muehlbauer, G.J., Schnable, P.S., Timmermans, M.C.P., Sun, Q., et al. (2012). Ontogeny of the Maize Shoot Apical Meristem. Plant Cell *24*, 3219–3234.

Takada, S., Hibara, K., Ishida, T., and Tasaka, M. (2001). The *CUP-SHAPED COTYLEDON1* gene of Arabidopsis regulates shoot apical meristem formation. Development *128*, 1127–1135.

Tanaka, W., Ohmori, Y., Ushijima, T., Matsusaka, H., Matsushita, T., Kumamaru, T., Kawano, S., and Hirano, H.-Y. (2015). Axillary Meristem Formation in Rice Requires the WUSCHEL Ortholog TILLERS ABSENT1. The Plant Cell *27*, 1173–1184.

Tang, L., Gao, H., Yoshihiro, H., Koki, H., Tetsuya, N., Liu, T., Tatsuhiko, S., and Xu, Z. (2017). Erect panicle super rice varieties enhance yield by harvest index advantages in high nitrogen and density conditions. Journal of Integrative Agriculture *16*, 1467–1473.

Tavakol, E., Okagaki, R., Verderio, G., J, V.S., Hussien, A., Bilgic, H., Scanlon, M.J., Todt, N.R., Close, T.J., Druka, A., et al. (2015). The Barley *Uniculme4* Gene Encodes a BLADE-ON-PETIOLE-Like Protein That Controls Tillering and Leaf Patterning. Plant Physiology *168*, 164–174.

Tian, C., Zhang, X., He, J., Yu, H., Wang, Y., Shi, B., Han, Y., Wang, G., Feng, X., Zhang, C., et al. (2014). An organ boundary-enriched gene regulatory network uncovers regulatory hierarchies underlying axillary meristem initiation. Molecular Systems Biology *10*, 755.

Truong, S.K., McCormick, R.F., Rooney, W.L., and Mullet, J.E. (2015). Harnessing Genetic Variation in Leaf Angle to Increase Productivity of Sorghum bicolor. Genetics *201*, 1229–1238.

Tsuda, K., Kurata, N., Ohyanagi, H., and Hake, S. (2014). Genome-Wide Study of KNOX Regulatory Network Reveals Brassinosteroid Catabolic Genes Important for Shoot Meristem Function in Rice. The Plant Cell *26*, 3488–3500.

Turner, A., Beales, J., Faure, S., Dunford, R.P., and Laurie, D.A. (2005). The Pseudo-Response Regulator Ppd-H1 Provides Adaptation to Photoperiod in Barley. Science *310*, 1031–1034.

Venglat, S.P., Dumonceaux, T., Rozwadowski, K., Parnell, L., Babic, V., Keller, W., Martienssen, R., Selvaraj, G., and Datla, R. (2002). The homeobox gene *BREVIPEDICELLUS* is a key regulator of inflorescence architecture in Arabidopsis. PNAS *99*, 4730–4735.

Vollbrecht, E., Reiser, L., and Hake, S. (2000). Shoot meristem size is dependent on inbred background and presence of the maize homeobox gene, *knotted1*. Development *127*, 3161–3172.

Vroemen, C.W., Mordhorst, A.P., Albrecht, C., Kwaaitaal, M.A.C.J., and Vries, S.C. de (2003). The *CUP-SHAPED COTYLEDON3* Gene Is Required for Boundary and Shoot Meristem Formation in Arabidopsis. The Plant Cell *15*, 1563–1577.

Waddington, S., M. CARTWRIGHT, P., and C, W. (1983). A Quantitative Scale of Spike Initial and Pistil Development in Barley and Wheat. Annals of Botany *51*, 119–130.

Wang, B., and Chee, P.W. (2010). Application of advanced backcross quantitative trait locus (QTL) analysis in crop improvement. Journal of Plant Breeding and Crop Science *2*, 221–232.

Wang, Z., Chen, F., Li, X., Cao, H., Ding, M., Zhang, C., Zuo, J., Xu, C., Xu, J., Deng, X., et al. (2016). Arabidopsis seed germination speed is controlled by SNL histone deacetylase-binding factor-mediated regulation of *AUX1*. Nature Communications *7*, 13412.

Westermann, J.-C., and Craik, D.J. (2010). Amino Acids, Peptides, and Proteins. In Comprehensive Natural Products II, (Elsevier Ltd.), p.

White, M.D., Kamps, J.J.A.G., East, S., Kearney, L.J.T., and Flashman, E. (2018). The plant cysteine oxidases from Arabidopsis thaliana are kinetically tailored to act as oxygen sensors. J. Biol. Chem. *293*, 11786–11795.

Xu, Y., Jia, Q., Zhou, G., Zhang, X.-Q., Angessa, T., Broughton, S., Yan, G., Zhang, W., and Li, C. (2017). Characterization of the *sdw1* semi-dwarf gene in barley. BMC Plant Biology *17*, 11.

Yan, L., Fu, D., Li, C., Blechl, A., Tranquilli, G., Bonafede, M., Sanchez, A., Valarik, M., Yasuda, S., and Dubcovsky, J. (2006). The wheat and barley vernalization gene *VRN3* is an orthologue of *FT*. PNAS *103*, 19581–19586.

Yao, R., Wang, L., Li, Y., Chen, L., Li, S., Du, X., Wang, B., Yan, J., Li, J., and Xie, D. (2018). Rice DWARF14 acts as an unconventional hormone receptor for strigolactone. J Exp Bot *69*, 2355–2365.

Yoshida, S., Kameoka, H., Tempo, M., Akiyama, K., Umehara, M., Yamaguchi, S., Hayashi, H., Kyozuka, J., and Shirasu, K. (2012). The D3 F-box protein is a key component in host strigolactone responses essential for arbuscular mycorrhizal symbiosis. New Phytol. *196*, 1208–1216.

Zitzewitz, J. von, Szűcs, P., Dubcovsky, J., Yan, L., Francia, E., Pecchioni, N., Casas, A., Chen, T.H.H., Hayes, P.M., and Skinner, J.S. (2005). Molecular and Structural Characterization of Barley Vernalization Genes. Plant Mol Biol *59*, 449–467.